

*Aus dem Fachbereich Biophysik  
Theoretische Medizin und Biowissenschaften  
der Medizinischen Fakultät  
der Universität des Saarlandes, Homburg/Saar*

# **ER-mitochondria contacts regulate a redox-driven signaling axis to control melanoma progression**

*Dissertation zur Erlangung des Grades eines Doktors der Naturwissenschaften*

**der Medizinischen Fakultät  
der Universität des Saarlandes**

**2020**

**vorgelegt von:**

Xin Zhang  
geb. am 22.06.1982 in Gansu, China

Tag der Promotion: 28th. September. 2020

Dekan: Univ.-Prof. Dr. med. Michael D. Menger

Berichterstatter: Prof. Markus Hoth

Prof. Gerald Thiel

# 1 Contents

1	Contents .....	1
2	Acknowledgments.....	5
3	Glossary .....	7
4	Summary .....	9
4.1	Zusammenfassung .....	9
4.2	Summary.....	11
5	Introduction.....	13
5.1	Skin and melanoma pathology .....	13
5.1.1	The human skin .....	13
5.1.2	Types of skin cancer and melanomas.....	14
5.1.3	Risk factors for carcinogenesis of NMSCs and melanomas .....	15
5.1.4	Epidemiology of melanoma .....	19
5.2	Calcium signaling in melanoma .....	21
5.2.1	Calcium signaling in cancer .....	21
5.2.2	The role of calcium signaling in melanoma pathogenesis .....	22
5.3	Redox signaling in melanoma .....	27
5.3.1	Redox signaling in cancer .....	27
5.3.2	Redox signaling in melanocytes and melanoma .....	28
5.4	Mitochondria in melanoma: Liaison between metabolism and signaling .....	31
5.4.1	Mitochondria as the hub of calcium and redox signaling .....	31
5.4.2	The mitochondrial function in melanoma .....	33
5.5	ER-mitochondria contacts in melanoma.....	34
5.6	The TMXs emerged from a genomic-wide screen for NFAT activation .....	36
5.6.1	Thioredoxin-related transmembrane protein: What is known.....	37
5.6.2	NFAT signaling in melanoma .....	38
5.7	Research focus and questions for the investigation.....	41
6	Materials and Methods.....	42
6.1	Materials .....	42
6.1.1	Chemicals .....	42
6.1.2	Solutions and Culture Media.....	43
6.1.3	Solutions and buffer recipes .....	44
6.1.4	Primers for PCR .....	45

6.1.5	siRNA and shRNA .....	45
6.1.6	Primary Antibodies .....	46
6.1.7	Assay kits .....	46
6.1.8	Peripherals.....	47
6.1.9	Devices .....	47
6.1.10	Microscopes .....	48
6.1.10.1	Zeiss Cell Observer Z1 .....	48
6.1.10.1.1	LED sets.....	48
6.1.10.1.2	Emission Filters and Dichroic Mirror Sets .....	49
6.1.10.1.3	Objectives .....	49
6.1.10.1.4	Cameras.....	50
6.1.10.2	Olympus IX70 Setup.....	50
6.1.11	Cell Lines .....	50
6.1.12	Genetically Encoded Protein Sensors .....	51
6.2	Methods .....	52
6.2.1	Cell culture .....	52
6.2.2	RT-PCR.....	53
6.2.2.1	RNA isolation .....	53
6.2.2.2	Reverse transcription .....	53
6.2.2.3	RT-qPCR.....	53
6.2.3	Western blotting .....	54
6.2.4	RNA oligonucleotide mediated gene silencing.....	55
6.2.5	NFAT1 translocation assay .....	57
6.2.6	Cell viability assay .....	57
6.2.7	Cell migration assay .....	58
6.2.8	Calcium measurement.....	59
6.2.8.1	Fura-2 AM based cellular calcium measurement .....	59
6.2.8.2	Compartmental calcium measurement.....	59
6.2.9	Intracellular H <sub>2</sub> O <sub>2</sub> measurement.....	60
6.2.10	Intracellular pH measurement .....	61
6.2.11	Mitochondrial ATP concentration measurement .....	61
6.2.12	Calcineurin activity assays .....	62
6.2.12.1	Dynamic measurement of calcineurin activity .....	62
6.2.12.2	Enzymatic end point measurement of calcineurin activity .....	62
6.2.13	Interleukin-8 secretion measurement .....	63

6.2.14	Electron microscopy analysis of MAM parameters.....	64
6.2.15	<i>In vivo</i> studies.....	64
6.2.16	Experimental data analysis and statistics .....	66
7	Results.....	67
7.1	The expression analysis of TMXs and NFAT1 in human melanoma .....	67
7.1.1	The mRNA expression of TMXs is elevated in melanoma cells .....	67
7.1.2	The mRNA expression of NFAT1 is elevated in melanoma cells .....	68
7.2	NFAT1 function is impaired by silencing of TMXs .....	70
7.2.1	NFAT1 translocation is inhibited by silencing of TMXs.....	70
7.2.2	NFAT1 transcriptional activity is reduced by silencing of TMXs.....	73
7.3	Silencing of TMXs does not affect SOCE.....	74
7.4	Silencing of TMXs increases cellular ROS production.....	75
7.5	Silencing of TMXs inhibits NFAT1 activation via the oxidative modulation .....	78
7.5.1	The NFAT1 translocation is redox dependent .....	78
7.5.2	The inhibition of NFAT1 activation induced by silencing of TMX1 can be reversed by antioxidants .....	79
7.5.3	Calcineurin is a redox-sensitive element of NFAT1 signaling pathway.....	81
7.5.3.1	Calcineurin activity is inhibited by silencing of TMXs.....	81
7.5.3.2	Calcineurin activity could be inhibited by H <sub>2</sub> O <sub>2</sub> .....	83
7.6	Mitochondria are major source for ROS generation following TMX silencing.....	84
7.6.1	Silencing of TMXs does not induce ER stress.....	84
7.6.2	Silencing of TMX1 does not affect ER redox homeostasis .....	85
7.6.3	Mitochondrial ROS is increased by silencing of TMXs .....	86
7.6.4	Elevated mitochondrial ROS is caused by altered mitochondrial metabolism ..	88
7.6.4.1	Mitochondrial calcium level is increased by TMX1 silencing .....	88
7.6.4.2	Mitochondrial ATP is elevated by TMX1 silencing.....	91
7.6.5	TMX1 silencing alters mitochondrial morphology .....	92
7.7	NOX4 is an alternative source of ROS.....	95
7.8	TMX-ROS-NFAT1 signaling axis controls melanoma behavior.....	97
7.8.1	TMX-ROS-NFAT1 axis promotes melanoma proliferation .....	97
7.8.2	TMX-ROS-NFAT1 axis promotes melanoma migration.....	99
7.8.3	TMX1 silencing does not affect BRAF-inhibitor sensitivity in melanoma .....	102
7.8.4	TMX1 silencing affects melanoma tumor growth <i>in vivo</i> .....	103
8	Discussion .....	105
8.1	The TMX proteins and NFAT1 are upregulated in melanoma and correlate with melanoma progression.....	105

8.2	The TMXs regulate NFAT1 activation via ROS, not Ca <sup>2+</sup> .....	107
8.3	The TMXs influence mitochondrial ROS production .....	109
8.4	The ER-mitochondria contact sites shape mitochondrial dynamics.....	110
8.5	TMXs and NFAT1 promote aggressive melanoma phenotypes .....	112
8.6	The TMX-NFAT1 axis regulates mitochondrial function and redox homeostasis in melanomas .....	115
8.7	ER-mitochondria contact sites and the TMX-ROS-NFAT1 axis in the perspective of melanoma therapeutics .....	116
8.8	Conclusion .....	118
9	References.....	120
10	Register of Graphs, Tables and Figures .....	143
11	Declaration.....	146
12	Publications.....	147
13	Curriculum Vitae .....	149

## **2 Acknowledgments**

I would like to express my deepest appreciation to my supervisor Prof. Dr. Ivan Bogeski for the constant support with my research work and professional development, without his persistence for the project we could not archive such progress and thoroughness. Ivan guided me during my Ph.D. study not only for how to investigate a scientific subject but also how to create meaningful cooperation in the academic field and conduct research resources with tactics. He accompanied me through the whole study period with patience, encouragement and assistance. He also gave me the opportunity to work independently and develop my confidence as a scientist. Altogether, I would like to thank him for the support, friendship and guidance in the past years.

I would also like to express my sincere gratitude to Prof. Dr. Markus Hoth for his friendly support and kindness during my study. He provided us generous supports over the developing of the project and offered us insightful suggestions about the research work. Moreover, he played a crucial role in the leading and integrating of all teams in the lab to create a friendly and innovative environment for science. His keen mind, gentleness and encouragement showed an excellent example as a mentor.

For all efforts towards the project, first I would like to especially thank my dear colleagues Dr. Christine S. Gibhardt, Dr. Adina Vultur, Ioana Stejerean and Sabrina Cappello for their great help and endless effort in conducting experiments, processing data, writing the draft for the publication and providing suggestions on the writing of this work. Without their contributions, this work would have not existed in this form. I would also like to express my gratitude to Prof. Dr. Barbara Niemeyer and Dr. Maik Konrad for their contribution in the initiation and developing of the project.

For experimental contribution and sharing of laboratory resources, I would like to acknowledge: Dr. Christina Körbel, Prof. Dr. Matthias W. Laschke and Prof. Dr. Michael D.

Menger for sharing laboratory resources and providing helps in the *in vivo* melanoma xenograft model (figure 25); Nasser Tahbaz, Lucas Mina and Prof. Dr. Thomas Simmen for conducting electron microscopy and data analysis (figure 18); our wonderful technician team, Andrea Paluschkiwitz, Sandra Janku and Alexandra Stark assisted in qPCR (figure 1 and 2) and western blot (figure 12) experiments. The XBP1s primer, PDI and BiP antibodies were kindly provided by Prof. Dr. Richard Zimmerman, Biochemistry, Saarland University (figure 12).

Additionally, I would like to thank the rest of technician team, Gertrud Schwär, Cora Hoxha and Carmen Hessig for their professional work and technical support on cell culture, buffer preparation and management of laboratory resources.

Many thanks to Dr. Adina Vultur and Scribbr for the English editing of the introduction, materials and methods and discussion sections of this thesis. I am grateful for the suggestions and supports from Ivan and Markus during the writing and revision of this dissertation.

Thanks to all my friends and colleagues at the UMG and Saarland University who made my time as a Ph.D. exciting and instructive. To the dear family members who supported me with all their strengths during my Ph.D. study, my appreciation is beyond any words.

### 3 Glossary

The units, measurements and abbreviations of the unexplained scientific terms used in the current study are all listed in the glossary. The other abbreviations in the text are explained when used for first time.

#### Units

---

µl	microlitre
µM	micromolar
g	gram
G	gravity
h	Hour
kDa	kilo dalton
M	molar
min	minute
ml	milliliter
mM	milli molar
nM	nano molar
RPM	rounds per minute
s	second
pmol	pico molar
mW	milli watt
mA	Milli ampere
V	volt

---

#### Abbreviations

---

AKT	AKT Serine/Threonine Kinase
Approx.	approximately
AP1	Activator Protein 1
ATP	Adenosine triphosphate
BCC	Basal Cell Carcinoma
BiP	Binding Immunoglobulin Protein
CRAC	Calcium Release-Activated Channels
ER	Endoplasmatisches Retikulum
ERo1	ER oxidase 1
ERK	Extracellular signal-Regulated Kinase
HIF1α	Hypoxia-inducible factor 1α
IP3R	Inositol trisphosphate Receptor
MAM	Mitochondria-Associated Membrane
MAPK	Mitogen-Activated Protein Kinase
MCU	Mitochondrial Calcium Uniporter
MITF	Microphthalmia-associated Transcription Factor
NFAT	Nuclear Factor of Activated T-cells

---

---

NF- $\kappa$ B	Nuclear Factor kappa-light-chain-enhancer of activated B cells
NMSC	Non-Melanoma Skin Cancer
NO	Nitric Oxide
NOX	NAD(P)H oxidase
RNS	Reactive Nitrogen Species
OCR	Oxygen Consumption Rate
OMM	Out Mitochondria Membrane
ORAI	ORAI Calcium Release-activated Calcium Channel Protein
OXPPOS	Oxidative Phosphorylation
PDI	Protein Disulfide Isomerase
PGC1 $\alpha$	Peroxisome proliferator-activated receptor $\gamma$ Coactivator 1 alpha
PI <sub>3</sub> K	Phosphatidylinositide 3-kinase
PM	Plasma membrane
PMA	Phorbol 12-myristate 13-acetate
PMCA	Plasma Membrane Ca <sup>2+</sup> ATPase
ROS	Reactive Oxygen Species
PTEN	Phosphatase and tensin homolog
PTP	Permeability Transition Pore
SCC	Squamous Cell Carcinoma
SKCM	TCGA Skin Cutaneous Melanoma
SOCE	Sarco/endoplasmic reticulum Ca <sup>2+</sup> -ATPase
STIM	Stromal Interaction Molecule
TMX	Thioredoxin related transmembrane protein
Trx	Thioredoxin
TXNDC15	Thioredoxin Domain Containing 15
UPR	Unfolded Protein Response
CaV	Voltage gated Ca <sup>2+</sup> channel
XBP1s	Splicing product of X-box Binding Protein 1

---

## **4 Summary**

### **4.1 Zusammenfassung**

Melanom ist die tödlichste Form von Hautkrebs und trat mit steigender Prävalenz in den vergangenen Jahrzehnten auf. Bei der Entstehung und dem Verlauf dieser Krebserkrankung spielen reaktive Sauerstoff Spezies (ROS), sowie die Dysregulation von Signalwegen eine wichtige Rolle. Außerdem führen die oxidative Stressantwort, sowie die Aktivierung von alternativen Signalwegen häufig zu Behandlungsesistenzen und einem erhöhten Metastasierungspotential, was Auswirkungen auf das Patientenüberleben hat. Zahlreiche wissenschaftliche Arbeiten konnten den Einfluss von oxidativem Stress auf verschiedene Signalwege in Schwarzem Hautkrebs nachweisen. Diese Signalwege können auf der anderen Seite wieder zu einer veränderten ROS Produktion oder antioxidativen Kapazität führen. Daher kann das bessere Verständnis der Interaktion von ROS und Redoxregulation von Signalwegen neue Einblicke in Behandlungsmöglichkeiten geben und diese verbessern.

Die Mitochondrien sind wichtige Zellorganellen, in denen durch oxidative Phosphorylierung ATP, sowie als molekulares Nebenprodukt ROS produziert werden. Durch die Nähe zum ER (Endoplasmatisches Retikulum) spielen Mitochondrien auch eine bedeutende Rolle in der Regulation von intrazellulärem Calcium und dem Feintuning nachfolgender Signalkaskaden. Es deutet viel darauf hin, dass Anomalien in den Mitochondrien, die im Mittelpunkt von Biogenese, Redoxregulation und Kontrolle von Signalwegen stehen, zur Melanomentstehung beitragen. Zusätzlich beeinflussen die Reprogrammierung, sowie Positionierung der Mitochondrien das Zellüberleben, sowie die Resistenzbildung gegenüber Therapien bei Krebs, eingeschlossen dem Melanom.

Daher haben wir in diesem Zusammenhang untersucht, wie die Veränderung von Kontaktstellen zwischen Mitochondrien und ER durch TMX1 und TMX3, den Oxidoreduktasen in der Mitochondrien assoziierten ER Membran (MAM), die Funktion der

Mitochondrien, von Zellsignale und die Melanom-Pathologie beeinflussen. In dieser Arbeit konnte gezeigt werden, dass TMX1, TMX3 und der Calcium/Calciumneurin-regulierte Transkriptionsfaktor NFAT1 im Vergleich zu Melanozyten und Keratinozyten in Melanom Zelllinien und Patientenproben überexprimiert sind. Der Knockdown von TMX1 und TMX3 führte durch einen Anstieg an mitochondrialen ROS, sowie einer erhöhten NAD(P)H Oxidase 4 (NOX4) Aktivität, zu einem Anstieg von ROS im Zytosol. Dadurch wurde die Translokation von NFAT1 in den Zellkern durch die Oxidation der Phosphatase Calcineurin verhindert. Durch die Inhibition der NFAT1-Aktivierung und die daraus folgende geringere transkriptionale Aktivität, wurde die Expression von Zielgenen beeinflusst. Die Inhibition von NFAT1 verursachte schließlich eine Hemmung der Melanomproliferation, der Migration *in vitro* und des Tumorwachstums *in vivo*.

Zusammenfassend lässt sich sagen, dass Mitochondrien-ER-Kontaktstellen die Melanom-Redox-Homöostase regulieren und den Signalweg von Calcineurin-NFAT1 beeinflussen. TMX und NFAT1 sind daher potenzielle Biomarker, die zur Melanomprogression beitragen.

## 4.2 Summary

Melanoma is the deadliest skin cancer with an increasing incidence in the past decades. The reactive oxygen species (ROS) and dysregulation of signaling pathways play important roles in the formation and progression of melanoma. Furthermore, the oxidative stress response and activation of alternative signaling pathways were reported as determinants of drug resistance, survival and metastasis of melanoma. There is abundant scientific literature demonstrating that the oxidative stress can influence multiple signaling pathways in melanoma and in return, the changes of these signaling pathways often lead to an altered ROS production or antioxidant capacity. Hence, understanding of the interaction between ROS and the redox regulation of signaling pathways could provide beneficial insights for treatment.

Mitochondria are organelles wherein the oxidative phosphorylation produces ATP as well as ROS as byproducts. Due to the proximity to the endoplasmic reticulum (ER), mitochondria also play a critical role in the regulation of intracellular calcium and the fine-tuning of the calcium-controlled signal cascades. Therefore, there are culminating evidences suggesting that mitochondria act as hubs of biogenesis, redox regulation and calcium signaling thereby controlling cellular function. Anomalies in mitochondrial function contribute to carcinogenesis of melanoma. Additionally, the reprogramming and positioning of mitochondria were shown as important factors in controlling cell survival and resistance against treatment in cancer including melanoma.

We investigated how the disturbance of contact sites between mitochondria and ER through manipulation of thioredoxin related transmembrane protein 1 (TMX1) and thioredoxin related transmembrane protein 3 (TMX3), oxidoreductases localized in the mitochondria-associated ER membrane (MAM) affect the mitochondrial function, cell signaling and melanoma pathobiology. In the present study, TMX1, TMX3 and a calcium/calcineurin-regulated transcription factor Nuclear Factor of Activated T-cells 1 (NFAT1) demonstrated up-

regulated expression in the melanoma cell lines and patient samples compared with healthy melanocytes and keratinocytes. The knockdown of TMX1 and TMX3 resulted in an elevated ROS via mitochondria and NAD(P)H oxidase 4 (NOX4) and NFAT1 inhibition via oxidation of the phosphatase calcineurin. The inhibition of NFAT1 led to a lower NFAT1 transcriptional activity, which affected expression of the target genes. Inhibition of NFAT1 eventually caused a suppression of melanoma proliferation, migration *in vitro* and tumor growth *in vivo*.

In conclusion, our study suggests that mitochondria-ER contact sites regulate melanoma redox homeostasis and influence calcineurin-NFAT1 signaling pathway. TMX and NFAT1 are thus potential biomarkers contributing to the progression of melanoma.

## **5 Introduction**

### **5.1 Skin and melanoma pathology**

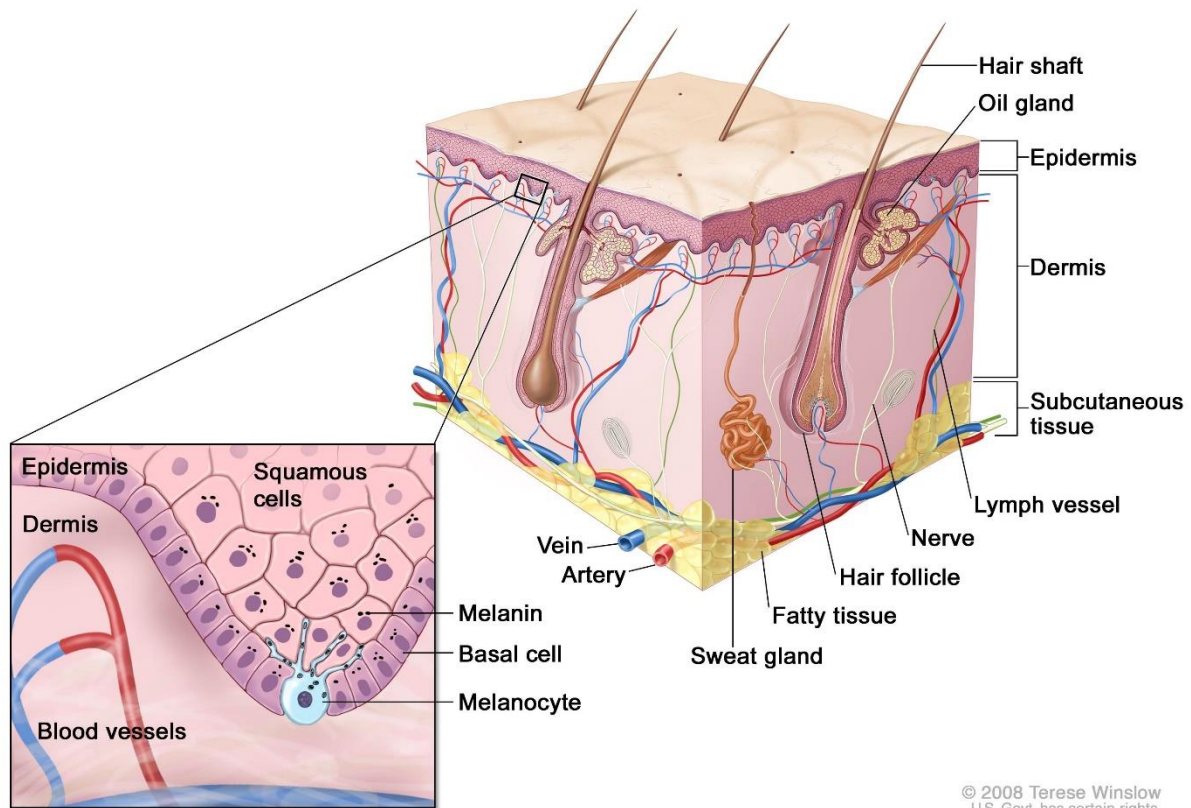
#### **5.1.1 The human skin**

The human skin is the largest organ of the integumentary system, which covers the surface of the body and serves as the first line of defense against various types of damage, harmful fluids, radiation and pathogens. As depicted in Graph 1, the skin consists of three different layers, namely the epidermis, dermis and subcutis.

The epidermis is the outer layer of the skin. It consists of three major cell types (keratinocytes, melanocytes and Langerhans cells), each of which has a different function. Keratinocytes are the predominant cell type in the epidermis; they produce keratin. They are developed from the stratum basale and migrate upwards to the stratum corneum after maturation. Dead keratinocytes in the corneum are constantly replaced by the new ones. Keratinocytes mainly function as a barrier against pathogens such as bacteria, viruses, parasites, fungi, ultraviolet (UV) radiation and dehydration. Melanocytes originate from the neural crest. They are responsible for melanin production and the pigmentation of the skin via their association with keratinocytes. In addition to melanin, they are able to produce signaling molecules such as cytokines, melanocortin peptides, catecholamines, serotonin and nitric oxide (NO) (1). Langerhans cells are dendritic cells responsible for cutaneous adaptive immune responses; they can promote CD4 T cell differentiation in a variety of inflammatory contexts (2).

The epidermis and dermis are connected by a complex layer called the dermo-epidermal junction, which contains the basement membrane. The dermis is located beneath the epidermis; it contains fibers composed of collagen and elastin proteins, as well as the gel-like extracellular matrix. The most important cells in the dermis are the fibroblasts, which produce collagen, elastin and other molecules. The sebaceous glands, sweat glands, hair follicles, some nerves and muscle cells are also embedded in the dermis. The bottom layer is the subcutis,

which is comprised of a collagen fiber network, adipocytes, blood and lymphatic vessels and nerves. The subcutis provides additional protection against external stresses such as mechanical force or coldness. With regard to the formation of melanoma, the epidermis and dermis, as the outer layers, are directly exposed to carcinogens. As a result, melanomas develop from the melanocytes in the basement layer.



© 2008 Terese Winslow  
U.S. Govt. has certain rights

**Graph 1: Anatomy of the Human Skin.** (Adapted from the University of California San Francisco/Melanoma Surgery/Department of Surgery; the link is as follows: <https://melanoma.surgery.ucsf.edu/conditions--procedures/melanoma.aspx>)

### 5.1.2 Types of skin cancer and melanomas

Based on their origins, skin cancers are generally categorized as being either non-melanoma skin cancers (NMSCs) or melanomas. Non-melanoma skin cancers develop from the basal cells and squamous cells in the epidermis, while melanomas originate from melanocytes derived from the neural crest. Melanomas and NMSCs are the most common types of cancer

in the fair-skinned population (3-5). About 80% of all NMSC are basal cell carcinomas, while squamous cell carcinomas account for approximately 20%; the other types only present around 1% of the diagnosed population (6).

There are four basic melanomas: superficial spreading melanomas, nodular melanomas, lentigo maligna melanomas and acral lentiginous melanomas. The common melanomas are generally cutaneous (7). The superficial spreading melanoma is the most common type, it tends to radial growth and covers the surface of skin. The thickness of superficial spreading melanomas is usually around 1 mm, but they can grow vertically and penetrate the skin. Nodular melanomas are characterized by rapid growth and invasiveness; they appear on the skin surface but can penetrate into the deeper layers very swiftly. Lentigo maligna melanomas are usually found in older populations as a result of long-term sun exposure, and the histological characteristic of it is the proliferation of atypical melanocytes at the dermo-epidermal junction. They are less aggressive compared to the other types of melanoma because they usually remain on the skin surface. When such a melanoma becomes invasive, it is termed a lentigo maligna melanoma (8). Acral lentiginous melanomas are common among Africans and Asians; they mainly develop on the feet or hands or under the nails. There are also several other types of melanoma, including amelanotic, polypoid and desmoplastic, but these are rarer and present in less than 5% of all cases. The staging of all melanomas is usually based on the thickness of tumor, ulceration status, the status of regional lymph node metastasis and distant metastasis. Further staging is usually based on information obtained from molecular diagnosis and biopsy.

### **5.1.3 Risk factors for carcinogenesis of NMSCs and melanomas**

With regard to the pathogenesis of NMSCs and melanomas, the risk of incidence depends on both the health status of the host and environmental factors. In terms of environmental factors, increased exposure to sunlight, namely photocarcinogenesis, is considered a major causal

factor for both types of skin cancer (5, 9-12). Chronic or intermittent sun exposure can lead to sunburn or skin lesions, which can develop into skin cancers (13, 14). Although the relationship between patterns of sun exposure and the formation of skin cancer is complicated (15, 16), it is generally agreed that UV irradiation from sunlight is the main risk factor. This conclusion has been drawn based on several different observations. Epidemiological studies have demonstrated that the incidence and mortality rates of NMSCs and melanomas are negatively correlated to geographic latitude of residence. Based on mouse experiments, skin cancer can be induced by UV irradiation. The UVB spectrum (280–320 nm) is particularly carcinogenic, while the contribution of UVA is less clear (17), and UVC rays are usually blocked by the ozone layer and the atmosphere. Furthermore, the deficiencies of UV-induced DNA damage repair increase susceptibility to skin cancer (18).

Ultraviolet irradiation-induced DNA damage is the critical initiating event for both NMSCs and melanomas. Such damage produces cyclobutane pyrimidine dimers which cause further DNA lesions and mutations as a result of errors in nucleotide excision repair (17, 19). Eventually, such mutations can lead to the activation of oncogenes or the silencing of tumor-suppressor genes and prompt a malignant transformation (20, 21). However, the driving mutations for NMSCs and melanomas differ. In the BCC, Patched and Smoothed in the Sonic hedgehog pathway are prevalent, while, in the SCC, the driver genes are TP53, epidermal growth factor receptor (EGFR), cyclin-dependent kinase 2A (CDKN2A), tyrosine kinase Fyn (FYN) and rat sarcoma (RAS) (22). A melanoma exhibits markedly basal mutation rates induced by UV irradiation, which are caused by the accumulation of cytidine to thymidine transitions (23, 24). Mutations of TP53 and CDKN2A have also been found to be inducible by UV in melanomas. Beyond DNA damage, UV irradiation can also cause sunburn, inflammation, immune suppression and ROS generation in the skin and elevate the risk of skin cancer (25).

From a host's perspective, there are many factors that can contribute to the carcinogenesis of NMSC or melanoma, including genetic heritage, age and phenotype characteristics. It is estimated that 5 to 12% of the worldwide incidence of melanomas can be attributed to inherited germline mutations (26, 27). The inheritance of melanoma is often observed in populations with lower risk susceptibility genes, but 5 to 10% of melanomas occurred in families prone to melanoma, which indicates that high penetrance susceptibility genes are also important (28, 29). The hereditary melanomas are linked to autosomal-dominant disorders; the associated genetic alterations include CDKN2A, CDK4 (cyclin-dependent kinase 4), the telomerase complex proteins telomerase reverse transcriptase (TERT), protection of telomeres 1, BRCA1-associated protein-1 (BAP1), microphthalmia-associated transcription factor (MITF), TP53, phosphatase and tensin homolog (PTEN) and xeroderma pigmentosum (XPA) (27, 30-36). The prevalence of these mutations in hereditary melanomas varies, but, generally, the risk of melanoma incidence for bearers is higher when compared to that of common individuals. Clinical surveillance is thus suggested on different degrees for the mutation bearers.

The phenotypic characteristics of a host, such as hair color, eye color, skin color and freckle density, are often investigated in cohort studies or meta-studies (37-40) for the purpose of evaluating melanoma risk. However, these factors are very interactive with environmental factors; for example, freckle density, red or blond hair, blue eyes and light skin are the phenotypes related to photosensitivity. This means that bearers have a greater sensitivity to UV irradiation, which is in turn associated with a higher risk of skin cancer (41, 42). The cause of these phenotypes is the amount and type of cutaneous melanin generated by the bearer (43, 44); thus, controlling genes such as melanocortin-1 receptor plays a critical role in the development of melanomas in the subpopulation bearing these phenotypes (45, 46).

Beyond the phenotypic characteristics, the nevi number is another important reference for the evaluation of melanoma risk. The melanocytic nevi are benign neoplasms or hematomas composed of melanocytes. They can be acquired over the course of an individual's lifetime or may be congenital, meaning that they developed during embryogenesis. As a risk factor, melanocytic nevi are generally associated with sun exposure, subpopulations with certain phenotype characteristics and bearers' genetic predispositions, so multiple approaches to categorization and parameters are applied in the studies regarding the evaluation of nevi and melanoma occurrence. According to case-control studies on patients and meta-studies on melanoma risk, melanocytic and atypical naevi are also very prominent risk factors, a finding that could be used for the prediction of malignant melanomas (47, 48). The total numbers of common naevi and clinically atypical naevi are often two important parameters for analysis (49), while a large number of acquired melanocytic nevi is often considered as representing a high risk for melanoma, as it may indicate a higher genetic tendency towards melanoma formation or high exposure to environmental agents. Acquired nevi on soles, palms and nail have been found to be less dangerous (49, 50). As atypical naevi are usually larger and have a more variegated appearance when compared with the common naevi, they may conceal an underlying dysplasia, which could lead to melanoma formation. Dysplastic melanocytic nevi and non-dysplastic nevi demonstrate different degrees of risk compared the familial or non-familial melanoma (51-54). Populations with familial melanomas and more atypical naevi are at much higher risk, while the estimation for populations without familial history of melanoma is usually lower.

In general, past studies on host-related risk factors have demonstrated a good degree of standardization, which led to variations in their results. The heterogeneity in the methods of determination used also affected the estimations of risk factors; thus, the assessment of these studies needs further effort in order to increase the accuracy for the prediction. The etiology

of melanoma is complex; thus, researchers are in agreement that environmental and host factors such as phenotype characteristics and naevi or dysplastic naevi counts are inter-related, which may have caused the inconsistencies in the previous studies. The genetic understanding of the formation of melanomas remains incomplete, but further exploration may provide important clues for explaining these risk factors.

#### **5.1.4 Epidemiology of melanoma**

Non-melanoma skin cancers represent 5.8% of cancers from all sites and cause 0.7% of cancer-related deaths; the global estimation for 2018 was approximately 1 million new cases and 65,000 deaths, with most of these cases being related to BCC and SCC; melanomas represent only 1.6% of all new cases but cause 0.6% of all deaths, which are around 60,000 new cases in 2018 (55). Malignant melanomas represent only about 5% of skin cancer diagnoses but account for more than 90% deaths associated with cutaneous tumors (56). Cutaneous melanomas account for more than 90% deaths of all melanoma cases (7, 57) and are considered to be the most rapidly increasing cancer in the white population. Globally, the incidence of melanoma has been increasing alarmingly over the past decades; in particular, the incidence rate of cutaneous melanoma was greater than that of any other malignancy (58). From 1970 to 2000, the incidence rates of melanoma increased approximately threefold in the United States and central Europe (4, 59-61), accompanied by a low level increase in mortality rates.

Because of the genetic backgrounds of various populations and differences in sun exposure correlated to distance from the equator, there is significant geographic variation in the incidences of NMSCs and melanomas globally. The highest rates for NMSCs and melanomas were reported in Australia and New Zealand (at 37 cases per 100,000 people), followed by Northern America and Western Europe; the lowest were in South-Central Asia (55, 62). A major explanation is the different genetic background of populations, as white populations

have the highest incidence rate, while Asian and African populations have significantly lower incidence rates; however, registration system and diagnosis criteria could also affect the validity of these statistics. In Europe, the melanoma incidence rate is less than 10~25 new cases per 100,000 inhabitants; Switzerland has the highest rates and Greece the lowest. According to some studies, there is also a gradient of NMSC and melanoma incidence and mortality from northern to southern and western to eastern Europe (61, 63), which has been suggested as correlating with the distribution of various ethnic groups and the level of development in these countries. In the United States of America, the incidence rate is 20~30 per 100,000 inhabitants; in Australia, the incidence is 50~60 per 100,000 inhabitants, which is the highest incidence recorded. With regard to mortality, Australia and New Zealand have the highest global melanoma mortality rates of around 3.5 per 100,000, while the rates in North America and Europe are 1.7 per 100,000 and 1.5 per 100,000, respectively (64, 65).

The age demographics of melanoma are quite particular when compared with other cancers. Melanomas affect more of the younger population between 20 to 40 years compared with the other cancers which are usually found in the older population up to 60 years. The median age of diagnosis for melanoma is around 57 years, but incidence rates start to increase from 30 years of age; around 50% of melanoma cases involve patients under 55 years of age, while approximately 30% occur among patients younger than 45 years. Incidences in populations under the age of 15 years are rare, but early over-exposure to UV is correlated with incidence in later life. In addition, the types of melanoma diagnosed in populations of different ages also display certain trends: Tumors among younger populations are less thick, while, in older populations, tumors are more often found on body parts that have been subjected to chronic exposure to sunlight and often are acral lentiginous or lentigo maligna types (3, 66). Those age-cohort studies that have attempted to explain these trends in melanoma incidence are

usually population dependent. In addition, the models used are generally difficult to interpret and fully fit to the clinical data on both incidence and mortality (61).

The differences in incidence rates of NMSCs and melanomas between the gender groups are age dependent, and the overall incidence rates for men are two times higher than for women, as are mortality rates. Generally, the incidence of melanoma is higher in female populations under the age of 50, but the incidence in men over 60 years increases sharply. The overall mortality rates are higher for men than for women due to the late presentation of the disease and poor diagnosis in older populations.

In general, epidemiological studies on melanoma have indicated an increasing trend in terms of incidence rates whereas mortality rates remained steady. Treating melanomas and NMSCs may represent a severe burden for healthcare systems in areas of high incidence. Thus, while research on the molecular basis of melanomas is challenging, it has the potential to yield results that are both of scientific and practical.

## **5.2 Calcium signaling in melanoma**

### **5.2.1 Calcium signaling in cancer**

The calcium ions are one of the most important second messenger molecules. They impact many aspects of physiological functions, including muscle contraction, neural signal transmission and immune cell activation. On the cellular level,  $\text{Ca}^{2+}$  ions are involved in the proliferation, migration, apoptosis gene transcription and control of signaling pathways (67). Because of this multi-faceted role played by calcium, the intracellular  $\text{Ca}^{2+}$  concentration is under stringent maintenance which limits the free cytosolic  $\text{Ca}^{2+}$  concentration to approximately 100 nM whereas the extracellular environment has a concentration of approximately 1-2 mM (68). Cytosolic  $\text{Ca}^{2+}$  is mainly controlled by three separate

mechanisms. First, the compartments in the cytosol, such as ER and mitochondria, can take up and release  $\text{Ca}^{2+}$ . Second, the channels and pumps on the plasma membrane, such as the calcium release-activated channels (CRAC) and plasma membrane  $\text{Ca}^{2+}$  ATPases (PMCA), can control the entry and extrusion of  $\text{Ca}^{2+}$ . Finally, cellular proteins such as calmodulin, which have a broad variety of affinities, can chelate  $\text{Ca}^{2+}$ . Thus, the universal mechanism for  $\text{Ca}^{2+}$  signaling is the entry of calcium via the plasma membrane or the release of calcium from intracellular stores. Entry through plasma membrane or release of calcium from stores leads to the elevation of the cytosolic  $\text{Ca}^{2+}$  level and  $\text{Ca}^{2+}$  binding to proteins, which could further activate downstream effectors such as transcription factors and enzymes and lead to physiological changes. In addition, dysfunctions in calcium signaling can cause many pathological states, including cancer. The changes observed in calcium signaling in cancer cells usually include increased stimulated  $\text{Ca}^{2+}$  influx, sustained  $\text{Ca}^{2+}$  oscillations, lower basal  $\text{Ca}^{2+}$  and up-regulated SOCE, all of which can alter cell proliferation, intercellular communication and cell migration and promote resistance to apoptosis and oxidative stress (69-71). The cause of such alterations is often the irregular expressions of key components in the calcium pathways (72), such as PMCA (73-75), STIM (Stromal Interaction Molecule) /ORAI (ORAI Calcium Release-activated Calcium Channel Protein) (76-78) or the transient receptor potential (TRP) channels (79, 80). There are also studies that have suggested that the deregulation of intracellular  $\text{Ca}^{2+}$  stores, mitochondria and ER is responsible for the evasion of apoptosis in cancer cells (81).

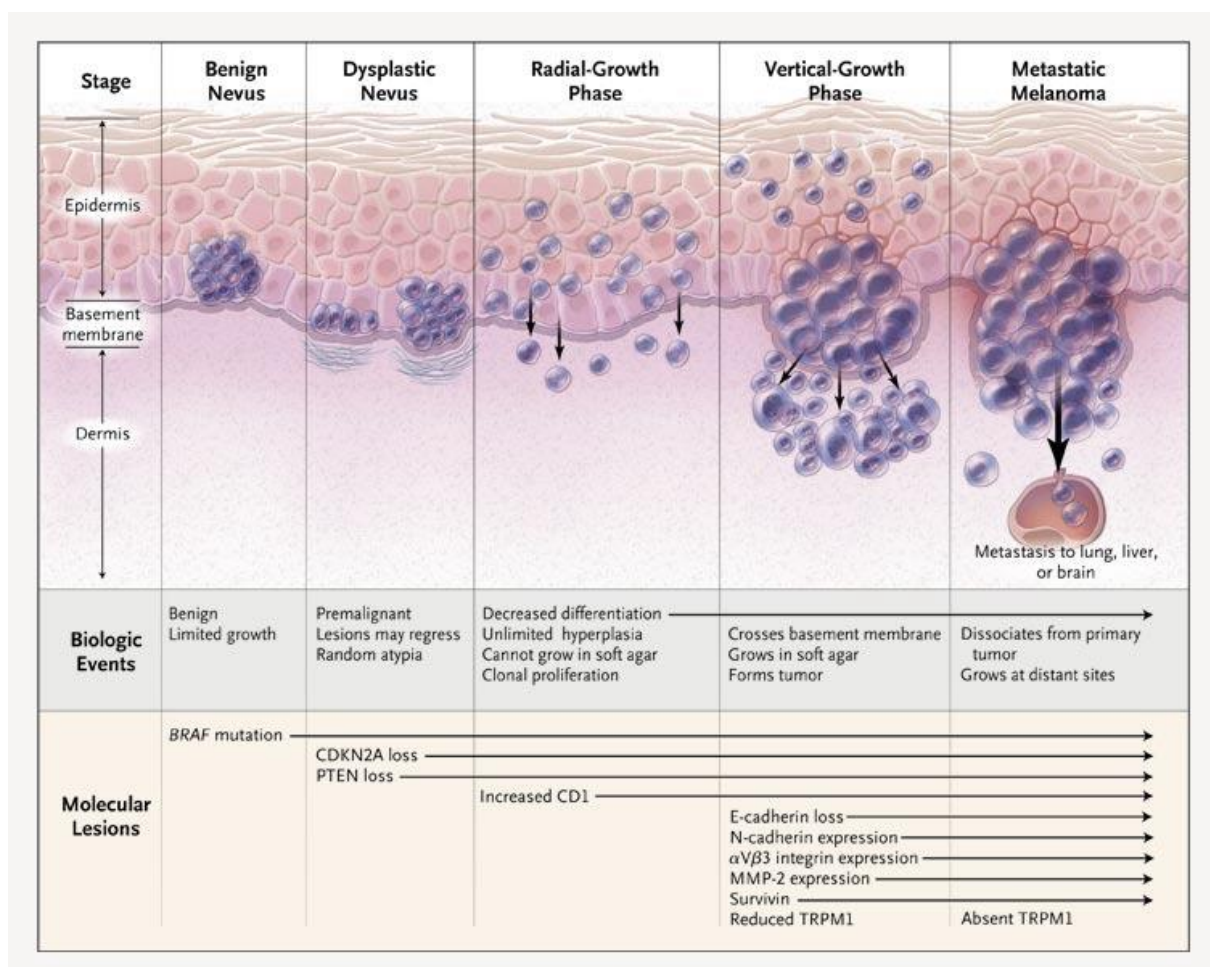
### **5.2.2 The role of calcium signaling in melanoma pathogenesis**

While the involvement of abnormal calcium signaling in melanoma pathology is indisputable as well as for the other malignancies, the key molecular players that affect melanoma pathology and underlying mechanisms remain to be identified in the field of melanoma research. Within the healthy human epidermis, a steep  $\text{Ca}^{2+}$  gradient is maintained. The  $\text{Ca}^{2+}$

level in the basal layer is relatively low, but it progressively increases towards the outer layer. The  $\text{Ca}^{2+}$  level is highest in the stratum granulosum and drops to a minimum in the stratum corneum. The  $\text{Ca}^{2+}$  gradient is determined by the  $\text{Ca}^{2+}$  uptake and release of keratinocytes. This  $\text{Ca}^{2+}$  gradient promotes the sequential differentiation of keratinocytes as they migrate from the bottom to the outer layer of the epidermis to form the impermeable barrier of the skin. Thus, calcium signaling plays an important role in cell adhesion, cell-to-cell communication and the intracellular signaling of keratinocytes. Since keratinocyte differentiation is crucial to the formation of an intact epidermal barrier, the disruption of the epidermal barrier is involved in the development of diseases, including BCC and SSC. In the epidermis, the keratinocytes work with the neighboring melanocytes to produce photo-protective melanin from the unique organelle melanosome, which is found in melanocytes. Through their interactions with keratinocytes, the proliferation, adhesion and migration of melanocytes are controlled (82, 83).

Melanomas derive from the melanocytes or their progenitor cells in the basal layer of the epidermis. The developments of melanomas reflect an interdependence between environmental and host factors; it is a result of causal mutation and the consequent dysregulation of signaling pathways. The Clark model of melanoma progression (depicted in Graph 2) describes the histological features that can be identified during the transformation of normal melanocytes into a malignant melanoma (84). On the molecular level, the concomitant multi-step mutations are critical contributors to this progression. In the first phase of the Clark model, the abnormal proliferation of melanocytes, which is caused by the exclusive somatic mutation of NRAS or BRAF, results in the activation of the ERK-MAPK pathway, leading to the formation of benign nevi. The growth of benign nevi is suppressed by the senescence which is controlled by the expression of INK4A. In the next phase, the melanoma cells acquire the mutation of CDKN2A, PTEN, P53 or MITF amplification (85, 86). The

deactivation of tumor-suppressor genes and increased expression of the oncogene lead to aberrant cell proliferation, DNA repair, susceptibility to cell death and the development of dysplastic nevi from benign nevi. Eventually, the alteration of the wingless-type mammary tumor virus integration-site family (WNT) pathway disrupts the association of E-cadherin and  $\beta$ -catenin. The loss of E-cadherin, the expression of N-cadherin and aberrant  $\alpha$ V $\beta$ 3 integrin further decrease the adhesion of melanoma cells, which leads to the metastasis of the melanoma (87). As a universal second messenger molecule,  $Ca^{2+}$  is involved in many of these signaling pathways. For example, the activation of mitogen-activated protein kinase (MAPK) and WNT can be triggered by a calcium influx (88, 89), and downstream extracellular signal-regulated kinase (ERK) is also regulated by calcium (90). In addition, important downstream transcription factors such as microphthalmia-associated transcription factor (MITF), NF- $\kappa$ B and NFAT are also calcium dependent (91, 92).



**Graph 2: Biologic Events and Molecular Changes in the Progression of Melanoma.**  
(Adapted from Arlo J. Miller and Martin C. Mihm, *N Engl J Med* 2006; 355:51-65.)

Along with its role, the basic questions concerning the involvement of  $\text{Ca}^{2+}$  signaling are as follows: 1) Are there any differences in  $\text{Ca}^{2+}$  signaling between melanocyte and melanoma cells? 2) How does  $\text{Ca}^{2+}$  signaling contribute to the progression of melanoma? 3) Which  $\text{Ca}^{2+}$  signaling pathways are involved? Many efforts have been made to answer these questions in recent decades. In the early 1980s, researchers found that the calcium chelator EGTA, and voltage-gated  $\text{Ca}^{2+}$  channels (CaV), can affect the proliferation and migration of melanoma cells and thus established the first link between  $\text{Ca}^{2+}$  signaling and melanoma (93). However, this did not exclude the possibility of the involvement of other channels (94). Allen and colleagues subsequently characterized the ion channels in four different human melanoma cell lines and concluded that the melanoma cell lines displayed different patterns of ion channel expression, including calcium channels such as CRAC and CaV (95). The transient receptor potential (TRP) channels, especially melastatin 1 (TRPM1), were found to be regulated by the transcription factor MITF in melanocytes and melanoma; TRPM1 has a lower expression in primary melanoma and was originally identified as a metastasis suppressor (96-99). The research on murine melanoma line B16 revealed that the expression of melastatin is inversely correlated to the metastatic potential of these melanoma cells (97, 98). The TRPM channels belong to a superfamily of up to 30 members that can transport  $\text{Ca}^{2+}$ ,  $\text{Mg}^{2+}$  and  $\text{Na}^{2+}$ . In addition to TRPM1, several other family members have been identified as functional in keratinocytes, melanocytes and melanoma. TRPV1, TRPV3, TRPV4 and TRPA1 are involved in the control of keratinocyte differentiation, inflammation response and hair growth (100-102); the TRPA1 and TRPML3 channels have also been found to be functional in melanocytes and melanoma cells (103, 104). To date, TRPM1 is generally agreed as the

channel required for melanin synthesis in melanocytes and cancer marker for the melanoma progression (105).

With regard to cytosolic  $\text{Ca}^{2+}$  homeostasis, the CRAC channels are the determinant factors. The STIM and ORAI isoforms are important regulators in both normal and tumor tissue (106, 107). While there are multiple isoforms of both, namely STIM1, STIM2, ORAI1, ORAI2 and ORAI3, the expression of the isoforms determines the SOCE response in different cells (108), and the amplitude of SOCE is determined by the relative expression of STIM and ORAI in such contexts (109). The first report on SOCE from melanoma cells was based on the findings that sustained SOCE could activate the protein kinase B/Akt signaling pathways, thus control proliferation of B16 melanoma cells, providing apoptosis resistance (110). This study features the mitochondria as the critical buffering pool to SOCE for keeping the ORAI channels open and maintaining robust  $\text{Ca}^{2+}$  entry since the expression of STIM1/ORAI is on the same level in both non-malignant and malignant B16 cells. The STIM and ORAI isoforms were also investigated in primary human melanocytes (111); and the study found that STIM2 and ORAI1 are the predominant isoforms expressed, and that SOCE controls endothelin-1-induced melanin production. This study also indicated that STIM and ORAI could potentially regulate the pigmentation of skin upon UV radiation; they thus play an important role in adaptive tanning, which is protective against skin lesions by UV irradiation. The same authors also examined the contribution of STIM and ORAI in human melanoma cells (112), finding that STIM2/ORAI-controlled SOCE is a critical factor in melanoma phenotype switching. The silencing of STIM2/ORAI1 could increase the MITF expression and proliferation of melanoma cells, but it reduces their potential for migration. Therefore, STIM2/ORAI1 could be pharmacologically targeted to limit the invasion and metastasis of melanoma. Further studies have found that SOCE regulates the proliferation and migration of melanoma via the Extracellular signal-Regulated Kinase (ERK) signaling pathway, which provides the link

between SOCE and MAPK signaling in melanomas (113). Other recent studies have identified different mechanisms with regard to SOCE and melanoma invasion. STIM1/ORAI1-mediated  $\text{Ca}^{2+}$  oscillations have been found to promote melanoma invasion by affecting invadopodium assembly and extracellular matrix (ECM) degradation (114). Finally, Soboloff and colleagues found that WNT5A controls protein kinase C-mediated phosphorylation and SOCE in invasive melanoma, which provides another clue as to the function of STIM/ORAI (115). Taken together, these studies highlight the heterogeneity of SOCE in melanoma, but they all provide important knowledge regarding melanoma proliferation and migration.

In summary, with regard to the role of calcium signaling in melanocytes and melanoma, the findings of previous studies provide important evidence and make it possible to identify interesting implications. However, due to the dynamic nature of calcium signaling and its complexity, additional research is required to fully answer the questions concerning the mechanisms and their potential use in therapeutics.

## **5.3 Redox signaling in melanoma**

### **5.3.1 Redox signaling in cancer**

The reactive oxygen species (ROS) are unstable and bio-reactive species containing oxygen, including superoxide anion ( $\text{O}_2^-$ ), hydrogen peroxide ( $\text{H}_2\text{O}_2$ ) and hydroxyl radicals ( $\text{OH}^\cdot$ ). They were considered as the byproducts from aerobic metabolism from mitochondria in the cells. These molecules have different physical and chemical properties that allow them to react with various biological targets, including lipids, DNA and proteins. Thus, ROS were considered as the damaging factors in cells (116). However, in recent decades, it has become apparent that ROS molecules can also serve as signals for regulating physiological and

pathological processes (117-119). The cysteine residues in the proteins exist in the form of thiolate anion, which is susceptible to oxidation; thus, the reversible oxidation of the thiol group serves as a biological function “switch” and a signal transduction mechanism (120-122).

In cancer cells, the constitutive activation of signaling pathways related to proliferation leads to higher levels of bio-synthesis and energy metabolism. As a consequent of abnormal metabolic activity, cancer cells usually generate more ROS from mitochondria, ER or the NADPH oxidases (123, 124), which leads to a markedly higher intracellular ROS level compared to that of normal cells (70). Therefore, it was proposed that an elevated ROS level causes DNA damage and genomic instability, which could lead to tumorigenesis. In addition, it was found that, in some cancer cells, the ROS are essential for proliferation, migration and survival. The widely accepted explanation of it is that the important signaling pathways in these cell can be activated by ROS molecules (125-128). Furthermore, to control their redox balance, cancers prompt a higher antioxidant activity (129, 130), which could be targeted for therapeutic purposes (131, 132). Thus, there are many drugs that are designed to affect the redox homeostasis or ROS-regulated signaling pathways to either eliminate cancer cells or sensitize them to other therapeutic measures. The main methods used to achieve such ends include 1) artificially inducing the generation of ROS, 2) depleting intracellular antioxidant pools such as GSH and NADPH, 3) inhibiting critical enzymes such as SOD, thioredoxin, NADPH oxidases and 4) manipulating ROS-related signaling pathways.

### **5.3.2 Redox signaling in melanocytes and melanoma**

Due to the complexity of their functions, ROS also play distinct roles in various aspects of melanoma development, including 1) melanomagenesis, 2) melanoma progression and metastasis and 3) therapeutic resistance.

Upon UV exposure, melanocytes produce melanin through a series of chemical reactions based on the precursor L-tyrosine. The end products are either eumelanin or pheomelanin,

which determine skin and eye color. The biosynthesis of pheomelanin requires glutathione; thus, UV-induced production of pheomelanin may compete with the antioxidant system for GSH and cause oxidative stress. Furthermore, under normal physiological condition, melanin protects the skin from UV and oxidative stress (133), but, in the presence of iron, pheomelanin and the intermediate product S-cystainyldopa can also serve as prooxidants in melanoma cells. The oxidized melanin can react with O<sub>2</sub> to form H<sub>2</sub>O<sub>2</sub> and other radicals; therefore, the synthesis of melanin can produce ROS and disturb homeostasis, and this likely contributes to oxidative stress-induced genome instability and the malignant transformation. Another source of ROS in melanocytes is UV-radiation-induced inflammation; phagocytic cells can produce both ROS and reactive nitrogen species (RNS) from the respiratory burst, and phagocytes can invade the tissue and release H<sub>2</sub>O<sub>2</sub>. Despite its potential to cause inflammation and DNA damage, UV radiation can result in an impaired antioxidant defense. According to some studies, UV radiation suppresses the enzymatic activity of catalase, glutathione reductase and SOD in skin cells (134-136). It has been reported that UVA radiation upregulates the expression of thioredoxin-interacting protein which inhibits the scavenging activity of thioredoxin and promotes melanoma intravasation (137). Thus, by weakening antioxidants, UV radiation can also cause an elevation of intracellular ROS level. To eliminate the detrimental effect of UV exposure and the bio-synthesis of melanin, cells require a more active antioxidant system; however, this, in turn, could also enhance cell's resistance to apoptosis and lead to a high stress tolerance, which could cause neoplastic transformation (138, 139). To eliminate the elevated ROS, cells of melanocytic origin have a higher antioxidant capacity when compared with keratinocytes (140). In primary melanomas, the expression of SOD and catalase is higher than in the normal skin and nevi (141, 142), which contributes to the resistance against internal oxidative stress. The third source of ROS involved in melanoma formation is related to the abnormal mitochondrial metabolic activity; in a fraction of melanoma cells, the oxidative phosphorylation (OXPHOS) is upregulated.

High level of mitochondrial respiration leads to excessive ROS generation, while drug resistance is also increased (143).

With regard to the progression of melanoma, ROS mainly serve as the signaling molecules influencing the major pathways for the regulation of proliferation, metastasis, angiogenesis, immune escape, microenvironment manipulation and stress resistance (140, 144). The constitutively activated MAPK signaling in melanomas via mutated BRAF is a key modulator of melanoma initiation and progression; furthermore, it can regulate ROS production and coordinate with P53 to suppress apoptosis (145). The downstream serine/threonine kinase Akt activated via MAPK signaling can decrease the activity of phosphatase and tensin homolog (PTEN), which results in the attenuation of the antioxidant network in a melanoma (146). Furthermore, it has been found that Akt can induce the expression of NOX4 in a melanoma and that the produced ROS contribute to metastasis (147).

As mentioned previously, the NF- $\kappa$ B signaling pathway is critical for cell survival and apoptosis control. In melanoma, anomalous NF- $\kappa$ B signaling has been found to be related to the intracellular H<sub>2</sub>O<sub>2</sub>, and the recruitment of co-activator AP-1 is correlated to the intracellular O<sub>2</sub><sup>-</sup>. Together the activation of this pathway contributes to increased apoptosis resistance in melanomas (148). In addition, ROS generated by NAD(P)H oxidase (NOX) can also activate the NF- $\kappa$ B to enhance the proliferation of melanomas (149). The chemokines produced by the activation of NF- $\kappa$ B can also lead to the autonomous growth and invasion of melanoma cells by autocrine and paracrine signals. AP-1 regulates the expression of matrix metalloproteinases (MMPs) 1 and 2 (150, 151); thus, together, the activation of NF- $\kappa$ B and AP-1 by ROS could contribute to melanoma progression by enhancing the potential for migration and invasion of melanomas.

Since ROS generation is higher in melanoma cells and they utilize an upregulated antioxidant system to control the redox balance, common strategies for targeted therapy are to induce

additional ROS generation or to inhibit the antioxidants with drugs. Buthionine sulfoximine (BSO), disulfiram (DSF) and 2-methoxyestradiol (2-ME<sub>2</sub>) were used in preclinical models to inhibit the endogenous antioxidants in melanoma (152-155). Both BSO and DSF have been used to manipulate the GSH pool, while DSF can also generate O<sub>2</sub><sup>-</sup> and induce apoptosis. 2-ME<sub>2</sub> was tested in a mouse model for inhibiting SOD activity (156). It was found to have a strong anti-angiogenic effect, which leads to the inhibition of tumor growth in melanomas (157). In a study on metabolic activity in melanoma subpopulations, it was found that blocking mitochondrial respiration and inducing mitochondrial oxidative stress can overcome the drug resistance of melanoma cells (143, 158). Chemotherapy, radiotherapy and immunotherapy, while not directly intended to disturb the redox state of cells, as well as therapy-induced apoptosis and other effects also promote ROS generation (159, 160).

## **5.4 Mitochondria in melanoma: Liaison between metabolism and signaling**

### **5.4.1 Mitochondria as the hub of calcium and redox signaling**

Mitochondria have become a focal point in biomedical research field in recent decades due to their critical role in both signaling and metabolism. Mitochondrial abnormalities are found to be involved in numerous pathologies, including cardiovascular disorders, neurodegenerative disorders, diabetes and cancer (161). These findings emphasize the importance of the precise regulation of mitochondrial calcium and ROS.

As the main bioenergetic organelles, mitochondria produce ATP through the OXPHOS of the substrate, which is essentially a process of electron transfer via the respiratory electron transfer chain complexes to O<sub>2</sub>. This electron transfer is also coupled to the export of protons, which drive ATP synthesis from complex V. However, the electron transfer is not completely efficient. Electrons may escape from the transporters and react with nearby O<sub>2</sub> which leads to

generation of ROS molecules (162, 163).  $\text{Ca}^{2+}$  plays an important role in OXPHOS by activating key enzymes such as isocitrate dehydrogenase, pyruvate dehydrogenase and ketoglutarate dehydrogenase (164, 165). Therefore,  $\text{Ca}^{2+}$  is taken up through the mitochondrial calcium uniporter (MCU) at the expense of mitochondrial membrane potential (166). As a consequence, mitochondrial ATP production and ROS generation are connected to mitochondrial calcium uptake; mitochondrial calcium uptake stimulates respiratory activity and ROS production, but the ROS in turn regulate MCU activity by oxidizing the active cysteine residues in the MCU complex and its regulators (167). Such  $\text{Ca}^{2+}$ -induced ROS generation is dependent on respiratory activity. Complexes I and III have been found to be the major sources of ROS, and the primary ROS molecules are very often  $\text{H}_2\text{O}_2$  and  $\text{O}_2^-$  (168-170). Mitochondrial  $\text{Ca}^{2+}$ -sensitive  $\text{K}^+$  has been identified to be another crosstalk pathway for  $\text{Ca}^{2+}$  and ROS; calcium-induced  $\text{K}^+$  influx to mitochondrial matrix can lead to alkalinization and ROS generation (171). Intrinsically, ROS can also regulate the activity of mitochondrial enzymes such as succinate dehydrogenase,  $\alpha$ -ketoglutarate dehydrogenase and aconitase to limit the respiration rate, perhaps as a feedback mechanism (172). In addition,  $\text{Ca}^{2+}$  also induces NO generation, which can inhibit ETC complexes and produce ROS (173, 174). Since mitochondrial calcium uptake can buffer the  $\text{Ca}^{2+}$  increase in the surrounding cytosol, the mitochondria are crucial players in the feedback and shaping of global  $\text{Ca}^{2+}$  signals (175, 176). Hence, the mitochondrial redox status is also influenced by global  $\text{Ca}^{2+}$  signaling. The mitochondria are very dynamic organelles whose structure, distribution and mobilization can be adjusted in response to energy requirements or signaling transduction (177). Thus, in a large background, the rearrangement of mitochondria could facilitate crosstalk between mitochondrial  $\text{Ca}^{2+}$ /ROS and inter-organelle communication (178-182).

The other function of mitochondria is sensing intracellular stress and inducing the apoptosis. Mitochondrial calcium overload can trigger the opening of permeability transition pores

(PTPs) on the out mitochondrial membrane (OMM) to initiate apoptosis. While the critical thiol oxidation of the PTPs serves as another sensing mechanism, the opening of PTPs could increase mitochondrial ROS production through the respiratory chain complexes (183, 184). Therefore, the inter-dependence between mitochondrial  $\text{Ca}^{2+}$  and ROS could be important for the regulation of stress-induced apoptosis.

#### **5.4.2 The mitochondrial function in melanoma**

As mentioned previously, the mitochondria integrate metabolic activities,  $\text{Ca}^{2+}$  signaling and redox signaling to regulate various aspects of physiological function in both healthy and cancerous cells. When it comes to melanoma research, mitochondria are studied in terms of the role they play in abnormal metabolic activity and their involvement in those signaling pathways that promote aggressive behavior in the hope of developing therapeutic strategies.

The metabolic shift between glycolysis and respiration depends on the availability of substrates and oxygen in normal cells. The shift of metabolic activity towards glycolysis in cancer cells under normoxia was termed Warburg effect, which is a hallmark of cancer (185). Studies focused on cell viability and intracellular ATP levels have suggested that melanocytes are more sensitive to the inhibition of mitochondrial respiration, while, in contrast, melanoma cells are more sensitive to the inhibition of glycolysis (186, 187). Further analyses of the metabolites of melanocytes and melanoma cells also indicate that glycolysis is more active in melanoma cells (188), although mitochondrial respiration occurs even under hypoxia. However, in some cell lines or in certain subpopulations of melanoma, mitochondrial respiration is upregulated, which suggests the existence of a switching mechanism that allows melanoma cells to adapt to the microenvironment (189).

The heterogeneity of melanoma metabolism is likely caused by the complexity of the driver signaling pathways during carcinogenesis and progression, which result in metabolic reprogramming to suffice the need for energy of cancer cells (190). The predominant

oncogenic mutation in melanoma, BRAF V600E, causes constant activation of the MAPK pathway through the BRAF-MEK-ERK axis. It has been reported that the inhibition of BRAF also causes downregulation of glycolytic enzymes and glucose transporters (186, 191), which correlates with the results obtained from studies on inhibition of ERK activation, suppression of downstream transcription factor hypoxia-inducible factor 1 $\alpha$  (HIF1 $\alpha$ ) and v-Myc avian myelocytomatosis viral oncogene homolog (MYC) (191). Furthermore, a recent study found that the inhibition of BRAF can force melanoma cells to switch to mitochondrial respiration and that BRAF suppresses PGC1 $\alpha$  via the downregulation of MITF (192, 193). This evidence suggests that the BRAF mutation can suppress OXPHOS and enhance glycolysis, both are possibly important for the malignant transformation of melanocytes, as the BRAF mutation occurs during the early stages of melanoma. However, mitochondrial respiration has been reported to be elevated in metastatic melanoma cells (194, 195) and in subpopulations of melanoma cells with characteristics such as slow-cycling and/or drug resistant (158, 189). Thus, plausible predictions are that elevated glycolysis is the metabolic feature of malignant transformation and it supports rapid proliferation in primary melanoma but that high-level mitochondrial respiration benefits the progression and survival of melanoma.

## **5.5 ER-mitochondria contacts in melanoma**

The ER is the largest membrane-bound organelle, and is involved in various cellular functions, including protein synthesis and Ca<sup>2+</sup> storage. Through electron microscopy, it was discovered that ER can form contact sites with organelles including mitochondria, Golgi complexes, peroxisomes, endosomes, lysosomes, lipid droplets and plasma membranes (196, 197). Among all of these contact sites, the ER-to-mitochondria contact sites are the most important and well characterized (198). They are defined as the regions where the membranes of two organelles are closely tethered by membrane proteins without any fusion or direct connection

(199, 200). The ER membrane at the contact sites is named the mitochondrial-associated ER membrane (MAM), which has been found to be a specialized membrane domain. The tethered network has a very dynamic structure that responds to different stimuli (201, 202). The length of ER-to-mitochondrial contacts has been measured at 10~30 nM (198). This proximity facilitates crosstalk between ER and mitochondrial functions, the majority of which is still not fully understood. To date, several main functions of the contact sites have been well characterized: inter-organelle lipid exchange; the regulation of mitochondrial biogenesis, mitochondrial dynamics and inheritance; coordinating  $\text{Ca}^{2+}$  transfer; and mediating stress response (203, 204). These functions are intertwined and form an integrated communication system between two organelles.

The role played by the ER-to-mitochondria contact sites and MAM in cancer and in melanomas in particular has not been fully investigated, although there is evidence that indicates their importance. For example, the MAM can function as a specialized “docking site” for signaling molecules to facilitate the regulation of nearby components from critical signal pathways. The promyelocytic leukemia protein (PML) located in the MAM could modulate the IP3R-Akt signaling pathway to control apoptosis (205) and determine cancer cell fate (206). The PTEN can also regulate the Inositol trisphosphate receptor-AKT Serine/Threonine Kinase (IP3R-Akt) signaling pathway after being recruited to the MAM. IP3R activation is an important event in determining ER  $\text{Ca}^{2+}$  release, which, as mentioned previously, initiates the SOCE response and ER-to-mitochondria calcium transfer. Thus, these studies imply that the ER-to-mitochondria contact sites could be the hotspots for controlling IP3R and  $\text{Ca}^{2+}$  signaling event, which governs many aspects of melanoma cellular function. Furthermore, the upstream activator of Akt, the target of rapamycin complex 2 (mTOR2), has been found to be recruited to the MAM by the stimulation of growth factor (207). mTOR is a crucial sensor for nutrient availability and metabolism control. Its activation in cancer cells leads to a

dependence on mitochondrial bioenergetics (208). Based on these studies, another clue could be the ER to mitochondria contact sites are possibly the fundamental structure for the “metabolism switching” in melanoma cells.

Another important role of ER-to-mitochondria contact sites concerns the mediation of stress response. ER stress is a complex signaling event triggered by the accumulation of unfolded proteins or the dramatic disruption of the ER homeostasis. During the ER stress response, the ER morphology changes, and the contact sites are strengthened to adapt to the stress; mitochondria have been found to relocate towards the perinuclear ER, perhaps to provide the ATP for the response (209). If the stress is severe enough to cause cell death, apoptosis will be activated to eliminate the cells. There are studies that have demonstrated that, during this phase, the docking proteins can prompt apoptosis by inducing ER-to-mitochondria  $\text{Ca}^{2+}$  transfer, which leads to mitochondrial calcium overload (210, 211). Melanoma cells are extremely resistant to therapies due to the suppression of apoptosis, particularly at advanced stages (212, 213). By overexpression of suppressive genes, activating survival pathways or inactivation of pro-apoptosis pathways, they acquired the resistance (214). Therefore, some drugs that target BRAF-mutated melanoma cells are intended to induce apoptosis via ER stress (215) or to exploit the possibility of increasing apoptosis to overcome drug resistance (216-218). However, in this context, the influence of contact sites has rarely been investigated, thus there still remain many possibilities to investigate in terms of the manipulating of contact sites to sensitize melanoma cells for these drugs.

## **5.6 The TMXs emerged from a genomic-wide screen for NFAT activation**

In 2013, Sonia Sharma *et al.* published a work on a genome-wide siRNA screen for NFAT1 activation (219), in which the authors attempted to identify novel regulators of STIM and ORAI channels. They used thapsigargin to maximally activate the SOCE in HeLa cells and

recorded the translocation of GFP-tagged NFAT1 as a readout. Among all the hits, the authors identified septins, which reorganize the plasma membrane domains and thus facilitate STIM1-ORAI1 communication, as novel coordinators of SOCE. It. Notably, a set of thioredoxin-related transmembrane protein TMX1, TMX3 and Thioredoxin Domain Containing 15 (TXNDC15) showed relatively high level of inhibition of NFAT1 activation after siRNA-guided knockdown in HeLa cells, which indicates their possible involvement in the cytosolic Ca<sup>2+</sup> handling.

### **5.6.1 Thioredoxin-related transmembrane protein: What is known**

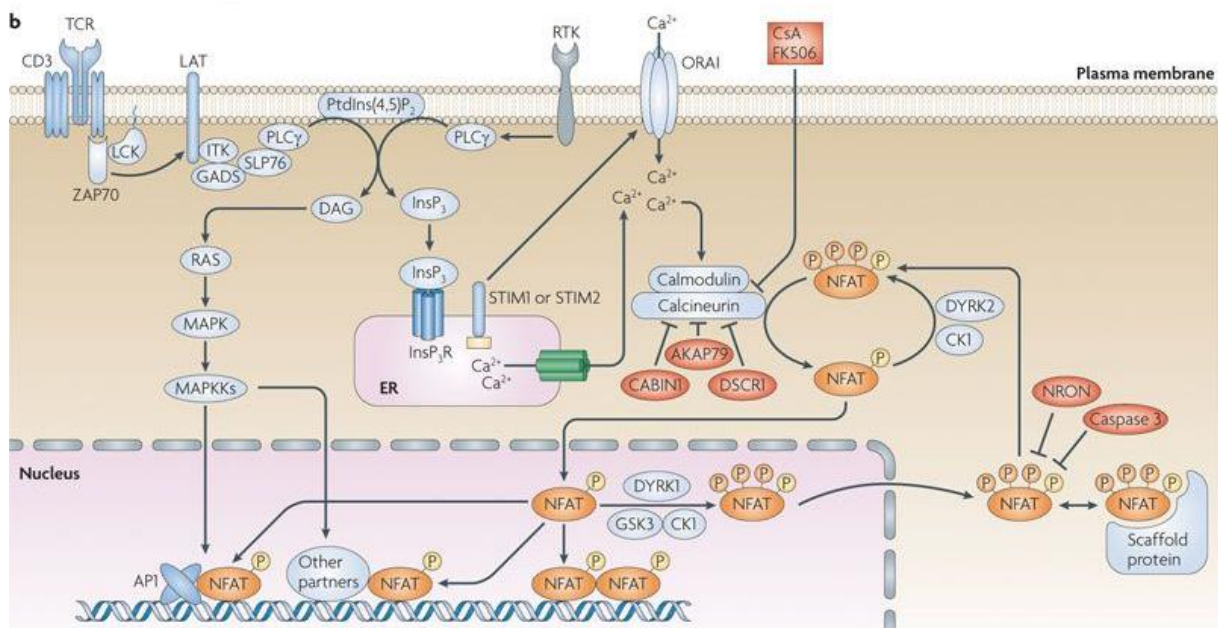
To date, four members of the TMX family have been identified. All of them possess a thioredoxin (Trx)-like domain with an active site sequence containing conserved cysteine residues, an N-terminal signal peptide and a transmembrane domain; thus, they are categorized as members of the thioredoxin (Trx) superfamily. The cellular localization of TMX proteins is distinct, but most characterizations have indicated that TMX1 (220), TMX2 (221), TMX3 (222) and TMX4 (223) are predominantly expressed in the ER, partially on the related membrane structures. The first ER residing Trx to be identified was the protein disulfide isomerase (PDI), so the TMX proteins are also referred to as the members of the PDI family due to their similarity in structure and function. The typical PDI proteins contain four domains, a, b, b' and a', which are homologous to the cytosolic thioredoxin. The catalytic domains a and a' contain tetrapeptide C-X-X-C active site sequences for disulfide bond exchange reactions, while the b domain is responsible for the interaction between enzyme and substrate proteins. The catalytic site in PDI is capable of both oxidation and reduction; thus, it can oxidize the substrate to reduce the active cysteine residues. In turn, the catalytic site can be oxidized by ER oxidase 1 (Ero1), and the electrons are ultimately transferred to molecular oxygen, which leads to the generation of H<sub>2</sub>O<sub>2</sub> (224, 225).

Functional studies on TMX proteins are relatively scarce, and these proteins' interaction partners and substrate proteins are largely unknown. TMX1 has been identified as a transforming growth factor- $\beta$ -responsive gene in the human adenocarcinoma cell line; when expressed in HEK293 cells, it suppresses brefeldin A-induced apoptosis, which leads to the conclusion that it may help to relieve ER stress through reversible oxidation of the active site (220, 226). Later, it was found that TMX1 is enriched in the MAM (227) and that it controls the reprogramming of the metabolism by modulating the ER-mitochondrial  $\text{Ca}^{2+}$  flux (228). Notably, from the result in the study mentioned above, TMX3 is also partially localized to the MAM, which indicates a possible role in regulating MAM homeostasis. However, the early study only revealed that TMX3 has an active site motif as C-G-H-C, which might be a substrate for Ero1 or an unidentified oxidase, but, intriguingly, during the unfolded protein response, TMX3 expression is not upregulated (222). Based on the literature, TMX1 and TMX3 share several features of particular interest: First, they share the same active site motif involved in disulfide bond formation and may be involved in ER oxidative stress regulation; second, they are all localized in the MAM, which is important for mitochondrial function modulation; and, third, their involvement in cytosolic  $\text{Ca}^{2+}$  has never been reported or studied.

### **5.6.2 NFAT signaling in melanoma**

The nuclear factor of activated T cells (NFAT) has been identified in nuclear extracts from activated T-cells, which binds to the interleukin-2 promoter (229, 230). It contains a cytosolic component which is regulated by phosphorylation via phosphatase calcineurin and nuclear GSK3 kinases, a nuclear co-activator activator protein 1 (AP1) and several other partners that are regulated by the RAS-MAPK signaling pathways (depicted in Graph 3). Originally, the NFAT1 was found to regulate T cell activation and differentiation, but it was later found to also be important in dendritic cells, B cells and megakaryocytes. In total, five family members have been identified thus far, but only four of them are regulated by cytosolic  $\text{Ca}^{2+}$  signaling,

which is the canonical pathway that has been extensively investigated and hence used frequently for screens. The primordial family member, NFAT5, is only activated by osmotic pressure stress. The members of the NFAT family play a crucial role in the development of many tissues, including skin (231), and the dysregulations of them are often involved in the development of cancer (232). The mutation of NFAT proteins is rare and not associated with cancer, but their overexpression and hyperactivity are involved in cancer progression and metastasis in lymphoma, breast cancer, prostate cancer, pancreatic cancer, T-cell acute lymphoblastic leukaemia (T-ALL), endometrial cancer and melanoma (233). This overview of previous studies indicates that the NFAT proteins can influence cell proliferation, migration and angiogenesis, as well as the immune response of cancer cells.



Nature Reviews | Immunology

**Graph 3: The Ca<sup>2+</sup>-NFAT Signaling Pathway.** (Adapted from Martin R. Müller and Anjana Rao, *Nat Rev Immunol* 2010;10:645-656.)

The regulation of NFAT proteins is a very complicated network that includes Ca<sup>2+</sup> signaling, phosphatases and kinases, various co-activators and an import and export system of the nucleus; thus, the mechanisms in the skin and melanomas are varied and not fully understood.

It has been suggested that the UV irradiation-induced calcium influx in the skin tissue can activate NFAT and contribute to the proliferation of keratinocytes (234, 235), but it also causes upregulation of COX-2, which is a proinflammatory, anti-apoptotic and pro-carcinogenic factor (236). In contrast, further studies have found that Notch 1 and NFAT pathways together control the growth and differentiation of keratinocytes and that the loss of Notch 1 can lead to lower-level NFAT signaling, which may cause keratinocyte tumor development (235, 237). The use of immunosuppressant cyclosporine A (CsA), which inhibits the phosphorylation of NFAT by calcineurin for organ transplants in patients, has been found to increase the risk of cancers by suppression of the immune system. (238).

The studies conducted over the past decade have indicated that NFAT signaling is involved in the proliferation, metastasis and apoptosis resistance of melanoma. Flockhart and colleagues found that, in metastatic melanomas, oncogenic BRAF V600E can activate NFAT2 and NFAT4, which leads to the expression of COX-2 and a poor prognosis (239). This work provided the first evidence that the NFAT signaling pathway is involved in major mutation events; however, this conclusion was based on a comparison between primary melanocytes and three BRAF mutation-positive cell lines, which meant that other melanoma cases were not considered. A later study found that permanently activated NFAT2 inhibits apoptosis in melanoma (240). More recent studies have found that NFAT1 promotes tumor growth and metastasis by increasing interleukin-8 and MMP3 expression; in addition, the expression of NFAT1 has been found to be inversely correlated with MITF expression in melanomas, which suggests that NFAT1 can promote melanoma dedifferentiation and immune escape (241, 242). Notably, as an alternative co-activator of NFAT proteins, FOXP3 expression is also related to the proliferation, apoptosis and modifying of the tumor environment in melanomas, which might be attributed to the NFAT pathway; however, due to the different models used in these studies, a more comprehensive overview is required (243-245). Finally, the inhibitor of

calcineurin CsA can also inhibit proliferation and induce apoptosis in melanoma cells (246, 247), but, due to the complexity of the signaling pathways in which calcineurin is involved, it is not clear if NFAT proteins are also responsible in this case.

## **5.7 Research focus and questions for the investigation**

As mentioned previously, the mitochondria are dynamic organelles that integrate  $\text{Ca}^{2+}$  signaling, redox regulation and bioenergetics to control important functions such as proliferation, migration and apoptosis in both normal and cancerous cells. As the communicative junction, the ER-mitochondria contact site is crucial for the integrated signal transduction, but a comprehensive understanding of the underlying mechanism in the context of melanoma pathogenesis and therapeutics is required. Previous studies on TMX1 and TMX3 have indicated their localization in the contact site and roles in controlling of cell metabolism in melanoma; however, the single cell-based model leaves many questions unanswered. Furthermore, TMX1 and TMX3 have been found to be the regulators of the NFAT1 signaling pathway, which plays important roles in many aspects of melanomas, but the mechanism behind this link was yet to be revealed.

## 6 Materials and Methods

### 6.1 Materials

#### 6.1.1 Chemicals

The chemicals, fluorescent dyes and other reagents used for this study are listed below. The chemicals for general use in the laboratory were purchased from Sigma-Aldrich (Darmstadt, Germany) if not included in the list.

**Table 1: Chemicals**

<b>Chemical</b>	<b>Supplier</b>	<b>Catalog-/Order-Number</b>
2-Mercaptoethanol	Sigma	M6250
Antimycin A	Sigma	A8674
Acrylamide-Bisacrylamide	Sigma	A2792
Accutase	Sigma	A6964
Agarose	Sigma	A9539
Bovine Serum Albumin	Sigma	A2153
Ammonium chloride (NH <sub>4</sub> Cl)	Sigma	A9434
Ammonium persulfate	Sigma	A3678
1,2-Bis(2-Aminophenoxy)ethane-N,N,N',N'-tetraacetic acid (BAPTA)	Sigma	A4926
Calcium chloride solution (CaCl <sub>2</sub> )	Sigma	21115
CellMask™ Green	ThermoFisher	C37608
Chloroform (99 %)	Sigma	C2432
Protease Inhibitor Cocktail	Roche	05892970001
Diethylpyrocarbonate (DEPC)	Sigma	D5758
Dimethylsulfoxide (DMSO)	Sigma	D2650
DTT	Sigma	D9779
Ethanol	Sigma	48075
Ethylenediaminetetraacetic acid	Sigma	E9884
EGTA	Sigma	E4378
FCCP	Sigma	C2920
Fetal bovine serum	Invitrogen/Gibco	10500064
Fura-2 AM	Invitrogen	F1221
FuGENE® HD	Promega	E2312
GKT137831	Cayman Chemical	17764
Glucose	Merck	108337
Glycine	Appllichem	A1067
Glycogen	Sigma	G1767
H <sub>2</sub> O <sub>2</sub> (10M)	Sigma	H1009
HEPES	Sigma	H7523
Insulin solution (human)	Sigma	I9278
Ionomycin	Sigma	I9657
Isopropanol	Sigma	W292907
M2 medium	Sigma	M7167

Magnesium chloride solution (MgCl <sub>2</sub> )	Sigma	M1028
Methanol	Sigma	322415
MitoTracker™ Deep Red FM	ThermoFisher	M22426
MitoTEMPO	Biomol	Cay16621
N-Acetyl-L-cysteine	Sigma	A9165
N,N,N',N'-Tetramethylethylenediamin (TEMED)	Sigma	T9281
NP-40	Sigma	73485
Oligomycin A	Sigma	75351
PEG-catalase	Sigma	C4963
Poly-L-ornithine hydrobromide	Sigma	P3655
Potassium bicarbonate (KHCO <sub>3</sub> )	Sigma	12602
Potassium chloride (KCl)	Sigma	P9333
Puromycin	VWR	540222-25
Rotenone	Sigma	R8875
Sodium chloride (NaCl)	Sigma	S7653
Sodium dodecyl sulphate (SDS)	Sigma	L3771
Streptavidin Peroxidase	Calbiochem	189733
Thapsigargin (Tg)	Invitrogen™	T7458
Trizma® hydrochloride	Sigma	T5941
Trizma® base	Sigma	T1503
Triton™ X-100	Sigma	X100
TRIzol® Reagent	Invitrogen™	15596026
TWEEN® 20	Sigma	93773

### 6.1.2 Solutions and Culture Media

The solutions, buffers and media in the following list were used for assays or cell culture according to the manufacturer's instructions.

**Table 2: Solutions and Culture Media**

Item	Supplier	Catalog-/Order-Number
Dulbecco's Phosphate Buffered Saline (DPBS)	Invitrogen/Gibco	14190094
L15 Leibovitz liquid medium	Merck/Biochrom	F 1315
MCDB 153 basal medium	Merck/Biochrom	F 8105
RPMI 1640 L-Glutamine+ Medium	Invitrogen/Gibco	21875-034
MEM-Medium + L-Glutamine	Invitrogen/Gibco	31095-029
Dulbecco's Modified Eagle Medium	Invitrogen/Gibco	11965-084
Opti-MEM™	Invitrogen/Gibco	31985070
Ringer's buffer	Home-made	-

### 6.1.3 Solutions and buffer recipes

The recipes for the home-made solutions are provided below. Unless indicated otherwise, these standard recipes were used for all experiments including calcium imaging and live-cell imaging.

**Table 3: Recipes for home-made solutions**

<b>Solution</b>	<b>Composition</b>
Ringer's solution (0mM Ca <sup>2+</sup> )	NaCl 145mM KCl 4mM Glucose 10mM MgCl <sub>2</sub> 2mM HEPES pH 7.4 10mM EGTA 1mM
Ringer's solution (0.25mM Ca <sup>2+</sup> )	NaCl 145mM KCl 4mM Glucose 10mM MgCl <sub>2</sub> 2mM HEPES pH 7.4 10mM EGTA 1mM CaCl <sub>2</sub> 0.25mM
Ringer's solution (0.5mM Ca <sup>2+</sup> )	NaCl 145mM KCl 4mM Glucose 10mM MgCl <sub>2</sub> 2mM HEPES pH 7.4 10mM EGTA 1mM CaCl <sub>2</sub> 0.5mM
Ringer's solution (1mM Ca <sup>2+</sup> )	NaCl 145mM KCl 4mM Glucose 10mM MgCl <sub>2</sub> 2mM HEPES pH 7.4 10mM EGTA 1mM CaCl <sub>2</sub> 1mM
Ringer's solution (2mM Ca <sup>2+</sup> )	NaCl 145mM KCl 4mM Glucose 10mM MgCl <sub>2</sub> 2mM HEPES pH 7.4 10mM EGTA 1mM CaCl <sub>2</sub> 2mM
Ringer's solution (10mM Ca <sup>2+</sup> )	NaCl 145mM KCl 4mM Glucose 10mM MgCl <sub>2</sub> 2mM HEPES pH 7.4 10mM

2% TU medium	EGTA 1mM CaCl <sub>2</sub> 10mM MCDB153 (80% of total volume) Leibovitz-15 Medium (20% of total volume) 2% FCS 1,68mM CaCl <sub>2</sub> (1,68mM) 2.5ng/ml Insulin
TGH lysis buffer (100mL)	1% Triton X-100 (10mL of 10% stock) 10% Glycerol (20mL of 50% stock) 5M NaCL 1ml 50mM 1M HEPES 5ml 50mM 200mM EGTA 0.5ml 1mM 1% sodium deoxycholate (10ml of 1% stock) dH <sub>2</sub> O 53.5ml

### 6.1.4 Primers for PCR

The primers used for qPCR experiments are listed below (From 5' to 3').

**Table 4: Primers for PCR**

Transcript	Forward	Reverse
TMX1	AGTCCTGGTGCTGTTGCTTT	TTCTCCCCATTCAGCAAAC
TMX3	TTGCTATGGATGGCTTCCTC	TGGGACTGTCAATTCATCCA
NFAT1	AAACTCGGCTCCAGAATCCA	TGGACTCTGGGATGTGAACT
NFAT2	GCTATGCATCCTCCAACGTC	AGTTGGACTCGTAGGAGGAG
NFAT3	ACACAGCCCTATCTTCAGGA	ATCTTGCCTGTGATACGGTG
NFAT4	ACCCTTTACCTGGAGCAAAC	CTTGCAGTAGCGACTGTCTT
NFAT5	CGTGTGTGTGGCTTCTATGT	TGCCTCTCAATCAGAGAGAG
XBPI	CACCTGAGCCCCGAGGAG	TTAGTTCATTAATGGCTTCCAGC
TBP	CGGAGAGTTCTGGGATTGT	GGTTCGTGGCTCTCTTATC

### 6.1.5 siRNA and shRNA

The siRNA and shRNA were used for the knockdown of target gene expression, the sequences are provided in Table 5. The scrambled control siRNA was purchased from the same supplier accordingly. For shRNA experiments, the pLKO.1 empty vector was used as the control. The design, synthesis, sequencing and quality check were all done by the manufacturers.

**Table 5: siRNA and shRNA**

Item	Sequence	Supplier	Catalog /Order Number
siTMX1	5'-GAGAAGAUCUUGAGGUUA A dTdT-3'	MicroSynth	481616
siTMX3	5'-GGAGUUCGAGGUUAUCCAA dTdT-3'	MicroSynth	2920934
siNFAT1	5'-CUGAUGAGCGGAUCCUUA A dTdT-3'	Sigma	SASI_H s01_001 95473
shTMX1_1	5'- CCGGCGTGCCAAGCAATAAGATTTACTCGAGT AAATCTTATTGCTTGGCACGTTTTTTG-3'	Sigma	TRCN0 0001502 91
shTMX1_2	5'- CCGGGCTGAAAGTAAAGAAGGAACACTCGAG TGTCCTTCTTACTTTCAGCTTTTTG-3'	Sigma	TRCN0 0003385 83

### 6.1.6 Primary Antibodies

The primary antibodies used for western blot analyses and immunohistochemistry are listed below.

**Table 6: Primary Antibodies**

Target	Supplier	Catalog-/Order-Number
TMX1	Abcam	Ab37876
TMX3	Provided by Prof. Lars Ellgaard (Copenhagen, Denmark)	/
GAPDH	Cell Signaling Technology	#2118L
BiP and PDI	Provided by Prof. Dr. Richard Zimmermann (Homburg, Germany)	/
NFAT1	Cell Signaling Technology	#5861S

### 6.1.7 Assay kits

Commercially available kits were used for specific assays and procedure. Any supplementary components were made following manufacturer's recommendations.

**Table 7: Commercially Available Kits**

Item	Supplier	Catalog-/Order-Number
Amaya Nucleofector™ Kits for Human Melanocytes (NHEM-neo)	LONZA	VPD-1003

Amaxa P2 Primary Cell 4D-Nucleofector®	LONZA	V4XP-2024
Amaxa SF Cell Line 4D-Nucleofector®	LONZA	V4XC-2024
Calcineurin cellular activity assay kit	ENZO	BML-AK816-0001
CellTiter-Blue®	Promega	G8081
Complete Proteinase-Inhibitor cocktail	Roche	05892791001
HTS Transwell®-24 well permeable support	Corning®	3422
HTS Transwell®-96 well permeable support	Corning®	3374
Human IL-8/CXCL8 DuoSet ELISA	R&D systems	DY208
HiSpeed Plasmid Maxi Kit	Qiagen	12662
Pierce™ BCA Protein Assay Kit	ThermoFisher	23225
QuantiTect SYBR Green kit	Qiagen	204145
Superscript II Reverse Transkriptase Kit	Invitrogen	18064-014

### 6.1.8 Peripherals

The peripheral items used for the experiments are listed below.

**Table 8: Peripheral materials**

Item	Supplier	Catalog-/Order-number
Baysilon-Paste high viscosity	GE Bayer Silicones	700514
Coverslip (25mm)	ORSATec / Kindler	02R1215-D
Immersol 518F fluorescence free, 23° C	Zeiss	444960-0000-000
Immersol 518F fluorescence free, 37° C	Zeiss	44970-9010-000
nitrocellulose membrane	GE Healthcare	10600003

### 6.1.9 Devices

The devices used in the experiments are listed below; small devices for general laboratory use are not listed.

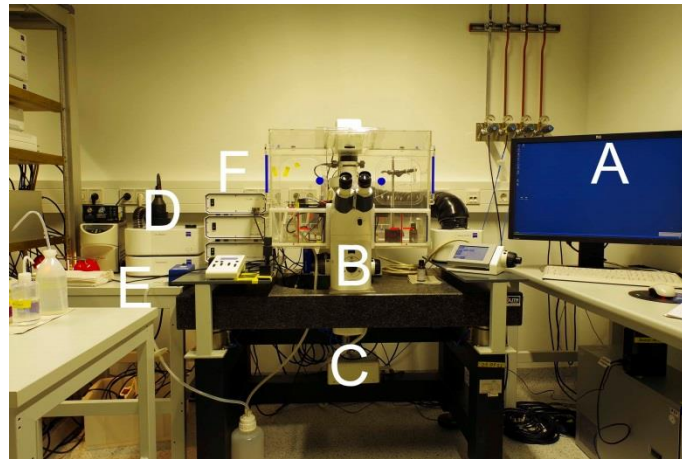
**Table 9: Devices**

Item	Supplier	Function
4D-Nucleofector™ System	LONZA	Transfection of siRNA
Nucleofector™ 2b Device	LONZA	Transfection of siRNA
Centrifuge 5415C	Eppendorf	Centrifugation
Infinite M200 Pro	Tecan	Plate reader
Nucleic Acid Electrophoresis Systems	BIO RAD	Electrophoresis
Cell Observer Z1	Zeiss	Live cell imaging
Evolve® 512 EMCCD Camera	PHOTOMETRICS	Live cell imaging
Olympus IX70	Olympus	Calcium imaging
Polychrom V	Till Photonics	Calcium imaging
CCD Camera Imago	Till Photonics	Calcium imaging

## 6.1.10 Microscopes

### 6.1.10.1 Zeiss Cell Observer Z1

The live cell imaging experiments performed for the current study were either done on an automatic Zeiss cell observer Z1 or a similar semi-automatic Zeiss cell observer D1 system including a Colibri LED light source, an incubation chamber with gas and temperature control units, fast acquisition cameras and a special trigger unit (used to achieve high frame rate imaging). The setup is as shown in the photo below.



**Graph 4: Zeiss Cell Observer Z1 imaging setup.** A: Computer B: Cell Observer Z1 C: Evolve®512 Delta EMCCD Camera D: Atmosphere control E: Temperature control F: Power supply unit

#### 6.1.10.1.1 LED sets

The LEDs are installed in a Colibri system. They provide light sources with fixed wavelength for the excitation of different fluorescent proteins or dyes. The excitation wavelengths of LED sets and beam combiners are listed below.

**Table 10: LED Sets on the Zeiss Colibri 2 System**

<b>LED (wavelength)</b>	<b>Beam Combiner</b>
400nM	Beam Combiner 425nm+Beam Combiner 490nm
420nM	Beam Combiner 425nm+Beam Combiner 490nm
490nM	Beam Combiner 565nm+Beam Combiner 490nm
505nM	Beam Combiner 565nm+Beam Combiner 490nm
555nM	Beam Combiner 565nm+Beam Combiner 490nm

### 6.1.10.1.2 Emission Filters and Dichroic Mirror Sets

The emission signals from the fluorescent proteins passed through a dichroic system and are filtered by the emission filter sets before being detected by the sensor of camera. The filter and dichroic mirror system are built on an automatic or semi-automatic revolver which can be controlled by a computer. The emission filter and matched dichroic mirrors are listed below.

**Table 11: Emission Filters and Dichroic Mirror Sets**

<b>Dichroic Mirror</b>	<b>Emission Filter</b>
FT 509nm	528nm/40
FT 505nm	525nm/50
FT 520nm	542nm/27
BS 458nm	483nm/32
FT 573nm	630nm/92

### 6.1.10.1.3 Objectives

Different objectives were used to visualize cellular signals. These objectives are listed below.

**Table 12: Objectives on the Zeiss Cell Observer**

<b>Manufacturer</b>	<b>Type</b>	<b>Magnification</b>	<b>Numerical Aperture</b>	<b>Serial number</b>
Zeiss	Fluar	2.5×	0.12	420120-9900
Zeiss	Fluar	10×	0.5	420140-9900
Zeiss	Fluar	20×	0.75	420150-9900
Zeiss	Fluar	40×	1.3	420260-9900
Zeiss	Fluar	100×	1.45	421190-9900
Zeiss	Plan-NEOFluar	40×	0.75	420360-9900

#### 6.1.10.1.4 Cameras

To achieve proper time resolution for live cell imaging, fast acquisition cameras were used for the experiments. The specifications of cameras are listed below.

**Table 13: Cameras for Live Cell Imaging**

Manufacturer	Type	Sensor	Array Size	Pixel Size
Zeiss	Axiocam 702 mono	IMX174 Exmor Pregius	1928×1200	5.86× μm
Photometrics®	Evolve® 512 Delta	E2V CCD97	512×512	16 <sup>2</sup> μm

#### 6.1.10.2 Olympus IX70 Setup

The Olypmus IX70 imaging setup was used for the ratiometric calcium imaging experiments; the components of full system are listed below.

**Table 14: Olympus IX70 Components**

Components	Function
Olympus IX70 microscope	Imaging
Computer	Data processing
Polychrome V Monochromator	Excitation light source
CCD-Camera T.I.L.L. Imago	Recording
20× Objective	Visualization
Filter sets	Customized for Fura-2 spectrum

#### 6.1.11 Cell Lines

All melanoma cell lines labeled with “WM” and “Lu” are a gift from Prof. Dr. Meenhard Herlyn (The Wistar Institute, Philadelphia, USA); additional melanoma cell lines were purchased from German Collection of Microorganisms and Cell Cultures GmbH and American Type Culture Collection. The primary human melanocytes were a gift from Dr. Hedwig Stanis-Bogeski (Dermatology, Göttingen).

Experiments on human cell lines or primary cells were approved by the local ethics committees. Culture medium, the origin and genetic information of all used cell lines are provided below.

**Table 15: Panel of Cell Lines Used for the Current Study**

<b>Cell line</b>	<b>BRAF</b>	<b>N-RAS</b>	<b>PTEN</b>	<b>Culture Medium</b>
WM3734	V600E	WT	WT	TU+2% FCS
Mel Juso	WT	Q61K	WT	RPMI 1640+10% FCS
WM164	V600E	WT	WT	TU+2% FCS
WM983B	V600E	WT	WT	TU+2% FCS
1205Lu	V600E	WT	Hem Del	TU+2% FCS
WM9	V600E	WT	Hem Del	TU+2% FCS
WM3918	WT	WT	N/A	TU+2% FCS
SK Mel 5	V600E	WT	WT	RPMI 1640+10% FCS
451Lu C2	V600E	WT	WT	TU+2% FCS
WM1366	WT	Q61L	WT	TU+2% FCS
HaCat	WT	WT	WT	DMEM+10% FCS
Melanocyte	WT	WT	WT	M2 medium+1% Pen/Strep
HeLa	-	-	-	DMEM+10% FCS+1% Pen/Strep

*\*Sequencing analyses of the Wistar melanoma cell lines were performed in the K. Nathanson laboratory, University of Pennsylvania, Philadelphia, USA. All melanoma cell lines have been fingerprinted for their uniqueness to exclude cross-contamination. (WT, wild type; Hem Del, hemizygous deletion). The mycoplasma contaminant tests were done with a commercially available kit.*

### **6.1.12 Genetically Encoded Protein Sensors**

Genetically encoded protein sensors are used for monitoring of cell signaling and activities of specific molecules in a quantitative and real-time manner in different intracellular compartments. Compared with broadly used fluorescent dyes, the protein sensors offer the opportunities for more precise monitor of the cellular physiological activities. In the current study, the protein sensors were applied to measure calcium, ROS and ATP concentration in compartments including cytosol, ER and mitochondria. The information for the labeled reporters and protein sensors is provided below.

**Table 16: Genetically Encoded Protein Sensors**

<b>Item</b>	<b>Feature</b>	<b>Targeted Compartment</b>	<b>Function</b>
NFAT1-GFP	GFP reporter	Cytosol	NFAT1 activation
HyPer3	Ratiometric	Cytosol	H <sub>2</sub> O <sub>2</sub> concentration
Mito HyPer	Ratiometric	Mitochondria	H <sub>2</sub> O <sub>2</sub> concentration
SypHer	Ratiometric	Cytosol	pH
Mito SypHer	Ratiometric	Mitochondria	pH
4mt D3cpV	FRET	Mitochondria	Ca <sup>2+</sup> concentration
4mt TNXL	FRET	Mitochondria	Ca <sup>2+</sup> concentration
MAM HyPer	Ratiometric	MAM	H <sub>2</sub> O <sub>2</sub> concentration
ER HyPer	Ratiometric	ER	H <sub>2</sub> O <sub>2</sub> concentration
CaNAR2 cyto	FRET	Cytosol	Calcineurin activity

## 6.2 Methods

### 6.2.1 Cell culture

All cell lines used in this study were cultured with corresponding media supplemented with fetal bovine serum and were maintained in a standard incubator with a temperature control at 37°C, supplied with 5% CO<sub>2</sub>. Specific culture conditions for the major cell lines used in this study are as follows.

#### WM3734

The WM3734 cell line was established on site at the Wistar Institute, Philadelphia, PA USA (M. Herlyn Laboratory) as previously published (248). The cells were isolated from a brain metastasis of human melanoma in a female patient. The cells were maintained in 2% TU medium and split twice a week.

#### Mel Juso

The Mel Juso cells originate from a human primary melanoma tumor, purchased from German Collection of Microorganisms and Cell Cultures GmbH. The cells were cultured in RPMI 1640 medium with 10% FCS and were split twice a week.

#### Melanocytes

Human melanocytes were used for comparisons to the melanoma cells in expression analysis. The melanocytes were isolated from neonatal foreskins obtained after circumcision from different donors and were cultured according to established protocols.

*\*The melanocytes were provided by Dr. Hedwig Stanisz-Bogeski (Dermatology, Universitätsmedizin Göttingen, Göttingen).*

## **6.2.2 RT-PCR**

### **6.2.2.1 RNA isolation**

The TRIzol™ reagent from Invitrogen was used to isolate total RNA from the cells and tissue sample in the present study. Briefly, cells were detached by incubation with accutase, they were centrifuged at 1500 rpm for 3 minutes. The pellet was then suspended by pipetting the TRIzol™ reagent. The samples were then stored at -20°C if not used immediately. The isolation proceeded by the sequential precipitation of total RNA using different solutions, following manufacturer's instructions. The yield of isolated total RNA was measured by reading the absorbance with a spectrophotometer; the RNA concentration was calculated using the formula:  $A_{260}$  (absorbance at 260nm)  $\times$  dilution  $\times$  40 =  $\mu$ g RNA/mL.

### **6.2.2.2 Reverse transcription**

Generally, 800 ng of total isolated RNA was reverse-transcribed to cDNA using SuperScript™ II reverse transcriptase following manufacturer's instruction; the link of the instruction is as follows:

[https://assets.thermofisher.com/TFS-Assets/LSG/manuals/superscriptII\\_pps.pdf](https://assets.thermofisher.com/TFS-Assets/LSG/manuals/superscriptII_pps.pdf)

### **6.2.2.3 RT-qPCR**

A volume of 0.5  $\mu$ L cDNA was used for q-PCR experiment using the SYBR Green Kit (Qiagen #204145) and Bio-Rad CFX96™ Real-Time System. The TATA box binding protein

(TBP) was set as the housekeeping gene. Analyses were performed using the  $2^{-\Delta\text{CT}}$  method. The qPCR experiments in the current study were run on either the Biorad® Light Cycler or Agilent technologies® stratagene mx3000p\*.

*\*The transfection, treatment of cells, sample collection and data analysis were performed by Xin Zhang, the RT-PCR experiments were performed by the laboratory technicians Andrea Paluschkiwitz (Universitätsmedizin Göttingen, Göttingen) and Sandra Janku (University of Saarland, Homburg-Saar).*

### **6.2.3 Western blotting**

To analyze the knockdown efficiency of the siRNA/shRNA or the expression of target proteins across a panel of melanoma cell lines and melanocytes, the western blot analyses were applied. The general experimental procedure is described below.

Generally,  $2 \times 10^6$  cells were harvested using accutase or trypsin, the cell pellets were stored at  $-80^\circ\text{C}$  before use. The tumor samples from mouse xenografts were fixed and embedded in paraffin, or frozen instantly on site using liquid nitrogen. The determination of the protein concentration was performed using the Bradford or BCA protein assay,  $25\mu\text{g}$  protein were loaded on 10% SDS-polyacrylamide gel for the electrophoresis. After the electrophoresis, the samples were transferred onto a nitrocellulose membrane and blocked in 5% BSA. The blots were incubated with specific primary antibodies overnight and then incubated with fluorescent secondary antibodies in dark, at room temperature for hours. The blots were scanned with a BioRad imaging system.

*\*The transfection, treatment of cells and tumor sample collection were performed by Xin Zhang, the running of gel and blotting were performed by technicians.*

## 6.2.4 RNA oligonucleotide mediated gene silencing

To study the physiological function of the TMX proteins and NFAT1, the RNA interference technique was used to knockdown the expression of the target proteins.

For the transient knockdown, the small interference RNA (siRNA) was introduced by electroporation-mediated transfection with a 2b or 4D Nucleofector machine from LONZA. The cells were suspended with a mixture of siRNA and salt free solution provided by the supplier, and were electroporated with optimized programs.

Briefly, two million cells were harvested by trypsinization and centrifuged at 1000 RPM for 3 min; the supernatants were discarded. The cells were suspended with 4 $\mu$ L of 20pmol siRNA in 100 $\mu$ L transfection solution and were loaded into cuvettes. Pre-optimized programs were used for the electroporation according to cell types. The programs defined the type, number and voltage of the electroporation to be executed. After the electroporation, cells were immediately transferred into pre-warmed growth medium, they were seeded and kept in the incubator until measurement started. The programs used for electroporation are listed as follows.

**Table 17: Programs Used for the Transfection by Electroporation**

System	Program	Cell Line
4D-Nucleofector™ System	CA137	WM3734
Nucleofector™ 2b Device	A24	WM3734
Nucleofector™ 2b Device	A24	Mel Juso

For the stable knockdown of TMX1, the Sigma MISSION® shRNA was transduced into WM3734 and 1205Lu melanoma cells with a lentiviral vector pLKO.1, the control cells were transduced only with scrambled pLKO.1 vector. All procedures followed the RNAi Consortium (TRC) Broad Institute, the detailed protocol can be found following the link below: <https://www.broadinstitute.org/rnai-consortium/rnai-consortium-shrna-library>.

The workflow for the generation of stable TMX1 and TMX3 knockdown cell lines was as follows:

Day 1: Seed 4 million recently thawed HEK293T cells in 10ml antibiotic-free medium in 10cm tissue culture dishes for packaging.

Day 2: Transfect the HEK293T cells with lentivirus plasmids of control, shRNA against TMX1 and TMX3 by lipofection. The composition of the mixture for transfection is as follows: 1) Packaging plasmid psPAX2 9 $\mu$ g; 2) Envelope plasmid PMD2.G 0.9 $\mu$ g; 3) empty vectors pLKO.1 or shRNA 9 $\mu$ g; 4) Opti-MEM to a total volume 225 $\mu$ L. The transfection reagent mixture is as follows: 1) lipofectamine 54 $\mu$ L; Opti-MEM 90 $\mu$ L.

Day 3: 18 hours after transfection, remove the medium and add fresh high-serum medium.

Day 4: 24 hours later, collect the medium with virus and add fresh medium.

Day 5: 24 hours after first collection, collect the medium with virus and discard packing cells.

The virus was stored in -80°C before use.

Day 6: Seed the target cells at 50%~60% confluence.

Day 7: Infection of cell lines with virus and 8 $\mu$ g/mL polybrene in complete medium, and incubate for 16 hours.

Day 8: Discard supernatant from dish and wash 3 times with PBS, then add fresh medium.

Day 9: After 24 hours, discard the supernatant and replace with medium plus 2 $\mu$ g/mL puromycin. Wait for the selection for 72 hours.

Day 12: Refresh the medium and wait for the recovery of cells.

*\*The establishment of TMX1 and TMX3 stable knockdown cell lines were performed by Xin Zhang, and the cell lines were shared to collaborators for subsequent experiments including*

*western blot analysis of cell signaling pathways, Matrigel invasion assay, mitochondrial respiration capacity analysis, electron microscopy analysis, determination of mitochondrial volume and surface by confocal microscopy, mouse model based work.*

### **6.2.5 NFAT1 translocation assay**

To monitor the activation of transcription factor NFAT1, a microscopy-based NFAT1 translocation assay was performed using GFP tagged NFAT1. Melanoma cells were seeded onto glass coverslips at a density of 200,000 cells per well (6-well plate) and left for adhesion overnight. The next day, the cells were transfected with a NFAT1-GFP construct using FuGENE<sup>®</sup> HD solution, 1µg plasmid plus 4µL FuGENE solution and 100µL Opti-MEM for each well in 2ml growth medium. Six hours later, the medium was refreshed. Twenty-four hours after the transfection, the cells were loaded in 0.25mM Ca<sup>2+</sup> or 1mM Ca<sup>2+</sup> Ringer's buffer and were stimulated with thapsigargin (1µM). The translocation of NFAT1 was then recorded by live cell imaging at 37°C. The increase in fluorescence intensity in the nucleus was calculated by an Axiovision software using marked regions of interest, and the results were normalized by calculating the ratio of  $F_n/F_0$  fluorescence intensity (ratio of fluorescence signal intensity number from frame N divided by the fluorescence signal intensity number from the first frame)

### **6.2.6 Cell viability assay**

To analyze the viability of melanoma cells, the CellTiter-Blue<sup>®</sup> Cell Viability Assay was used following the manufacturer's protocol. The assay is developed on the conversion of resazurin into its fluorescent form by viable cells. Since nonviable cells or metabolically interfered cells lose the capacity to reduce the resazurin, emitted fluorescence signals can be used as a

reference of cell viability. Thus the assay provides a simple and reliable method to measure the viability of the cells. The details of the procedure are as follows.

The collected cells were suspended in full medium, and 10 $\mu$ L of the suspension was loaded into a counting cassette. The cell number was determined either with a Moxi™ Z Mini Automated Cell Counter or a Life Technologies® Countess II FL Cell Counter. The cells were seeded at a density of 5,000 cells/well (96-well plate), or 10,000 cells/well (48-well plate) in 200 $\mu$ L or 400  $\mu$ L growth medium respectively. Generally, 6 hours after the seeding, the cells were treated with activators/inhibitors for the specified time duration. After the treatment or the incubation time, 20 $\mu$ L (96-well plate) or 40 $\mu$ L (48-well plate) CellTiter-Blue were added per well and incubated with the cells for 3 hours. After the incubation, the plates were shaken for 20 seconds and the fluorescence signals emitted at the wavelength of 590nm (but excited at a wavelength of 560nm) were measured by a TECAN M200 plate-reader. The background signal from the wells filled only with medium and CellTiter-blue was subtracted from the measured wells, and the fluorescence intensity in arbitrary units was used to determine cell viability.

### **6.2.7 Cell migration assay**

The migration assay was performed using a HTS transwell® permeable support (Corning®, Kennebunk ME, USA) with 8- $\mu$ m pore size inserts. Cells were seeded at 50,000 cells per well (96-well plate) or 100,000 per well (24-well plate) in FBS-free medium containing 50ng/mL Wnt5a recombinant protein and were made to migrate towards a lower compartment containing preconditioned medium supplemented with 10% FBS. After 48 h, cells that migrated across the membrane were detached by digestion with accutase and suspended in PBS with 5% FCS, then counted using a Moxi Z Mini cell counter (ORFLO technologies, Ketchum, USA) or Life Technologies® Countess II FL Cell Counter.

## **6.2.8 Calcium measurement**

### **6.2.8.1 Fura-2 AM based cellular calcium measurement**

Measurements with the ratiometric calcium binding dye Fura-2 AM were performed for the quantification of cellular calcium concentrations. Melanoma cells were seeded at a density of 200,000 cells per well onto coverslips in 6-well plates and were incubated overnight for adhesion. The cells were stained with 1 $\mu$ M Fura-2 AM in growth medium for 30 min at room temperature in the dark. The measurements were performed in Ringer's buffer (pH 7.4) containing 155mM NaCl, 2mM MgCl<sub>2</sub>, 10mM glucose, 5mM HEPES and different concentrations of CaCl<sub>2</sub> or 0mM CaCl<sub>2</sub> plus 1mM EGTA and 3mM MgCl<sub>2</sub>. The cells were loaded with calcium free Ringer's buffer for the measurement of basal calcium levels, then the cells were perfused with 1 $\mu$ M of the SERCA (sarco/endoplasmic reticulum Ca<sup>2+</sup>-ATPase) inhibitor thapsigargin (Tg) which triggers a strong and irreversible depletion of ER Ca<sup>2+</sup>, leading the activation of SOCE. After the intracellular calcium level returned to resting level, the extracellular calcium concentration was increased by perfusion of the cells with Ringer's buffer containing 0.25mM or 1mM Ca<sup>2+</sup> to record the Ca<sup>2+</sup> influx through the plasma membrane channels. Time-lapse ratio-metric images were recorded with an Olympus IX70 microscope at a pace of one frame per 5 seconds. The results were analyzed with the TILLVISION software (FEI Munich, GmbH).

### **6.2.8.2 Compartmental calcium measurement**

To measure the calcium dynamics in different cell compartments, the genetically encoded protein sensors were introduced into the cells by transfection using FuGENE<sup>®</sup> HD solution. Generally, the plasmids were transfected 24 hours before the imaging experiment. The live cell imaging experiments were performed on the Zeiss Cell Observer using Zeiss Axiovision or ZEN software. The measurements were performed using Ringer's buffer (pH 7.4) containing 155mM NaCl, 2mM MgCl<sub>2</sub>, 10mM glucose, 5mM HEPES and different

concentrations of  $\text{Ca}^{2+}$ . Thapsigargin was used for depleting the ER store, and the extracellular calcium concentration was altered by perfusion or adding Ringer's buffer with various  $\text{Ca}^{2+}$  concentrations. The results were analyzed with the Zeiss software. For different sensors, the formulas described below were used for the calculation of the ratio representing the relative calcium concentration.

$$\text{FRET donor Ratio} = [(fret_{gv} - bg_{fret}) - cf_{don} * (don_{gv} - bg_{don}) - cf_{acc} * (acc_{gv} - bg_{acc})] / (Donor_{gv} - bg_{donor})$$

$$\text{Ratio } F_n \text{ to } F_0 = (Intensity_n - bg_n) / (Intensity_0 - bg_0)$$

$$\text{Ratio } CH_1 \text{ to } CH_2 = (Channel_1 - Channel_{bg}) / (Channel_2 - Channel_{bg})$$

(\*Regarding the subscripts in formula: gv=given; bg=background; don=donor; acc=acceptor; n= frame n; 0= frame 0; CH1=channel 1; CH2=channel 2; CF=correction factor.)

## 6.2.9 Intracellular $\text{H}_2\text{O}_2$ measurement

The concentration of  $\text{H}_2\text{O}_2$  in different cellular compartments such as ER and mitochondria were measured using the protein sensor HyPer3, ER HyPer and mito-HyPer respectively. The protein sensors were introduced into cells by transfection using FuGENE<sup>®</sup> HD solution as described before. The live cell imaging was performed on the Zeiss Cell Observer. The LEDs with excitation wavelengths of 420nm and 505nm were used and the emission signals were collected through the YFP filter with a passing wavelength of  $542\text{nm} \pm 14$ . The cells were loaded with the Ringer's buffer (pH 7.4) containing 155mM NaCl, 2mM  $\text{MgCl}_2$ , 10mM glucose, 5mM HEPES and 0.25mM  $\text{CaCl}_2$ , and were pre-incubated for 5min before imaging. On average, at least 3 different fields were recorded for each coverslip. To measure the signal of the fully reduced HyPer probes and subtract it as the background signal, cells were incubated with 100 $\mu\text{M}$  N-acetylcysteine (NAC), 1mM DTT or 100nM Mito TEMPO for

25min. Results were analyzed using Zeiss Axiovision or ZEN software and are presented as ratio values of the emission or the relative percentage numbers of the control group.

### **6.2.10 Intracellular pH measurement**

To monitor the pH of the cellular compartments as a control for the HyPer probes, the pH sensitive mutant SypHer probes were used for experiments in parallel. The transfection and measurement of the SypHer probes were done following the same procedure as with HyPer probes mentioned above. The results were analyzed with the same software accordingly and presented as the ratio of emissions from excitation wavelengths of 505nm and 420nm.

### **6.2.11 Mitochondrial ATP concentration measurement**

The mitochondria targeted FRET protein sensor ATeam1.03 was used to measure the basal mitochondrial ATP concentration. Briefly, cells were seeded on the glass coverslips following the same procedure for imaging experiments. The ATeam1.03 plasmid was transfected using FuGENE<sup>®</sup> HD solution 24 hours prior to the measurements. Cells were loaded with Ringer's buffer containing 0.25mM Ca<sup>2+</sup> and were imaged at 37 °C with the excitation wavelengths of 420nm and 505nm; and emission wavelengths of 483±16 nm and 542±14 nm. To measure the minimum level of ATP and subtract the signal from the ATP generated from other sources than mitochondrial respiration, 4µM oligomycin was used to fully block the ATP generation from the ATP synthase. Results were analyzed with Axiovision software and are presented as FRET donor ratio.

## **6.2.12 Calcineurin activity assays**

### **6.2.12.1 Dynamic measurement of calcineurin activity**

The dynamic phosphorylation activity of cytosolic calcineurin upon activation by calcium entry was measured with the FRET protein sensor CaNAR2-cyto. Melanoma cells were seeded onto glass coverslips and were incubated 4 to 6 hours for adhesion. The plasmid was transfected using FuGENE<sup>®</sup> HD solution 48 hours prior to the measurements. Cells were loaded with Ca<sup>2+</sup> free Ringer's buffer at the beginning of measurements, the Ca<sup>2+</sup> influx and subsequent activation of calcineurin was induced by adding 1 $\mu$ M thapsigargin, 1 $\mu$ M ionomycin and Ringer's buffer containing 2mM Ca<sup>2+</sup> to elevate the final extracellular Ca<sup>2+</sup> concentration to 1mM. The FRET signal was collected through an emission filter with a wavelength of 542 $\pm$ 14nm. The FRET/CFP ratio was calculated using the Axiovision software and is presented as the relative phosphatase activity of calcineurin.

### **6.2.12.2 Enzymatic end point measurement of calcineurin activity**

A commercially available kit for cellular calcineurin activity (BML-AK816-0001, Enzo Life Sciences, USA) was purchased and used for the end point measurement of calcineurin phosphatase activity in melanoma cells. Melanoma cells were transfected with the siRNA, and 2x10<sup>6</sup> cells were seeded in a T25 cell culture flask. By 48 h, the cells were washed with cold TBS for 3 times and were incubated with 0.5mL accutase for detachment. The cells were suspended, and the cell number in suspension was determined with a Moxi mini cell counter. Then the cells were wash once with a TBS solution and were centrifuged at 1500rpm for 5min. The supernatant was discarded and the pellet was lysed with the lysis buffer, then stored at -80°C before further measurement. For the measurement of phosphatase activity, the lysate was thawed on ice and desalted by gel filtration with a desalting column filled with activated resin. The desalted extracts were pipetted into microplates and were incubated with the substrate or the substrate plus inhibitors and EGTA as the negative control for 30min. The

samples were then incubated with 100 $\mu$ L BIOMOL<sup>®</sup> GREEN reagent for 30min in the dark. Next, the OD<sub>620nm</sub> of the mixture was measured with a TECAN M200 pro microplate reader. In principle, the free phosphates will react with the green reagent, the signal emitted by the end product can be detected as a reference to phosphatase activity. Data were presented as the raw OD<sub>620nm</sub> values from plate reading.

### **6.2.13 Interleukin-8 secretion measurement**

Interleukin-8 (IL-8) secretion from melanoma cells was measured with the enzyme-linked immunosorbent assay (ELISA). The CXCL8/IL-8 DuoSet kit (R&D system) was purchased and used for the quantification of the IL-8 in the supernatant of culture medium according to manufacturer's instruction.

Briefly, the WM3734 cells were transfected with the siRNA against TMX1 or TMX3 by electroporation and were seeded into a 6-well plate at a density of 0.75x10<sup>6</sup> cells per well. After 48 hours, the cells were treated either with 10 $\mu$ g/mL human insulin, 100nM thapsigargin alone or 100nM thapsigargin and 100nM phorbol 12-myristate 13-acetate (PMA) together in 0.5mL medium for 12 hours. Then the medium was collected from the plates and was centrifuged at 1500 RPM for 5min. After centrifugation, the supernatant was collected and stored at -80 °C. For preparation of coated plates, the Falcon clear bottom 96-well plate was coated with 100 $\mu$ L of the capture antibody at a concentration of 4 $\mu$ g/mL overnight. Before using, the plates were blocked with 1% BSA in PBS for 1 hour. Then, 100 $\mu$ L of the supernatants were added to the wells and were incubated with a capture antibody for 2 hours. Next, the detection antibody was added after intensive washing. After 2 h incubation, the streptavidin-horseradish peroxidase and substrate solution containing hydrogen peroxide and tetramethylbenzidine (TMB) were added for the revelation. The absorbance of end products was measured with a ClarioStar<sup>®</sup> plate reader at 450nm, the absorbance at 570nm was

measured as a correction. All procedures were performed at room temperature. Between blocking, antibody incubations and substrate addition the wells were washed intensively with 0.05% Tween<sup>®</sup>20 in PBS.

#### **6.2.14 Electron microscopy analysis of MAM parameters**

A monolayer of cells was fixed in 2% paraformaldehyde and 2% glutaraldehyde in 100mM sodium cacodylate buffer (pH 7.4) for 20 minutes. Then the cells were collected with scrapper as pellets. The pellets were fixed in osmium tetroxide 1% for the secondary fixation. The samples were washed and dehydrated, stained in 1% uranyl acetate. After the staining, the samples were treated with propylene oxide, and were then infused with embedding media (Embed 812); blocks were kept at 60 °C for hardening at least 48 h. The samples were then imaged using a digital camera mounted on a Philips 410 TEM, the images were processed with the “Mega View III” software.

For the melanoma cell line 1205Lu, the distance between mitochondria and ER, and the length of ER mitochondria contact sites (MAM length) were measured and shown in nanometer units. Mitochondrial proximity to the plasma membrane was quantified by measuring the distance between the closest mitochondria to the plasma membrane.

*\*The electron microscopy analyses were performed by Nasser Tahbaz and Lucas Mina, together with Prof. Dr. Thomas Simmen (Department of Cell Biology, University of Alberta, Canada).*

#### **6.2.15 In vivo studies**

The mouse experiments received permission from the local governmental animal care committee (Landesamt für Verbraucherschutz des Saarlandes), and were performed in consent

to the German legislation on protection of animals and the National Institutes of Health Guide for the Care and Use of Laboratory Animals. The 8 weeks old male athymic nude NOD.Cg-Prkdc<sup>scid</sup> Il2rg<sup>tm1Wjl</sup>/SzJ (NSG) mice were purchased from Charles River Laboratories, Sulzfeld, Germany. For the experiment, mice were divided randomly to 3 groups (7 mice per group) for inoculation: (A) shRNA control (control), (B) shTMX1\_1 (TMX1 kds 1), and (C) shTMX1\_2 (TMX1 kds 2). Mice were maintained in ventilated cages under specific pathogen-free conditions with temperature and humidity control, light time per day was set to 12h. All mice were maintained at the animal care facility of the Institute for Clinical and Experimental Surgery at Saarland University during experiment. Free access to tap water and standard pellet food were provided to all mice. The health status of mice was monitored by technician daily. Mice were each inoculated s.c. with 100,000 WM3734 cells suspended in a mixture of equal Matrigel (BD Matrigel™ Basement Membrane Matrix) and growth media. Tumor size was measured every 2-3 days by a single veterinarian who was blinded to the experimental groups, using a caliper. Tumor volumes were calculated using the formula:

$$V = \frac{\pi \times L \times W^2}{6}$$

Tumor samples with diameters larger than 15 mm before sacrifice were fixed and embedded in paraffin or frozen instantly after collection using liquid nitrogen. Immunoblots with tumor lysates were performed using 25 µg of total protein.

*\*The mouse experiments were performed by Xin Zhang, Dr. Adina Vultur, Dr. Christina Körbel, in collaboration with Prof. Dr. Matthias W Laschke and Prof. Dr. Michael D Menger (Institute for Clinical and Experimental Surgery, Saarland University, Homburg-Saar). The tumor samples were used for subsequent experiments to examine expression and cell signaling.*

### **6.2.16 Experimental data analysis and statistics**

The data obtained from all experiments were analyzed using TILL Vision, Zeiss Axiovision, Zeiss Zen, Biorad Quantity One, ImageJ with plugins and Microsoft Excel. The values are presented as mean  $\pm$  SEM if not mentioned otherwise. The unpaired two-sided Student's *t* test was used for data with normal distribution, the P-values are stated in the figure legends (\*  $P < 0.05$ , \*\*  $P < 0.01$ , \*\*\*  $P < 0.005$ ).

## **7 Results**

### **7.1 The expression analysis of TMXs and NFAT1 in human melanoma**

The pathogenesis of melanoma is a multiple-stage malignant transformation of the proliferative benign melanocytes to the invasive and metastatic melanoma cells. The acquisition of malignant competence is frequently caused by mutations, amplifications or deletions of certain precursor genes. Thus, genetic heterogeneity is one prominent characteristic of melanoma and hence there are only few biomarkers for this aggressive disease. In the current study, we investigated the role of TMX oxidoreductases and NFAT transcription factors in the human melanoma and addressed questions regarding if they are regulators of melanoma pathobiology and their potential connections with melanoma aggressive behavior.

#### **7.1.1 The mRNA expression of TMXs is elevated in melanoma cells**

We initiated our study with the assessment of expression status of TMXs proteins in the melanoma cells. The expression of TMX1 and TMX3 was quantified on the mRNA level with qPCR across a panel of distinct human melanoma cell lines. As shown in the Figure 1A and 1B, on the mRNA level, TMX1 and TMX3 are generally expressed in the melanocytes, keratinocytes and melanoma cells. The expression of TMX1 and TMX3 in melanoma cells is heterogeneous at the first glance. However, compared with the normal melanocytes and keratinocytes, in around 70% of the melanoma cell lines analyzed, the expression of TMX1 is significantly up-regulated while 6 out of 10 cell lines have a higher expression of TMX3, which indicates for a general upregulation of these genes in melanoma cell lines.

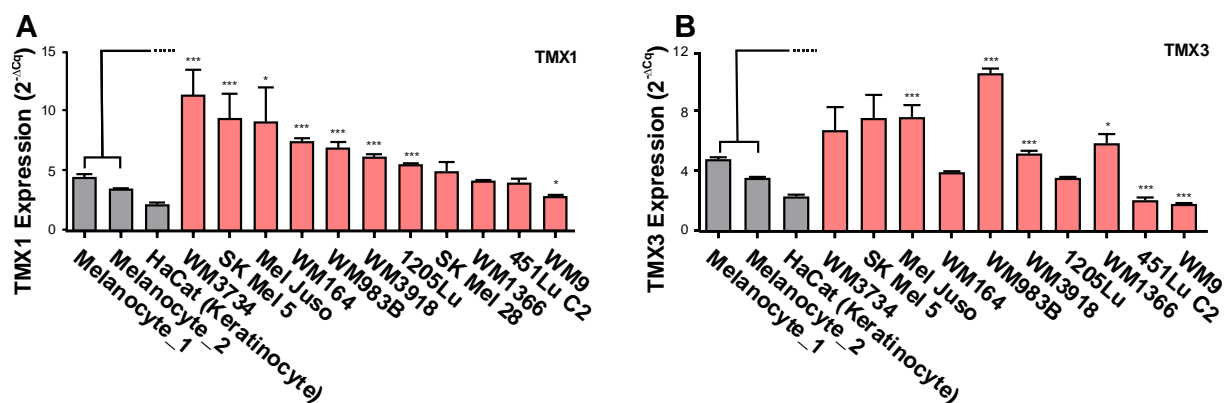


**Figure 1: mRNA expression of TMX1 and TMX3 in melanoma cell lines.** (A) The mRNA expression of TMX1 quantified by the qPCR in a panel of melanocytes from two donors, keratinocyte and 11 melanoma cell lines. (B) The mRNA expression of TMX3 quantified by qPCR cross a panel of melanocytes from two donors, keratinocyte and 10 melanoma cell lines. (The data were normalized to the expression of TATA box bind protein and presented as mean±SEM of 3 independent experiments. The significance test was performed between individual melanoma cell lines and the two melanocyte cell lines.)

### 7.1.2 The mRNA expression of NFAT1 is elevated in melanoma cells

To analyze the expression of NFAT in melanoma, we first quantified the mRNA expression of all five NFAT isoforms in two cell lines with qPCR. The results in the Figure 2A suggest that the NFAT1 is the predominant isoform among all family members in our cell lines. Then we selected a panel of 10 melanoma cell lines and quantified the mRNA level of NFAT1 to establish a general view of its expression. Interestingly, in 9 out of 10 cell lines the NFAT1 is expressed on an astonishingly higher level when compared with the melanocytes and keratinocyte, in which NFAT1 is nearly undetectable (Figure 2B). This finding indicates a strong functional relevance of NFAT1 in cultured melanoma cells.

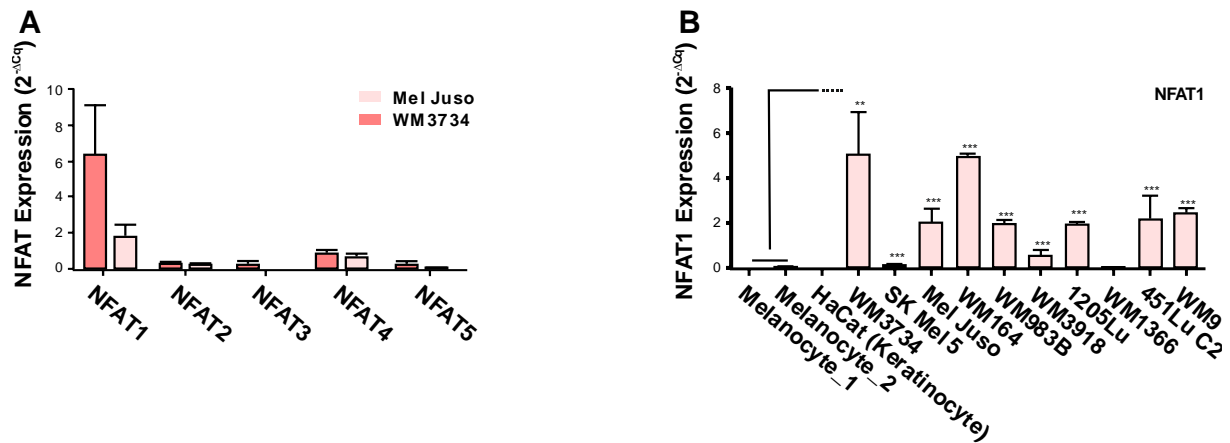


**Figure 2: mRNA expression of NFAT in melanoma cell lines.** (A) The mRNA expression of all NFAT isoforms quantified by the qPCR in two melanoma cell lines. (The data were normalized to the expression of TATA box bind protein and presented as mean of 3 independent experiments.) (B) The mRNA expression of NFAT1 quantified by the qPCR in a panel of melanocytes from two donors, keratinocyte and 10 melanoma cell lines. (The data were normalized to the expression of TATA box bind protein and presented as mean±SEM of 3 independent experiments. The significance test was performed between individual melanoma cell lines and the two melanocytes.)

The higher mRNA expression of TMX and NFAT1 in melanoma cells indicates that the abundance of these proteins might also be elevated in melanoma. Therefore, the Western Blot analyses were performed with the lysates from 10 melanoma cell lines and melanocytes from two different donors. As shown in our publication (Panel 1C)(249), though the protein expression does not fully match the mRNA expression pattern shown in Figures 1 and 2, the WB clearly shows that TMX1 as well as NFAT1 protein are significantly higher in the melanoma cell lines compared with the melanocytes. Regarding the expression of NFAT1, it is not detected in the melanocytes while the expression in 9 out of 10 melanoma cell lines are relatively high. Interestingly, the WM1366 melanoma cell line, which originates from a vertical growth phase melanoma and has slower proliferation rate and low migration potential does not express NFAT1 at all. These results indicated that the expression of TMX1 and

NFAT1 mRNA and proteins are relatively high in the melanoma cell lines, their expression is relevant in the cultured cell lines.

## **7.2 NFAT1 function is impaired by silencing of TMXs**

### **7.2.1 NFAT1 translocation is inhibited by silencing of TMXs**

In a previous study it was suggested that there is functional interaction between NFAT1 and TMX1, TMX3 in Hela cells. To explore how TMX1 and TMX3 could regulate NFAT1, we used a more detailed method based on the time-lapse fluorescent microscopy and GFP-tagged NFAT1 construct, in which the nuclear translocation of NFAT1 induced by stimulus can be tracked and assessed. First, we tested if the NFAT1 can be activated following a physiological stimulus such as insulin in the melanoma cells. Based on the expression analysis of TMXs and NFAT1, the WM3734 cells which have a high TMX1 and NFAT1 expression were used as the primary cell line. The Mel Juso cell line which has a high TMX1 expression but only moderate NFAT1 expression was used as a secondary cell line. By investigating these two cell lines, we also aimed to understand the impact of BRAF mutation in this context since the WM3734 is a BRAF V600E line and the Mel Juso is a BRAF wild type line.

As shown in Figure 3, the translocation of tagged NFAT1 can be induced by the addition of 50 µg/ml human insulin in the ringer buffer with 0.25mM Ca<sup>2+</sup>. After the stimulation, the nuclear signaling of NFAT1-GFP was strongly elevated (quantified by  $F_n/F_0$ , upper panel). This indicates that the induction of NFAT1 in melanoma cells is relevant to physiological stimulations.

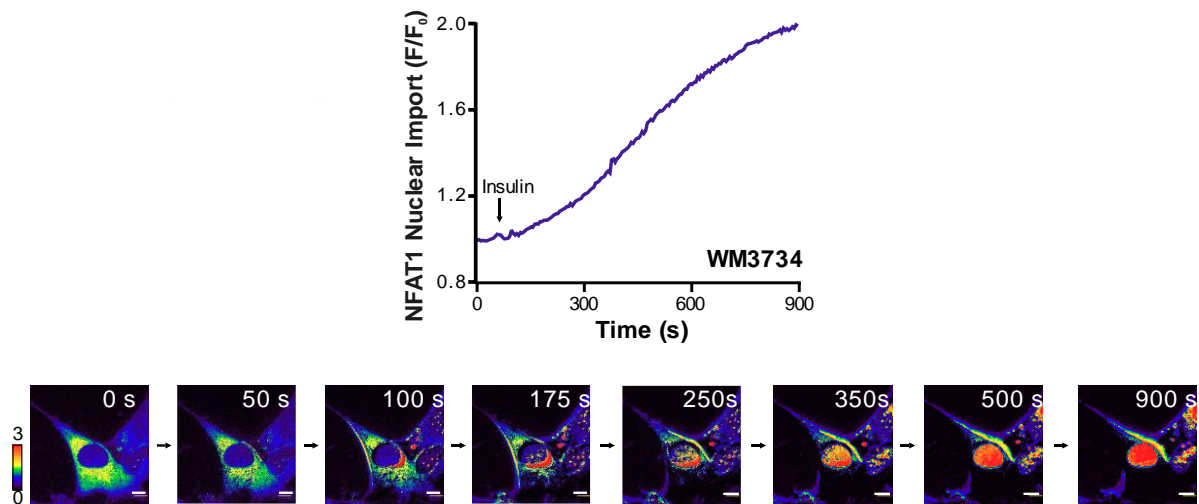


**Figure 3: Nuclear import of NFAT1 in melanoma cell.** The NFAT1 translocation following 50 $\mu$ g/ml human insulin stimulation was recorded with time-lapse fluorescent microscopy for 900s in the WM3734 melanoma cells. (Upper panel: Quantification; Lower panel: representative images for the changes over the time course)

Next, we used small interference RNA (siRNA) to silence the TMX1 and TMX3 on both cell lines for 48 hours, and then analyzed the NFAT1 translocation induced by Tg. As shown in Figure 4, the silencing of TMX1 and TMX3 inhibits the NFAT1 translocation in the WM3734 and Mel Juso cells (Figure 4B and E) around 25%~40% (Figure 4C and F) which confirms that the TMX1 and TMX3 can inhibit the activation of NFAT1 in the melanoma cell lines regardless of their BRAF mutation status. To further confirm the validity of this signaling axis, the assay was performed on two additional melanoma cell lines (Figure 4J-M). The results show a consistent inhibition of NFAT1 translocation caused by silencing of TMX proteins, which indicates the mechanism under this signaling axis may be universal in melanoma cell lines. To test this, we overexpressed the NFAT1-GFP in the WM1366 cells, which do not have endogenous NFAT1 and performed the same assay. Nonetheless, the results show a similar pattern (Figure 4N-O). To summarize, these results show that NFAT1 is ready for activation in melanoma cells generally, and the activation is expression-independent.

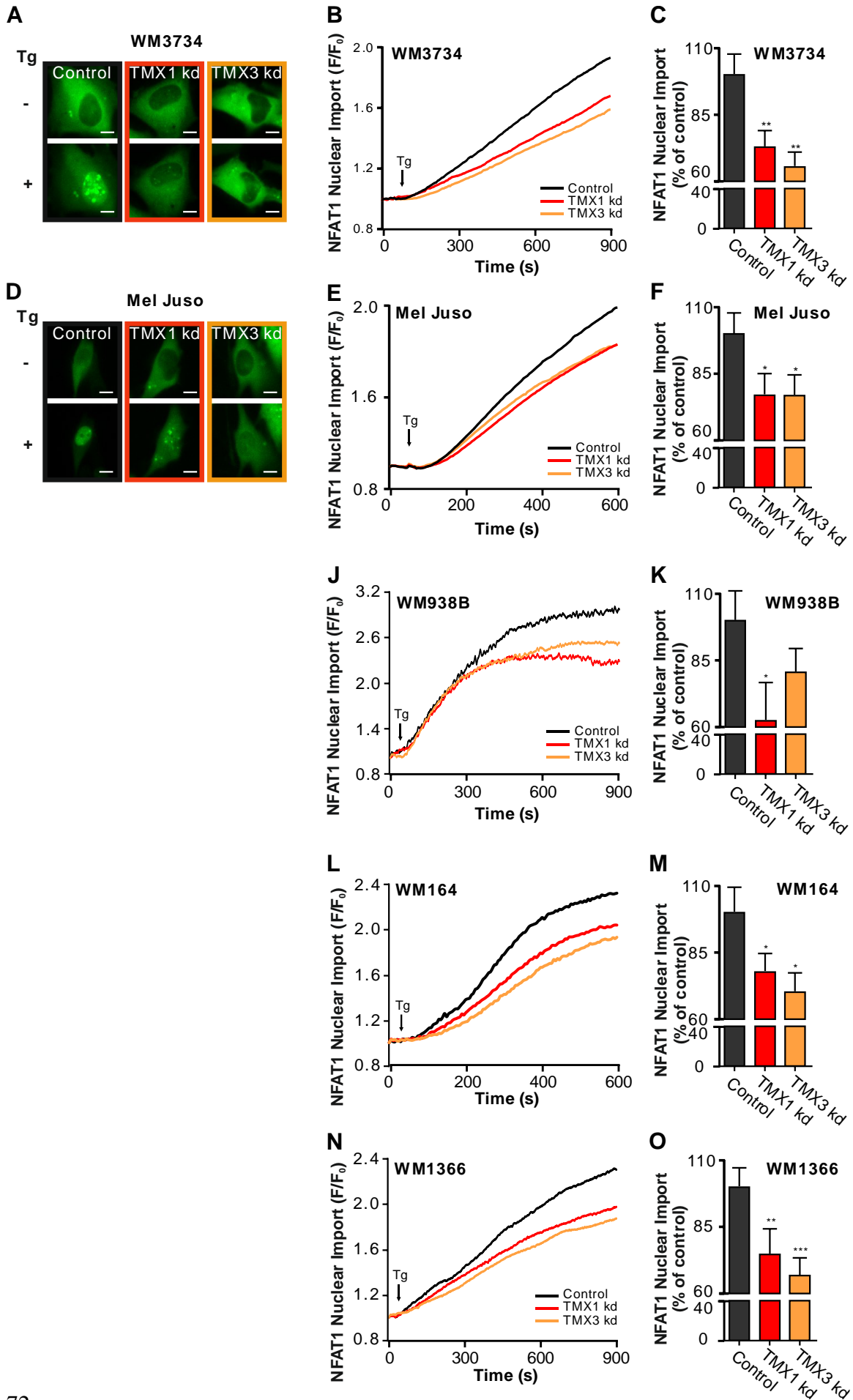


**Figure 4: NFAT1 translocation is inhibited following TMX silencing in melanoma cell lines.** (A) and (D): Representative images from the recorded NFAT1 translocation movie on the TMX1 and TMX3 silenced WM3734 and Mel Juso cells. (B), (E), (J), (L), (N): Fold change of NFAT1 translocation from the live cell imaging experiment on a time course. (C), (F), (K), (M), (O): Quantification of the end point from the NFAT1 translocation experiment. Data were collected from 3 independent experiments and presented as mean±SEM. (The analyzed cell number N: WM3734, control=142, TMX1 kd=116, TMX3 kd=148; Mel Juso, control=75, TMX1 kd=47, TMX3 kd=67; WM938B, control=16, TMX1 kd=12, TMX3 kd=27; WM164, control=46, TMX1 kd=56, TMX3 kd=44; WM1366, control=53, TMX1 kd=49, TMX3 kd=63.)

### 7.2.2 NFAT1 transcriptional activity is reduced by silencing of TMXs

The inhibition of nuclear translocation of NFAT1 can lead to decreased transcriptional activity and a lower expression of downstream target genes. To check if the inhibition of NFAT1 translocation influenced the transcriptional activity of NFAT1, the production of interleukin-8 (IL-8) which was reported as a target gene of NFAT1 (242) was assessed by enzyme-linked immunosorbent assay (ELISA) assay. The WM3734 cells were transfected with siRNA against TMX1 and TMX3, after 48 hours the cells were incubated with either 10µg/ml insulin, 100nM Tg or 100nM Tg and 100nM PMA together for 12 hours to induce the secretion of IL-8. As the end point, the growth medium was collected for the measurement of the IL-8 secreted from cells.

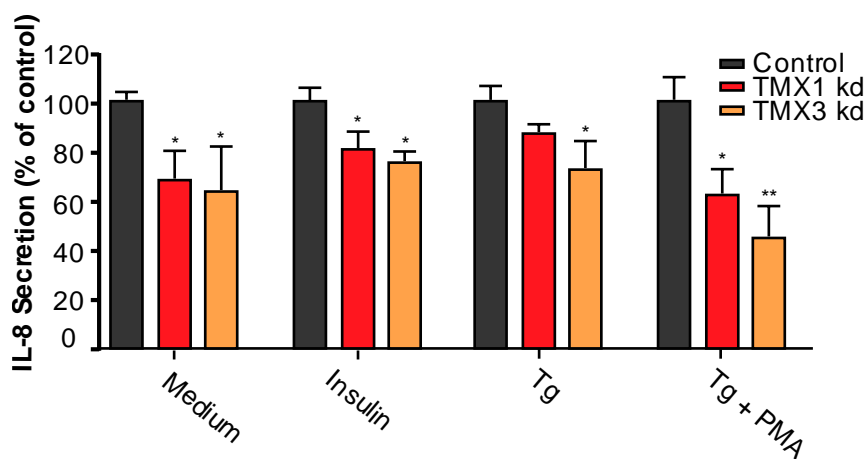


**Figure 5: IL-8 secretion from melanoma cells is decreased following TMX silencing.** The interleukin-8 secreted by TMX-silenced cells following different stimulation was measured with ELISA assay. The data are normalized as percentage of the control group and presented as mean $\pm$ SEM of 4 independent experiments.

As shown in Figure 5, the basal IL-8 production is inhibited by silencing of TMX1/TMX3 by up to 30~40% upon the stimulation with pre-conditioned medium which is supposed to contain growth factors secreted from the melanoma cells. Following stimulation with human insulin the IL-8 secretion is also inhibited by around 20%~30%. With more robust stimulations such as Tg and Phorbol 12-myristate 13-acetate (PMA), an activator of protein kinase C, the IL-8 production is even inhibited up to 20%~50%. These data confirm that the transcriptional activity of NFAT1 could be reduced by the knockdown of TMX proteins on both constitutional level or upon various stimulations. Based on these results, we conclude that the oxidoreductases TMX1 and TMX3 can regulate NFAT1 in melanoma cells as well as reported in Hela cells. The silencing of TMX1 and TMX3 thereby inhibit the activation of NFAT1 and impair the expression of downstream genes.

### **7.3 Silencing of TMXs does not affect SOCE**

The activation of NFAT1 is canonically driven by the elevation of cytosolic Ca<sup>2+</sup> following the signal transmission from plasma membrane. Therefore, we investigated if the silencing of TMX1/TMX3 affected the dynamics of cytosolic Ca<sup>2+</sup> using live cell calcium imaging. The TMX1/TMX3 silenced cells were loaded with Fura 2, placed into a Ca<sup>2+</sup> free ringer buffer and measured to assess the cytosolic Ca<sup>2+</sup> resting levels. The cells were then treated with Tg to induce the depletion of the ER Ca<sup>2+</sup> stores. A few minutes later, the cells were perfused with ringer buffer containing 1 mM Ca<sup>2+</sup> for quantifying Ca<sup>2+</sup> influx via the ORAI channels on the plasma membrane. At the end, the cells were perfused with Ca<sup>2+</sup> free ringer buffer

again to monitor the clearance of cytosolic calcium. To our surprise, the results (Figure 6A) show that in WM3734 cells, the basal cytosolic  $\text{Ca}^{2+}$  level, the depletion of ER as well as the calcium influx via SOCE are not dramatically affected by the knockdown of TMX proteins (Figure 6B). These results indicate that the impairment of NFAT1 function caused by silencing of TMX1/TMX3 is not due to alterations in SOCE, which remains functional and intact.

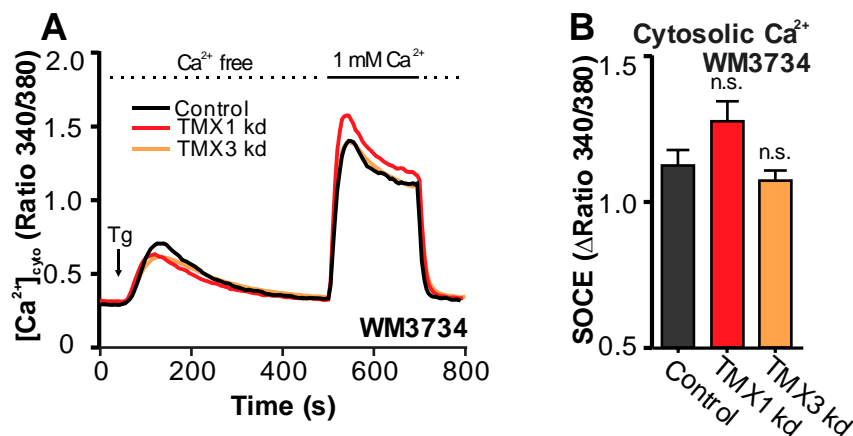


**Figure 6: Cytosolic calcium measurement on WM3734 cells following TMX silencing.** The cytosolic calcium was measured with ratiometric dye Fura-2 and live cell imaging on TMX-silenced WM3734 cells. Data are presented as mean±SEM. (The analyzed cell number N: control=30, TMX1 kd=49, TMX3 kd=52)

#### 7.4 Silencing of TMXs increases cellular ROS production

The  $\text{Ca}^{2+}$  measurements imply that TMX1/TMX3 silencing-induced impairment of NFAT1 function is through an alternative mechanism other than the disturbance of cellular  $\text{Ca}^{2+}$  dynamics. TMX oxidoreductases are involved in oxidative folding of proteins in the ER and their localizations are also confirmed in the related membrane network such as MAM. As mentioned before, such tethered membrane network is involved in the regulation of homeostasis of the organelles on both sides, accordingly it is plausible that these oxidoreductases could play a role in the regulation of ER-Mitochondria cross-talk and thus influence redox homeostasis. Hence, we next investigated if the silencing of TMX1/TMX3

affected the intracellular redox state with the genetically encoded protein sensor HyPer. First, we measured the cytosolic H<sub>2</sub>O<sub>2</sub> level with HyPer3 probe in the TMX1/TMX3 silenced cells. As shown in Figure 7A, the transient knockdown of TMX1/TMX3 results in a significant increase of HyPer3 signal on both WM3734 and Mel Juso cells. After the measurement, the cells were incubated with 100 $\mu$ M N-acetylcysteine (NAC) to fully reduce the probe and set the ratio number to the background level for the calibration of the relative increase of signals. The quantification of HyPer signals shows that the cytosolic signal level is increased by more than 2 folds in the WM3734 cells, and around 20%~60% in the Mel Juso cells (Figure 7B and C). The signal of HyPer3 probes can also be affected by the pH of the compartment due to a structural imperfection, so we measured the cytosolic pH with the pH reporter SypHer probe which is a mutant of HyPer with critical cysteine replacement. The results show that there is no apparent change of cytosolic pH in both cell lines (Figure 7D and E). We also performed the same assay on the NFAT1-negative WM1366 cells (Figure 7F) to see if the induction of ROS is cell line-dependent, the result indicates that the induction caused by knockdown of TMX proteins is common in the melanoma cell lines. All together, these results show that the increase of cytosolic H<sub>2</sub>O<sub>2</sub> level is caused by the knockdown of TMX proteins and the BRAF or NFAT1 expression is not relevant. Thus, we conclude that the knockdown of TMX proteins increases cellular ROS production in melanoma cells regardless of their BRAF mutation status and NFAT abundance.

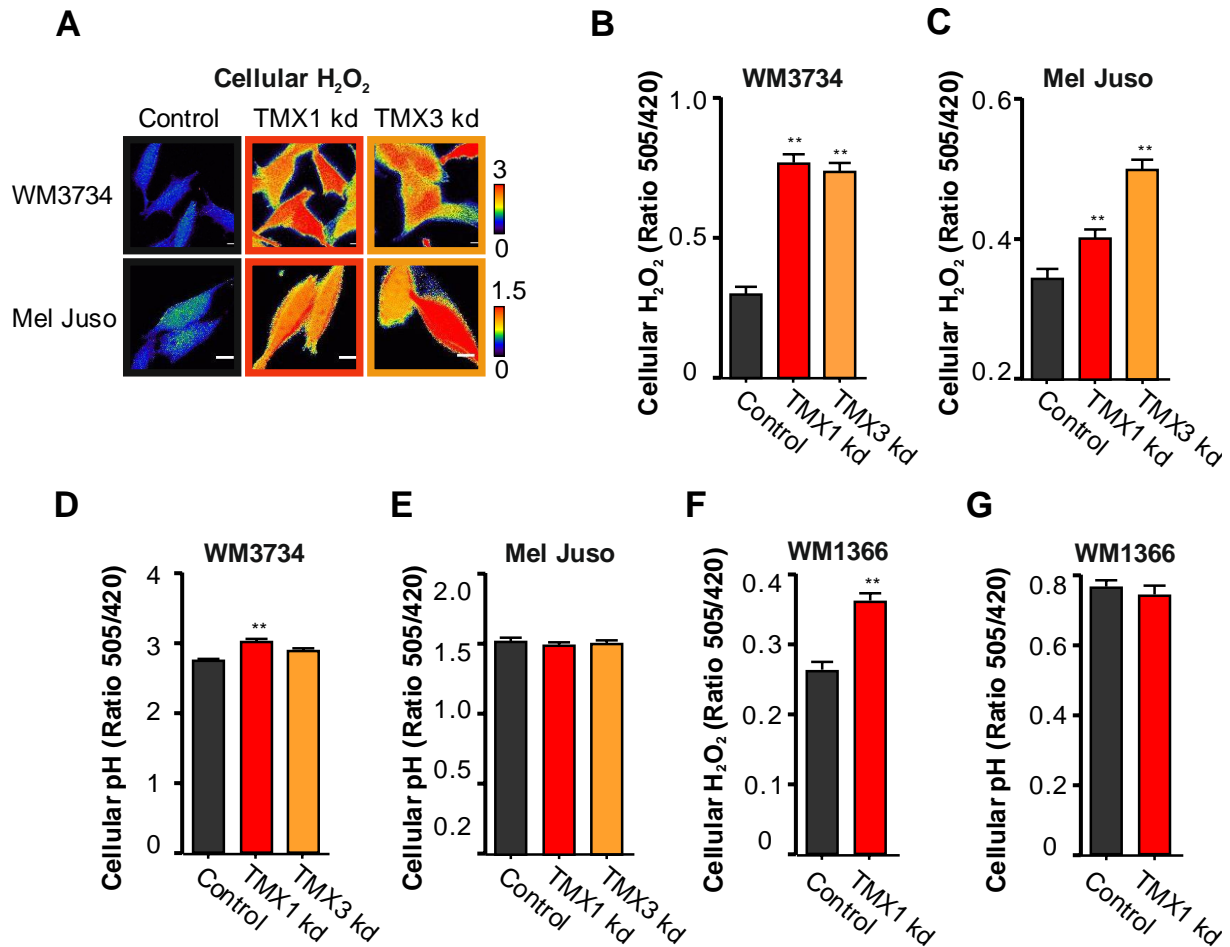


**Figure 7: Cytosolic  $H_2O_2$  concentration was elevated by TMX silencing.** (A) Representative images from the HyPer3 measurement on the TMX-silenced WM3734 cells and Mel Juso cells. (B, C and F) The quantification of the HyPer3 ratio values. Data are presented as mean $\pm$ SEM of at least 3 independent experiments. (The analyzed cell number N: WM3734, control=168, TMX1 kd=209, TMX3 kd=192; Mel Juso, control=297, TMX1 kd=343, TMX3 kd=440; WM1366, control=144, TMX1 kd=170.) (D, E and G) The quantification of the SypHer ratio values. Data are presented as mean $\pm$ SEM of 3 independent experiments. (The analyzed cell number N: WM3734, control=142, TMX1 kd=153, TMX3 kd=164; Mel Juso, control=72, TMX1 kd=95, TMX3 kd=101; WM1366, control=134, TMX1 kd=136.)

## 7.5 Silencing of TMXs inhibits NFAT1 activation via the oxidative modulation

### 7.5.1 The NFAT1 translocation is redox dependent

The signaling cascade of NFAT1 activation consists many proteins which can be regulated via reduction and oxidation reportedly. Based on our data, it is possible that the inhibition of NFAT1 activation by silencing of TMX1/TMX3 is caused by the elevation of cellular  $H_2O_2$ . Therefore, we tested the effect of  $H_2O_2$  on the NFAT1 activity by exposing the cells to different concentrations of extracellular  $H_2O_2$ . As shown in Figure 8A, extracellular  $H_2O_2$  inhibits NFAT1 translocation in a dose-dependent manner in WM3734 melanoma cells. The evaluation of dose effect curve pointed an  $IC_{50}$  value at an extracellular concentration of approximately  $13.2\mu M$  (Figure 8B). These results indicate that the NFAT1 translocation is a redox-dependent event and thus the elevation of cytosolic ROS can lead to its inhibition.

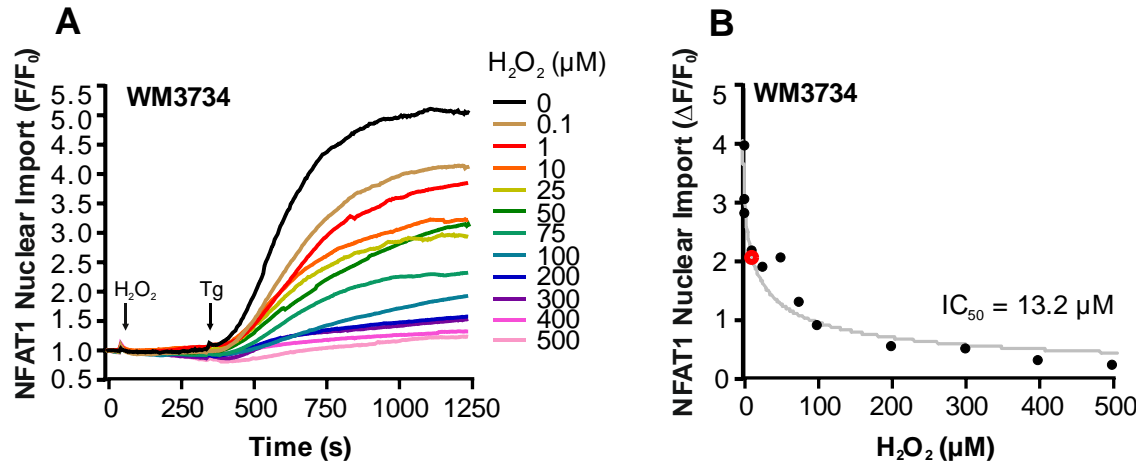


**Figure 8: The NFAT1 translocation is inhibited by extracellular  $H_2O_2$  in a dose-dependent manner.** (A) The NFAT1 translocation is inhibited by pre-incubation with various concentrations of extracellular  $H_2O_2$  to the WM3734 cells. Data are presented as mean of at least 4 cells from one experiment. (B) The quantification of the NFAT1 nuclear import by the end point and determination of  $IC_{50}$ .

### **7.5.2 The inhibition of NFAT1 activation induced by silencing of TMX1 can be reversed by antioxidants**

The thiol group of protein cysteine residues is very often a target for functional regulation via oxidation. The reductases in the cytosol reverse the oxidation using reducing resources in the cells such as glutathione and/or NADPH. Furthermore, the cells also have a well-balanced enzyme system for the degradation of ROS. The superoxide dismutase (SOD), peroxidases and catalases can catalyze the degradation of harmful ROS molecules and prevent oxidative damage. Thus, to test if the inhibition of NFAT1 caused by the silencing of TMX1/TMX3 can be reversed and prevented by antioxidants and ROS scavengers, the NFAT1 translocation assay was performed on the TMX1-silenced cells incubated with or without NAC (antioxidant and reducing reagent), PEG-catalase (ROS scavenger) and Dithiothreitol (DTT, reducing reagent). As shown in Figure 9A and B, NAC can partially rescue the inhibition of NFAT1 translocation induced by the silencing of TMX1 in both cell lines. Moreover, DTT and catalase can also reverse the NFAT1 inhibition in TMX-silenced WM3734 cells (Figure 9C), while NAC alone does not affect the NFAT1 translocation. The result from Mel Juso cells shows a similar trend though the statistics are insignificant because of the low sample numbers (Figure 9D). Based on these results, we conclude that the inhibition of NFAT1 caused by the silencing of TMX1 and TMX3 is mediated by the elevation of cellular ROS.

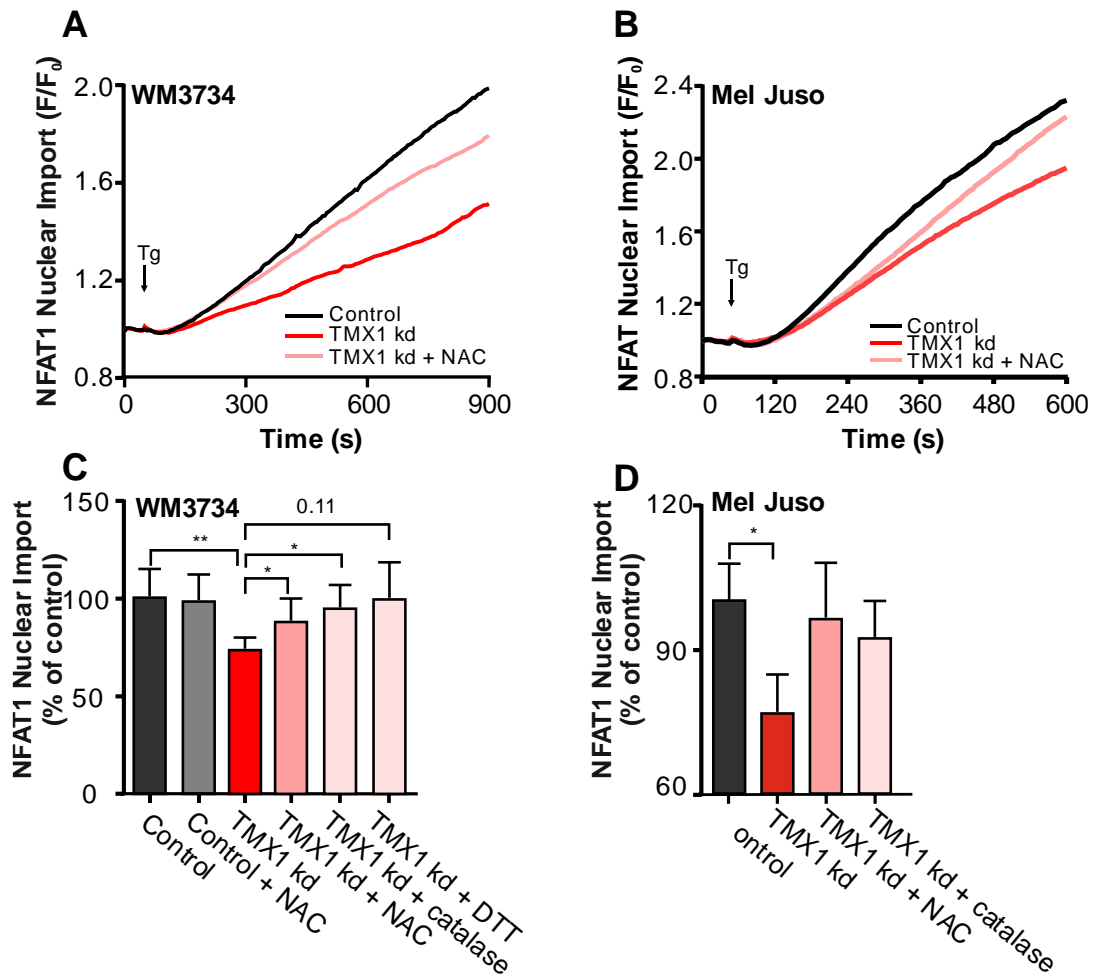


**Figure 9: The inhibition of NFAT1 activation induced by TMX1 silencing can be reversed by antioxidants.** (A) and (B) The NFAT1 translocation on TMX1-silenced WM3734 and Mel Juso cells, the cells were incubated with 100 $\mu$ M NAC for 48 hours prior to the assay and recorded with live cell imaging. Data are presented as mean of 3 independent experiments. (The analyzed cell number N: WM3734, control=73, TMX1 kd=57, TMX1 kd+NAC=63; Mel Juso, control=63, TMX1 kd=47, TMX kd+NAC=39.) (C) and (D) The Quantification of the end point from NFAT1 translocation assay on TMX1-silenced WM3734 cells and Mel Juso cells pre-incubated with 100 $\mu$ M NAC (48h), 50U/mL PEG-catalase (48h), 1mM DTT (20min). Data are presented as mean $\pm$ SEM of 3 independent experiments (+NAC) and (+catalase), 1 experiment (+DTT). (The analyzed cell number N: WM3734, control=73, control+NAC=19, TMX1 kd=57, TMX1 kd+NAC=63, TMX1 kd+catalase=58, TMX1 kd+DTT=22; Mel Juso, control=63, TMX1 kd=47, TMX kd+NAC=39, TMX1 kd+catalase=99.)

### **7.5.3 Calcineurin is a redox-sensitive element of NFAT1 signaling pathway**

#### **7.5.3.1 Calcineurin activity is inhibited by silencing of TMXs**

Several elements of the NFAT1 signaling pathway can be redox regulated. In principle, the ORAI channels on the plasma membrane consist of cysteine residues, which are prone to oxidation; the methionine oxidation of calmodulin could also be involved as well as the phosphatase calcineurin, which contains a reactive cysteine in its catalytic core and multiple cysteine residues around the catalytic site. Calcineurin dephosphorylates NFAT1 to initiate the nuclear transportation of NFAT1, thus it plays a critical role in the signaling cascade. Therefore, first we explored if calcineurin was the target for the oxidative modulation induced by the silencing of TMX1/TMX3 with a genetically encoded sensor CaNAR2-cyto. This protein sensor contains a sequence with dephosphorylation sites similar to the NFAT proteins and is therefore a mimic of natural target of calcineurin. Upon the dephosphorylation the configuration of this sensor changes, which leads to the decrease of distance between the CFP/YFP pair resulting an enhancement of FRET signal. The changes of FRET signal ratio indirectly report the phosphatase activity of calcineurin. As shown in Figure 10A, the silencing of TMX1/TMX3 leads to suppressed calcineurin activity, which is activated by Tg-induced calcium influx. The quantification of the basal levels and post-activation levels of calcineurin activity show that the silencing of TMX1/TMX3 decreases the basal as well as the induced calcineurin activity significantly in comparison with the control group (Figure 10B and C). To test if the inhibition is indeed due to oxidative modification, the cells were incubated with NAC after the siRNA transfection. The results in Figure 10 D and E show that indeed NAC restores the inhibited calcineurin activity in TMX-silenced WM3734 cells. The basal calcineurin activity at resting level (Figure 10D) as well as the maximum activity upon activation (Figure 10E) is restored to nearly the same level compared with control group.

According to these results, we conclude that the inhibition of NFAT1 nuclear import is caused by the inhibition of calcineurin activity.

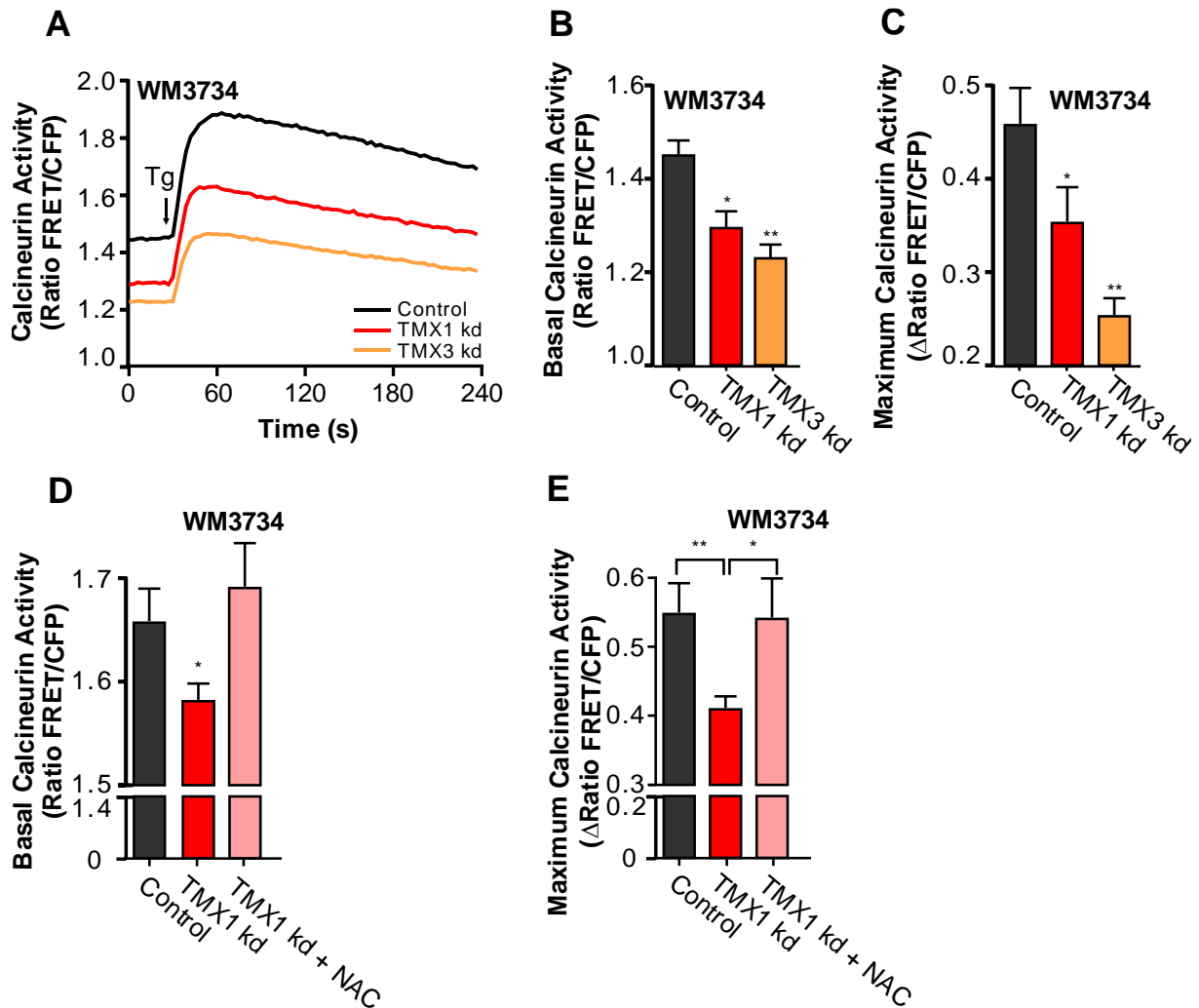


**Figure 10: The phosphatase activity of calcineurin is inhibited by TMX silencing.** (A) The cytosolic calcineurin activity of TMX-silenced melanoma cells was measured with CaNAR2-cyto protein sensor upon 1 $\mu$ M Tg+1 $\mu$ M Ionomycin induced calcium influx in Ringer's buffer with 1mM free Ca<sup>2+</sup> and shown as curves on a time course. Data are presented as mean of 3 independent experiments. (The analyzed cell number N: control=49, TMX1 kd=48, TMX3 kd=63.) (B) The quantification of the basal calcineurin activity in WM3734 cells at resting state. (C) The quantification of the maximum calcineurin activity induced by Tg+Ionomycin, the ratio values from basal activity are subtracted from the maximum ratio value. (D) and (E) The quantification of basal and maximum calcineurin activity measured on the TMX1-silenced WM3734 cells with/without 100 $\mu$ M NAC pre-incubation for 48 hours. Data are presented as mean $\pm$ SEM of 2 independent experiments. (The analyzed cell number N: control=15, TMX1 kd=24, TMX1 kd+NAC=19.)

### 7.5.3.2 Calcineurin activity could be inhibited by H<sub>2</sub>O<sub>2</sub>

To further test the redox sensitivity of calcineurin, we exposed melanoma cells to various concentration of H<sub>2</sub>O<sub>2</sub> for 5 min before the stimulation with Tg in Ringer's buffer with 1mM free Ca<sup>2+</sup>. We again used CaNAR2-cyto sensor to determine calcineurin activity. As shown in Figure 11A, the calcineurin activity shows a H<sub>2</sub>O<sub>2</sub> concentration dependence in the time-lapse assay. The normalized results show that the maximum calcineurin activity is inhibited by the extracellular H<sub>2</sub>O<sub>2</sub> in a dose-dependent manner (Figure 11B). In all, these data indicate that calcineurin activity depends on the intracellular redox state; thus, the TMX silencing induced excessive ROS is responsible for the inhibition of NFAT1 nuclear import.

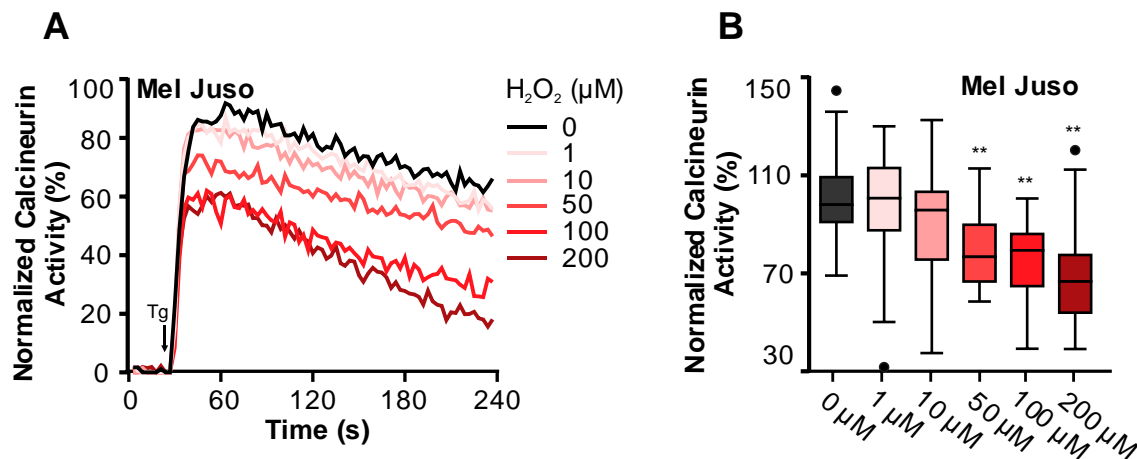


**Figure 11: Calcineurin activity is inhibited by H<sub>2</sub>O<sub>2</sub> in melanoma.** (A) Mel Juso cells were pre-incubated with different concentration of extracellular H<sub>2</sub>O<sub>2</sub> in Ringer's buffer containing 1mM free Ca<sup>2+</sup> for 5min, then cells were stimulated with Tg and the cytosolic calcineurin was measured with CarNAR2-cyto sensor. Data is normalized according the basal calcineurin activity and presented as the mean of at least 20 cells. (B) The quantification of maximum calcineurin activity. Data is presented as mean±SEM of at least 20 cells from 1 experiment.

## **7.6 Mitochondria are major source for ROS generation following TMX silencing**

### **7.6.1 Silencing of TMXs does not induce ER stress**

Based on our results from cytosolic ROS measurements, the elevated cellular H<sub>2</sub>O<sub>2</sub> levels in melanoma cells indicate that the redox balance is disturbed by silencing of TMX1 or TMX3. However, the source of this ROS production remains elusive so far. The TMX1 and TMX3 are anchored within the ER membrane with the active site hanging in the ER lumen. It is possible that the knockdown of TMX1/TMX3 might disturb the oxidative folding of proteins and lead to the ER stress, which may consequently induce oxidative stress in the cytosol in extreme cases. To test this theory, we investigated if the silencing of TMX induced ER stress in melanoma cell lines by measuring ER stress markers such as XBP1 splicing products, Bip and disulfide isomerase protein expression (PDI). The splicing product of X-box binding protein 1 (XBP1) was quantified by qPCR, and the protein expression of protein disulfide isomerase and binding immunoglobulin protein (BiP) were assessed with WB. As shown in Figure 12A, compared with the positive control group which was treated with thapsigargin for 4 hours, the XBP1s mRNA level is not increased in TMX1/TMX3 silenced melanoma cells. Furthermore, the Figure 12B shows that the PDI and BiP expression are also not elevated following TMX1/TMX3 silencing (Figure 12B). These findings indicate that silencing of the TMX proteins, despite their important role in oxidative folding, does not lead to significant accumulation of unfolded proteins and unfolded protein response (UPR) in the ER.

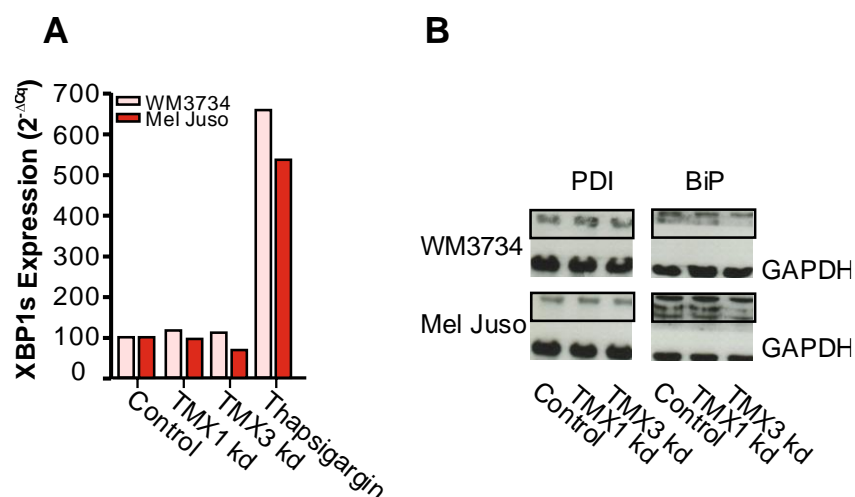


**Figure 12: TMX silencing does not trigger ER stress in melanoma cells.** (A) The splicing product of XBP1 was quantified by qPCR from samples collected 48 hours after the siRNA transfection, the positive control was treated with 1 $\mu$ M Tg for 4 hours to induce the ER stress. Data are presented as mean of 2 independent experiments. (B) The expression of PDI and BiP proteins was quantified by Western Blot from the lysates collected 48 hours after the siRNA transfection, the GAPDH was used as the loading control. The blots are representative images of two independent experiments.

### 7.6.2 Silencing of TMX1 does not affect ER redox homeostasis

To further check if the ER redox homeostasis was disturbed by the silencing of TMX, we measured ER H<sub>2</sub>O<sub>2</sub> levels with the genetically encoded protein sensor ER HyPer in TMX1-silenced WM3734 and Mel Juso cells. The cells were transfected with the siRNA against TMX1 and scrambled control; and the plasmids of ER HyPer were transfected 24 hours prior to the measurement. Forty-eight hours after the siRNA transfection, the cells were placed into a Ringer's buffer with 0.25mM Ca<sup>2+</sup> and imaged. As shown in Figure 13 (A and B), the silencing of TMX1 increases the ER H<sub>2</sub>O<sub>2</sub> level moderately in both cell lines. However, this result needs to be interpreted with particular care. The ER lumen is a highly oxidizing compartment due to its function in oxidative folding of proteins. Hence, the majority of the HyPer probes within the ER lumen are at least partially oxidized (Figure 13C). Nonetheless, the probes can still detect H<sub>2</sub>O<sub>2</sub> increase when applied externally (Figure 13D). These data

suggest that the ER lumen is very likely not the main source of ROS following the silencing of TMX1/TMX3, though the contribution can't be fully excluded.

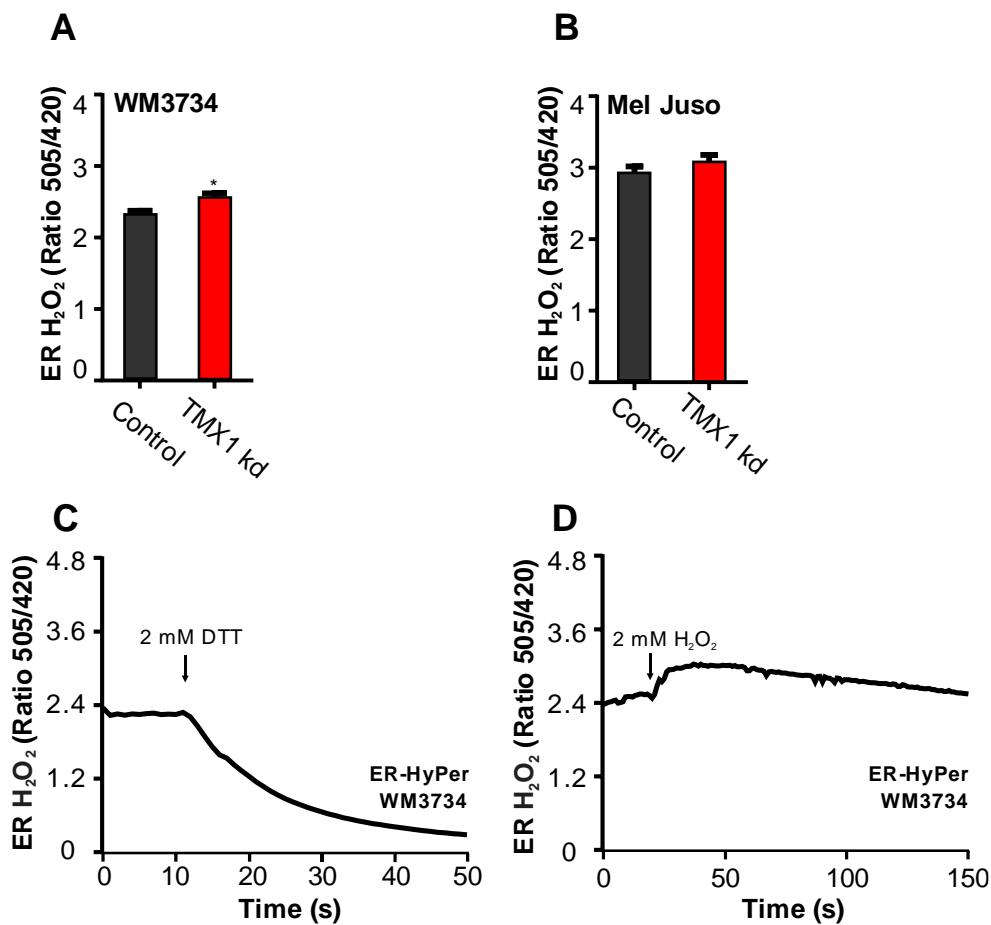


**Figure 13: The ER lumen is not a major source of H<sub>2</sub>O<sub>2</sub> in melanoma cells following TMX1 silencing.** (A) and (B) The quantification of results from ER HyPer experiment on the TMX1-silenced WM3734 cells and Mel Juso cells 48 hours after the siRNA transfection. Data are presented as mean±SEM of 3 independent experiments. (The analyzed cell number N: WM3734, Control=169, TMX1 kd=179; Mel Juso, Control=211, TMX1 kd=249.) (C) and (D) DTT and H<sub>2</sub>O<sub>2</sub> titration of ER HyPer probes on native WM3734 cells. Data are presented as mean±SEM of 4 cells from 1 experiment.

### 7.6.3 Mitochondrial ROS is increased by silencing of TMXs

TMX1 and TMX3 are enriched in the MAM section of ER and mitochondria contact sites reportedly. These contact sites have profound influence on many functions of the two organelles. Thus, the silencing of TMX1/TMX3 may lead to disrupted mitochondrial function,

which might induce generation of ROS. We next measured H<sub>2</sub>O<sub>2</sub> levels in mitochondria with the genetically encoded protein sensor mito-HyPer2 in WM3734 and Mel Juso cells. As seen, the silencing of TMX1/TMX3 results in a significant increase of HyPer signal ratio (Figure 14A) in both cell lines. The quantification of the HyPer probe ratio shows that silencing of TMX1 and TMX3 induced dramatic H<sub>2</sub>O<sub>2</sub> generation on the WM3734 and Mel Juso cells (Figure 14B and C). Using a mito-SypHer sensor we monitored the mitochondrial pH under the same conditions described above. Our results show the silencing of TMX1/TMX3 does not cause overt changes of mitochondrial pH (Figure 14D and E).

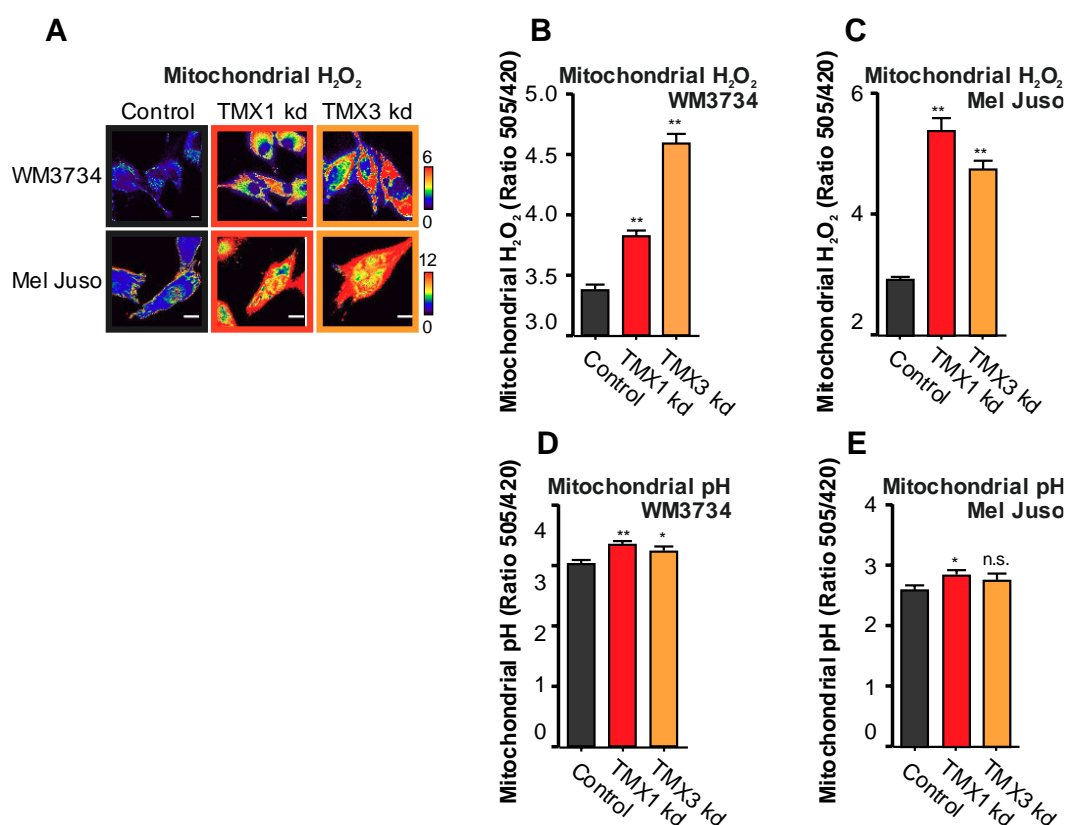


**Figure 14: TMX silencing induces significant increase of mitochondrial ROS.** (A) Representative images of mito-HyPer2 measurements on TMX-silenced WM3734 and Mel Juso cells. (B) Quantification of mito-HyPer2 ratio on the WM3734 cells 48 hours after the siRNA transfection. Data are presented as mean±SEM of at least 3 independent experiments. (The analyzed cell number N: control=546, TMX1 kd=510, TMX3 kd=621.) (C) Quantification of mito-HyPer2 ratio on the Mel Juso cells 48 hours after the siRNA transfection. Data are presented as mean±SEM of at least 3 independent experiments. (The analyzed cell number N: control=416, TMX1 kd=418, TMX3 kd=442.) (D) Quantification of

mito-SyPer ratio on the WM3734 cells 48 hours after the siRNA transfection. Data are presented as mean $\pm$ SEM of 3 independent experiments. (The analyzed cell number N: control=87, TMX1 kd=85, TMX3 kd=105.) (D) Quantification of mito-SyPer ratio on the Mel Juso cells 48 hours after the siRNA transfection. Data are presented as mean $\pm$ SEM of 3 independent experiments. (The analyzed cell number N: control=74, TMX1 kd=73, TMX3 kd=83.)

## **7.6.4 Elevated mitochondrial ROS is caused by altered mitochondrial metabolism**

### **7.6.4.1 Mitochondrial calcium level is increased by TMX1 silencing**

The mitochondrial ROS generation is coupled to the mitochondrial oxidative phosphorylation and respiration activity. The irregular mitochondrial ROS generation is frequently caused by either the electron leakage from the disrupted of electron transfer chain (ETC) or a hyper-activation of oxidative phosphorylation which produces ROS molecules as a “by-product” (162, 250). The accumulation of mitochondrial  $\text{Ca}^{2+}$  ( $[\text{Ca}^{2+}]_{\text{mito}}$ ) can drive the activation of the mitochondrial metabolic machinery and enhance the ATP synthesis. Hence, because of the dependence of ATP synthesis on  $[\text{Ca}^{2+}]_{\text{mito}}$ , the  $[\text{Ca}^{2+}]_{\text{mito}}$  is a good indicator for mitochondrial metabolic activity. Accordingly, we measured mitochondrial calcium dynamics with a genetically encoded  $\text{Ca}^{2+}$  sensor 4mt-D3cpV in WM3734 cells with stable TMX1 knockdown. As shown in Figure 15A, the silencing of TMX1 leads to an increase in resting  $[\text{Ca}^{2+}]_{\text{mito}}$  as well as in SOCE-induced  $[\text{Ca}^{2+}]_{\text{mito}}$  influx. The quantification data in (Figure 15B) shows the basal  $[\text{Ca}^{2+}]_{\text{mito}}$  is increased slightly by the silencing while the uptake is increased significantly compared with the control (Figure 15C). However, due to the low  $K_d$  of 4mt-D3cpV, the sensor could be saturated and will no longer answer to the elevation of  $\text{Ca}^{2+}$  upon a dramatic change. To address this issue, we used alternative genetically encoded protein sensor 4mt-TNXL, which has a higher  $K_d$  and performed the same measurements as with 4mt-D3cpV. As shown in Figure 15D, the  $[\text{Ca}^{2+}]_{\text{mito}}$  dynamics show a similar pattern, thus

confirm that the  $[Ca^{2+}]_{mito}$  levels are increased by of TMX1 silencing. Furthermore, the quantification data show the basal  $[Ca^{2+}]_{mito}$  is increased significantly (Figure 15E) as well as mitochondrial  $Ca^{2+}$  uptake (Figure 15F).

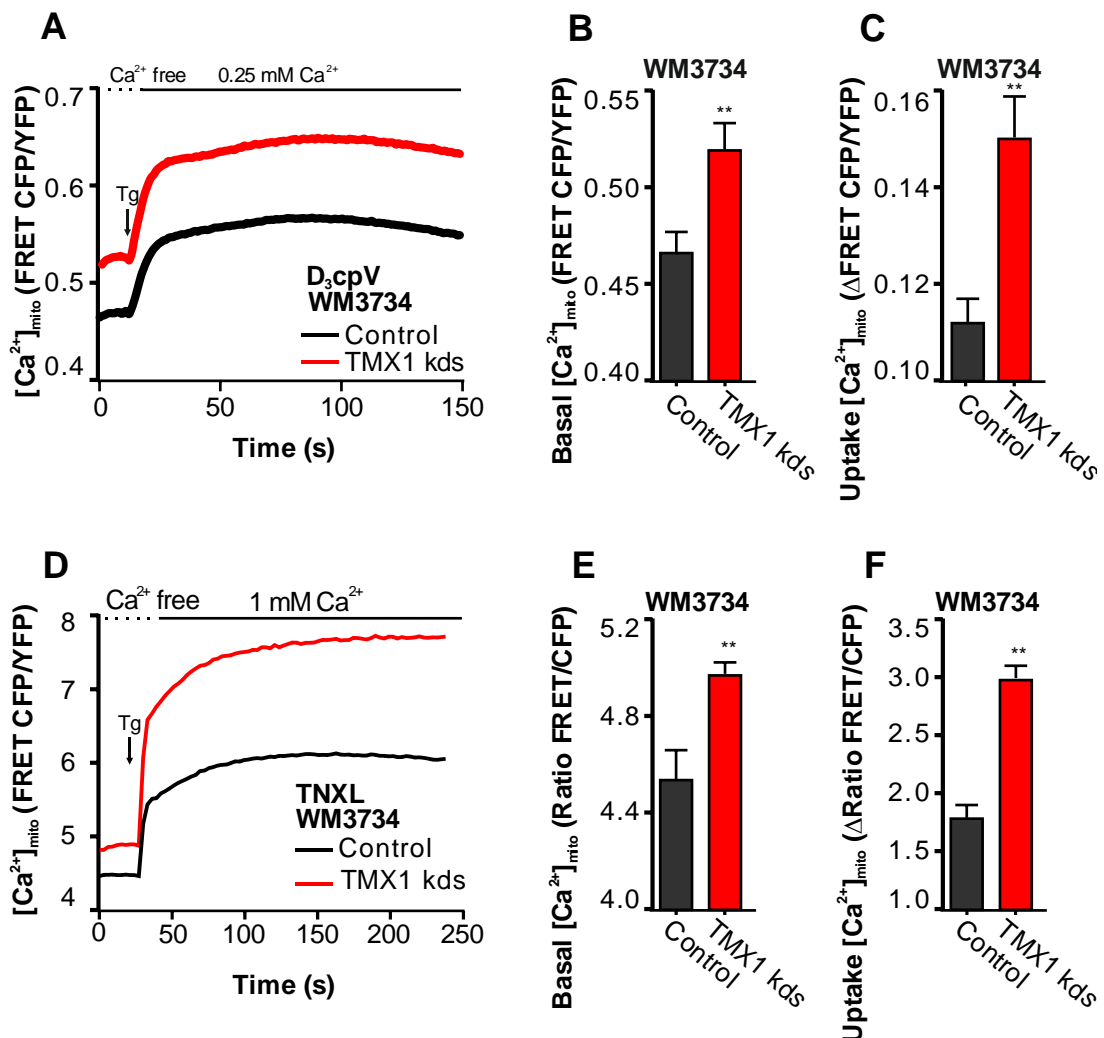


**Figure 15: Mitochondrial calcium uptake is increased following TMX1 silencing.** (A) The mitochondrial  $Ca^{2+}$  uptake was measured with genetically encoded protein sensor 4mt-D<sub>3</sub>cpV on WM3734 cells with a stable expression of shRNA against TMX1. Data are presented as mean of 3 experiments on a time course. (B) Quantification of the basal mitochondrial  $Ca^{2+}$  level from data in (A). Data are presented as mean±SEM. (The analyzed cell number N: control=62, TMX1 kd=45.) (C) Quantification of the mitochondrial  $Ca^{2+}$  uptake (basal-plateau) from data in (A). Data are presented as mean±SEM. (The analyzed cell number N: control=62, TMX1 kd=45.) (D) The mitochondrial  $Ca^{2+}$  uptake was measured with genetically encoded protein sensor 4mt-TNXL on WM3734 cells with a stable expression of shRNA against TMX1. Data are presented as mean of 1 experiment on a time course. (E) Quantification of the basal mitochondrial  $Ca^{2+}$  level from data in (D). Data are presented as mean±SEM. (The analyzed cell number N: control=94, TMX1 kd=83.) (F) Quantification of

the mitochondrial  $\text{Ca}^{2+}$  uptake (basal-plateau) from data in (D). Data are presented as mean $\pm$ SEM. (The analyzed cell number N: control=94, TMX1 kd=83.)

Next, we used a more detailed protocol, which separates the calcium transfer from ER and from PM into mitochondria. The cells were transiently transfected with siRNA against TMX1 and D<sub>3</sub>cpV sensor as before. Forty-eight hours later the cells were imaged in Ringer's buffer with 0 mM  $\text{Ca}^{2+}$  for a few seconds. Thereafter, the ER  $\text{Ca}^{2+}$  store depletion was triggered with Tg, in order to monitor calcium transfer from ER to mitochondria. To evaluate the PM-mitochondria  $\text{Ca}^{2+}$  transfer the extracellular  $\text{Ca}^{2+}$  was elevated to 1 mM. As shown in Figure 16A-C, the ER-mito transfer is decreased albeit the PM-mitochondria  $\text{Ca}^{2+}$  transfer is increased by silencing of TMX1-silenced cells. Thus, our data suggest that the increased calcium transfer from the plasma membrane is largely responsible for the increased  $[\text{Ca}^{2+}]_{\text{mito}}$  following TMX1 silencing, and the transfer from ER is restrained. Taking the difference between the extracellular compartment and the ER into account, the overall effect of TMX1 silencing should lead to an elevated mitochondrial calcium dynamic. These results also hint that mitochondrial metabolism should be enhanced in due by the elevation of mitochondrial calcium level.

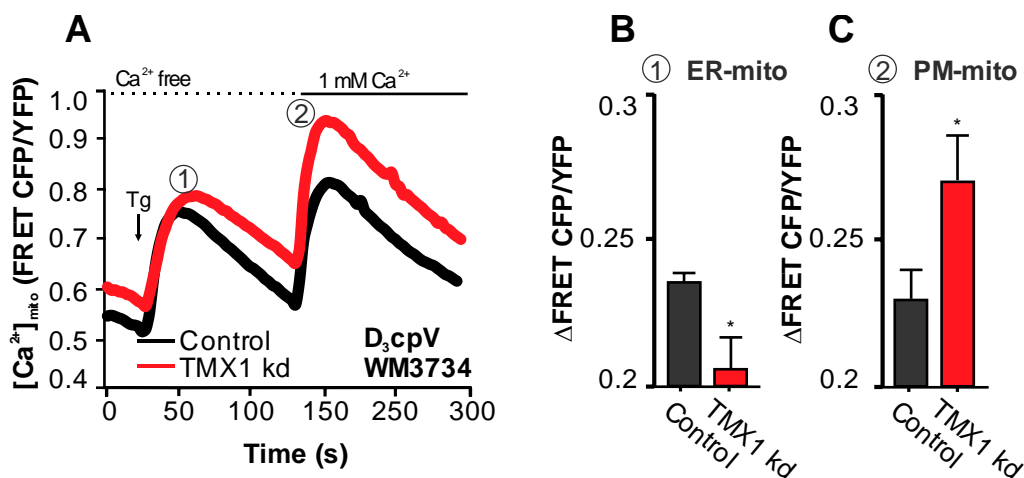


**Figure 16: The PM to mitochondria calcium transfer is increased following TMX1 silencing.** (A) The mitochondrial  $\text{Ca}^{2+}$  uptake was measured with genetically encoded protein

sensor 4mt-D<sub>3</sub>cpV on WM3734 cells 48 hours after the siRNA transfection. Data are presented as mean of 3 independent experiments on a time course. (B) Quantification of the ER-mito calcium transfer from data in (A). (The analyzed cell number N: Control=124, TMX1 kd=109.) (C) Quantification of the PM-mito calcium transfer from data in (A). (The analyzed cell number N: Control=124, TMX1 kd=109.)

#### 7.6.4.2 Mitochondrial ATP is elevated by TMX1 silencing

To test our speculations on the role of TMX1 on mitochondrial metabolic activity, we measured mitochondrial ATP in the stable knockdown cell lines with a genetically encoded mitochondria targeted ATeam1.03 protein sensor. The results shown in Figure 17A confirm that the mitochondrial ATP level is higher in the TMX1-silenced cell lines. The quantification data in Figure 17B depicts a significant increase in the resting mitochondrial ATP in both TMX1-downregulated melanoma lines.

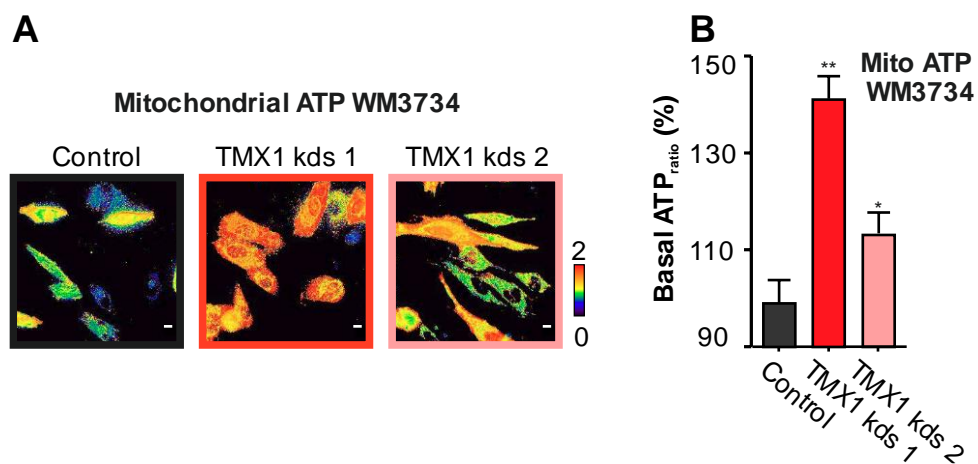


**Figure 17: The basal mitochondrial ATP level is increased following TMX1 silencing.** (A) The representative images from mito-ATeam1.03 measurements in WM3734 cells stably expressing shRNA against TMX1. Bars represent 10 $\mu$ m. (B) Quantification of basal mitochondrial ATP data, all data were normalized to the Control and shown in percentage. Data are presented as mean $\pm$ SEM of 3 independent experiments. (The analyzed cell number N: Control=481, TMX1 kds 1=583, TMX1 kds 2=419.)

Additionally, to confirm the mitochondrial metabolism is altered by the silencing of TMX1, the oxygen consumption rate (OCR) of TMX1-silenced WM3734 cells was examined with a Seahorse XF96 extracellular Flux Analyzer by our collaborators in the Biochemistry department. As shown in their results (Panel EV5G, H, I)(249), the TMX1-silenced WM3734 cells show a higher basal OCR as well as maximal OCR compared with the control. Although from the quantification data, one of the clones does not show a significant increase of basal and maximal respiration (TMX1 knockdown stable 1, TMX1 kds1), the overall trend shows a strong increase of OCR which confirms that the capacity of oxidative phosphorylation is increased following silencing of TMX1.

Summarized, our data shows that the silencing of TMX1 can alter the mitochondrial metabolism via an increase of the mitochondrial calcium uptake, which further boosts the capacity of mitochondrial respiration. The higher mitochondrial respiration produces more ATP and increases the rate of ROS generation.

### **7.6.5 TMX1 silencing alters mitochondrial morphology**

The altered mitochondrial  $\text{Ca}^{2+}$  levels could be caused by several factors including the up-regulation of mitochondrial calcium uniporter (MCU) or other channels, but the proximity of mitochondria to the calcium stores and channels also plays an important role. Since the calcium data show a strong increase of PM to mitochondria calcium transfer while the ER to mitochondria calcium transfer is reduced, the positioning of mitochondria and communication between mitochondria and ER in this case may be critical for the outcome. The similar observations were reported before, that during T cell activation, the cell polarization causes re-organization of the mitochondrial network to facilitate mitochondrial calcium uptake (251), and the sustained absorption of calcium by mitochondria can extend the calcium influx via plasma membrane and activation of T cells. In these observations, the structural changes are

initiative and critical for the following response in calcium signaling. To examine if the silencing of TMX1 caused any structural and morphological alterations of mitochondria, the mitochondrial morphology in the TMX1-silenced stable melanoma cell lines was examined with 3D confocal fluorescent microscopy by our collaborator Dr. Miso Mitkovski. As shown in Panel 5(G, H)(249), the silencing of TMX1 leads to a significant increase of mitochondrial total volume and surface, alterations that could lead to a higher exposure of mitochondria to the surrounding environment. Thus, the area of mitochondria exposed to the plasma membrane might be affected by the knockdown of TMX1. Further examination of the mitochondrial content in the vicinity of the plasma membrane with ImageJ software showed Panel 5(I, J)(249) that the area occupied by peripheral mitochondria is increased more than two folds in the TMX1 silenced cells. These data suggest the knockdown of TMX1 may lead to re-organization of mitochondria network and alteration of mitochondria morphology.

Based on the analysis of mitochondrial calcium uptake and morphology, it is postulated that the alteration of MAM structure might be responsible for the re-organization of mitochondria upon TMX1 knockdown. Therefore, the MAM structure and the mitochondrial positioning in the stable knockdown cells were investigated by our collaborators in Canada using electron microscopy. The quantified data show that the distance between mitochondria and PM is reduced by nearly 40% (Figure 18B), while the distance between mitochondria and ER is increased by nearly 25% (Figure 18C) in the TMX1-silenced melanoma cells. And the MAM length is shortened by nearly 30% (Figure 18D). These data suggest the knockdown of TMX1 shortens MAM length and causes a positioning shift of mitochondria network from ER adjacent area to the plasma membrane peripheral in melanoma cells (Figure 18A). Based on these findings, we conclude that the disturbance of MAMs and the mitochondrial re-positioning caused by the knockdown of TMX1 enhance the exposure of mitochondria to PM, ultimately lead to a higher exposure of mitochondria to calcium hotspots near the PM.

Consequently, the plasma membrane-derived mitochondrial  $\text{Ca}^{2+}$  uptake is increased upon SOCE activation.

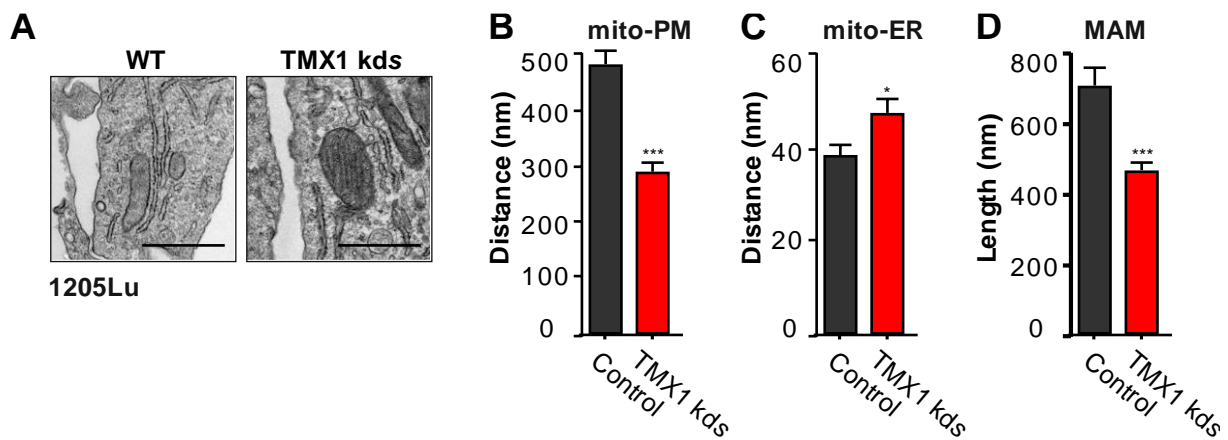


**Figure 18: Mitochondrial repositioning towards the plasma membrane in melanoma cells following TMX1 silencing.** (A) Representative images of the electron microscopy from TMX1-silenced 1205Lu cells. (B) Quantification of the distance between mitochondria and plasma membrane. Data are presented as mean±SEM. (The analyzed cell number N: Control=100, TMX1 kds=100.) (C) Quantification of the distance between mitochondria and ER. Data are presented as mean±SEM. (The analyzed cell number N: Control=60, TMX1 kds=60.) (D) Quantification of MAM length. Data are presented as mean±SEM. (The analyzed cell number N: Control=60, TMX1 kds=60.)

*\*The establishment of TMX1 stable knockdown cell line is done by Xin Zhang. The electron microscopy experimental data were generated by Nasser Tahbaz, Lucas Mina and Prof. Dr. Thomas Simmen, data processing was done by Xin Zhang.*

The disturbance of MAM structure can cast strong influences on the function and homeostasis of it reportedly. The structural studies already proved that the TMX1 silencing led to mitochondria repositioning and morphology changes, yet we searched for a direct observation of the redox homeostasis in MAM upon the silencing of TMX proteins. The MAM targeted HyPer sensor (unpublished work) was used to measure the  $\text{H}_2\text{O}_2$  level upon a 48h transient silencing of TMX1 and TMX3. As shown in Figure 19A, although some of the protein sensors are retained in part of the whole mitochondria to ER network, the expression of this sensor is seemingly in a cross section of ER and mitochondria. The quantifications from

Figure 19B show that indeed the silencing of TMX1 or TMX3 induces a relatively significant increase of H<sub>2</sub>O<sub>2</sub> in MAM domain.

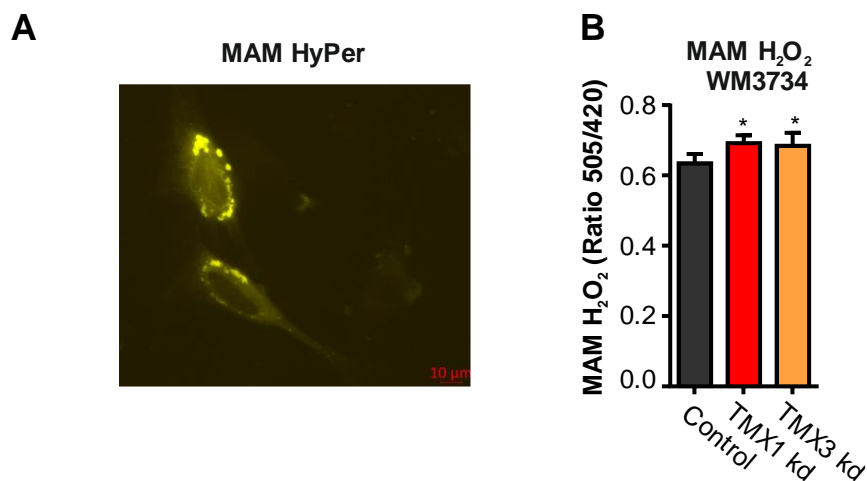


**Figure 19: Mitochondrial repositioning disturbed redox homeostasis in MAM.** (A) Representative image of the MAM-HyPer protein sensor in WM3734 cells. (B) Quantification of the H<sub>2</sub>O<sub>2</sub> level in MAM upon transient silencing of TMX1 and TMX3. Data are presented as mean±SEM of 2 independent experiments. (The analyzed cell number N: Control=17, TMX1 kd=15, TMX3 kd=10.)

In summary, our data on mitochondrial function and morphology suggest that the silencing of TMX1 can alter the mitochondrial morphology and positioning which lead to an increase of mitochondrial calcium uptake, higher metabolic activity and ultimately the elevated mitochondrial ROS production. The disturbance also caused a disruption of MAM redox homeostasis directly, leading to higher level of H<sub>2</sub>O<sub>2</sub> accordingly. Our findings highlight TMX oxidoreductases as important elements in regulating the MAM stability and mitochondrial architecture.

## 7.7 NOX4 is an alternative source of ROS

The NADPH oxidase (NOX) family enzymes are a set of oxidases that generate superoxide via oxidation of NADPH. There is growing evidence that NOX enzymes together with the

mitochondria are major intracellular sources of ROS. The NOX4 has been suggested to be a membrane bound protein localized in PM, mitochondria and ER (252-255). Accordingly, we asked if NOX4 played a role in the ROS induction by upon TMX1 silencing. For this purpose, we measured cellular H<sub>2</sub>O<sub>2</sub> concentration in TMX1-silenced cells with additional NOX4 knockdown or treatments with the NOX4 inhibitor GKT137831. Our results show that both silencing of NOX4 or suppression of its activity lead to reduction in ROS levels in TMX1-silenced cells (Figure 20A-B). Importantly, the knockdown or the inhibition of NOX4 causes only a minor change of cellular pH in WM3734 cells (Figure 20C).

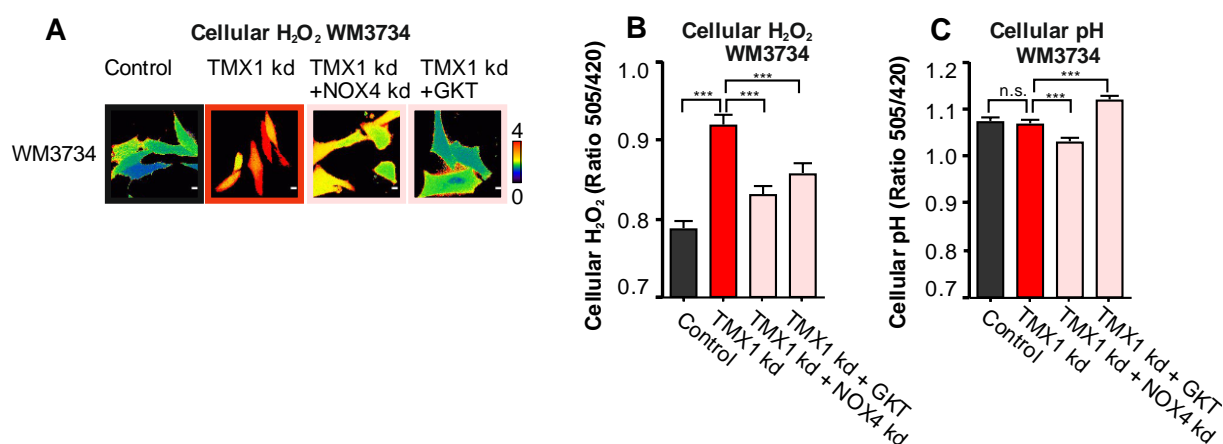


**Figure 20: The NOX4 is an alternative source of excessive cellular ROS.** (A) Representative ratiometric images of HyPer3 measurement on the WM3734 cells transfected with TMX1 siRNA, both TMX1 siRNA and NOX4 siRNA or treated with the NOX4 inhibitor GKT137831 (140nM) for 48 hours. Bars represent 10 $\mu$ M. (B) The quantification of the HyPer3 data. Data are presented as mean $\pm$ SEM of 3 independent experiments. (The analyzed cell number N: Control=837, TMX1 kd=888, TMX1 kd+NOX4 kd=793, TMX1+GKT=844.) (C) The quantification of the SypHer data as pH control for HyPer3. Data are presented as mean $\pm$ SEM of 3 independent experiments. (The analyzed cell number N: Control=265, TMX1 kd=233, TMX1 kd+NOX4 kd=187, TMX1+GKT=194.)

In sum, we conclude that the elevation of cytosolic ROS in the TMX1/TMX3-silenced cells is caused by the increased ROS production both from mitochondria and NOX4, though the proportion of the contributions between them remain undetermined.

## **7.8 TMX-ROS-NFAT1 signaling axis controls melanoma behavior**

### **7.8.1 TMX-ROS-NFAT1 axis promotes melanoma proliferation**

The TMX1 was reported as a suppressor of melanoma previously but notably only in a single cell line based study (228). The role of NFAT1 in melanoma was mostly yet to be revealed. Since the known literature never investigated these two elements in an integrative way on melanoma pathology, we next proceeded to investigate the impact of TMX-ROS-NFAT1 axis on melanoma pathology. Our data indicated that TMX1 and NFAT1 might have a close association with melanoma progression; hence we first started with examining the proliferation of melanoma cells upon suppression of TMX1/3 and NFAT1.

As shown in Figure 21A, the silencing of TMX1/TMX3 significantly inhibits the proliferation of WM3734 and Mel Juso cells (19% and 21% for TMX1; 29% and 39% for TMX3) around at 48 hours after the siRNA transfection while the inhibition on the WM1366 cells (non-NFAT1 expression line) is less pronounced (10% for TMX1; 8% for TMX3). To test if oxidative stress controls these effects on cell proliferation, the cells were treated with antioxidants. NAC and the mitochondria targeted antioxidant mTEMPO were used on the TMX1-silenced WM3734 cells. Figure 21C shows that both antioxidants can reverse the TMX1-silencing induced inhibition of proliferation, but NAC has a stronger potency. The three cell lines used for our experiment have different BRAF (mutation), NRAS (mutation) and NFAT1 (expression) status, so the data hint for a more general mechanism among melanoma cells. Based on these results, we conclude that the TMX-NFAT1 axis controls proliferation of melanoma cells regardless of their mutation status. Notably, NFAT1 expression affects the potency of TMX knockdown induced inhibition of proliferation, the inhibition of its activation also causes additional suppression of melanoma proliferation.

The siRNA mediated silencing usually provides only a very limited time window to examine the role of a certain protein. In order to examine the long-term effects of TMX silencing, we

measured proliferation in melanoma cells with stable TMX1 downregulation. As shown in Figure 21B, the proliferation of two cell lines with stable knockdown of TMX1 is also suppressed by 30%~40%, a finding that confirms that silencing of TMX proteins causes inhibition of melanoma cell proliferation in 2D culture in both short and long periods.

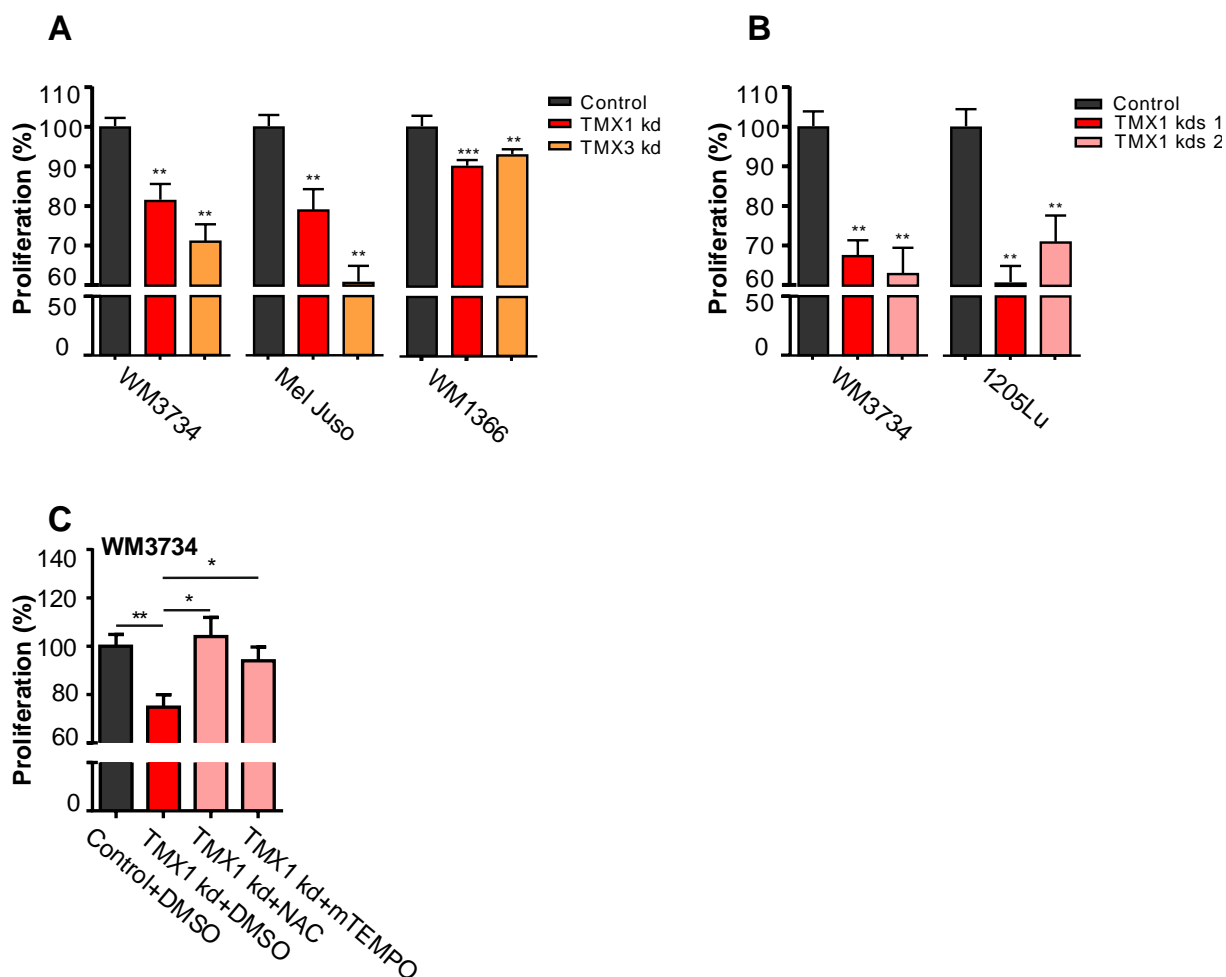


**Figure 21: Proliferation of melanoma cells is inhibited following TMX silencing.** (A) The proliferation was measured by cell titer blue assay on WM3734, Mel Juso and WM1366 cells 48 hours after transfection of siRNA against TMX1 and TMX3. Data are normalized to the percentage of control and presented as mean±SEM of at least 4 independent experiments. (B) The proliferation was measured by cell titer blue on WM3734 cells and 1205Lu cells stably expressing shRNA against TMX1. Data are normalized to the percentage of control and presented as mean±SEM of 3 independent experiments. (C) The NAC and mTEMPO were used to rescue the proliferation inhibition induced by TMX1 kd on WM3734 cells. After the siRNA transfection, the antioxidants were added and incubated with the cells for 48 hours, the proliferation was assessed with cell titer blue assay. Data are normalized to the percentage of control and presented as mean±SEM of 3 independent experiments.

Next, we tested if silencing of NFAT1 could induce similar effects on melanoma cell proliferation. Our data show that silencing of NFAT1 mediated by siRNA significantly inhibits the proliferation of both WM3734 and MelJuso melanoma cell lines (Figure 22A). To further test the role of NFAT1, we treated the cells with various concentrations of dipyridamole, a drug that disrupts NFAT1-calcineurin interaction. Our results show an inhibition of melanoma cell proliferation in a dose-dependent manner during a period of 72 hours by disrupting NFAT1 docking to calcineurin (Figure 22B). In all, these data suggest that TMX1/TMX3 and NFAT1 promote melanoma cell proliferation, and suppression of these proteins has a negative effect on the proliferation of melanoma cells in 2D culture.

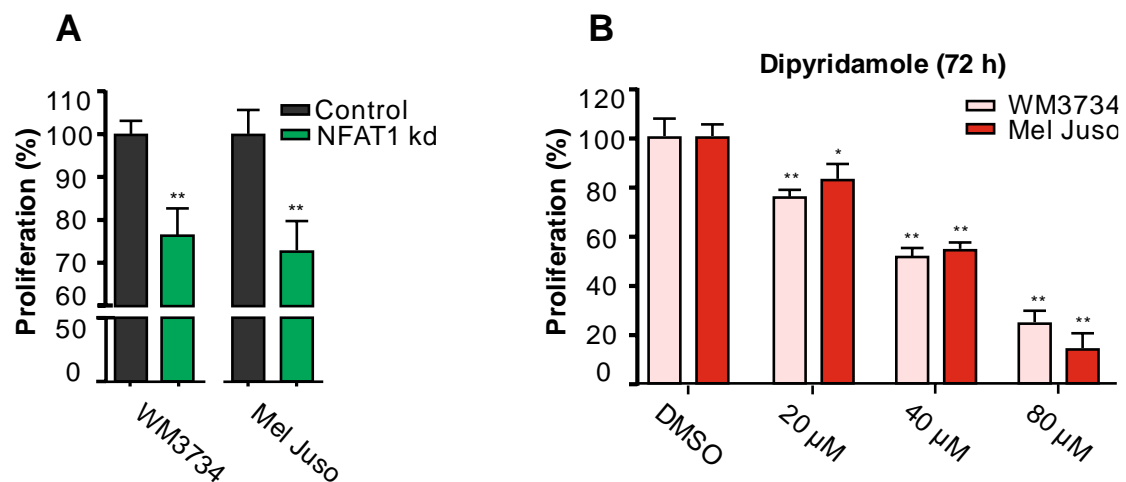


**Figure 22: The proliferation of melanoma cells is inhibited by suppression of NFAT.** (A) The proliferation was measured with cell titer blue assay on WM3734 cells and Mel Juso cells 24 hours after the transfection with siRNA against NFAT1. Data are normalized to the percentage of control and presented as mean±SEM of 3 independent experiments. (B) The proliferation was measured with cell titer blue assay on WM3734 cells and Mel Juso cells 72 hours after treatment with various concentration of Dipyridamole. Data are normalized to the percentage of control and presented as mean±SEM of 3 independent experiments.

### 7.8.2 TMX-ROS-NFAT1 axis promotes melanoma migration

Cellular invasiveness is the important parameter correlated with progression of cancers (256). We thus investigated if TMX-ROS-NFAT1 axis played a role in the migration of melanoma

cells. Figure 23A shows that silencing of TMX1/TMX3 inhibits migration of WM3734 cells by up to 35% and 50%, respectively. But this effect was not observed in the NFAT1-negative WM1366 cells, which indicates that NFAT1 may be more critical in the regulation of migration. Moreover, the inhibition of melanoma cell migration is reversed by NAC and mTEMPO suggesting involvement of redox regulation (Figure 23B). Furthermore, Inhibition of NFAT1-calcineurin interaction or calcineurin activity by dipyridamole or Cyclosporine A also suppresses the migration of WM3737 and 1205Lu cells significantly (Figure 23C). As depicted, the Dipyridamol treatment reduces WM3734 and 1205Lu cell migration by around 25% and 45%; Cyclosporine A inhibits the migration by nearly 40% in WM3734 cells and 30% in 1205Lu cells. The invasion measurements also show that stable knockdown of TMX1 may inhibit the invasion of WM3734 cells into Matrigel (Panel 6H) (249). Taken together, our data suggest that the TMX1, TMX3 and NFAT1 promote melanoma cell migration and invasion via redox-regulated mechanisms.

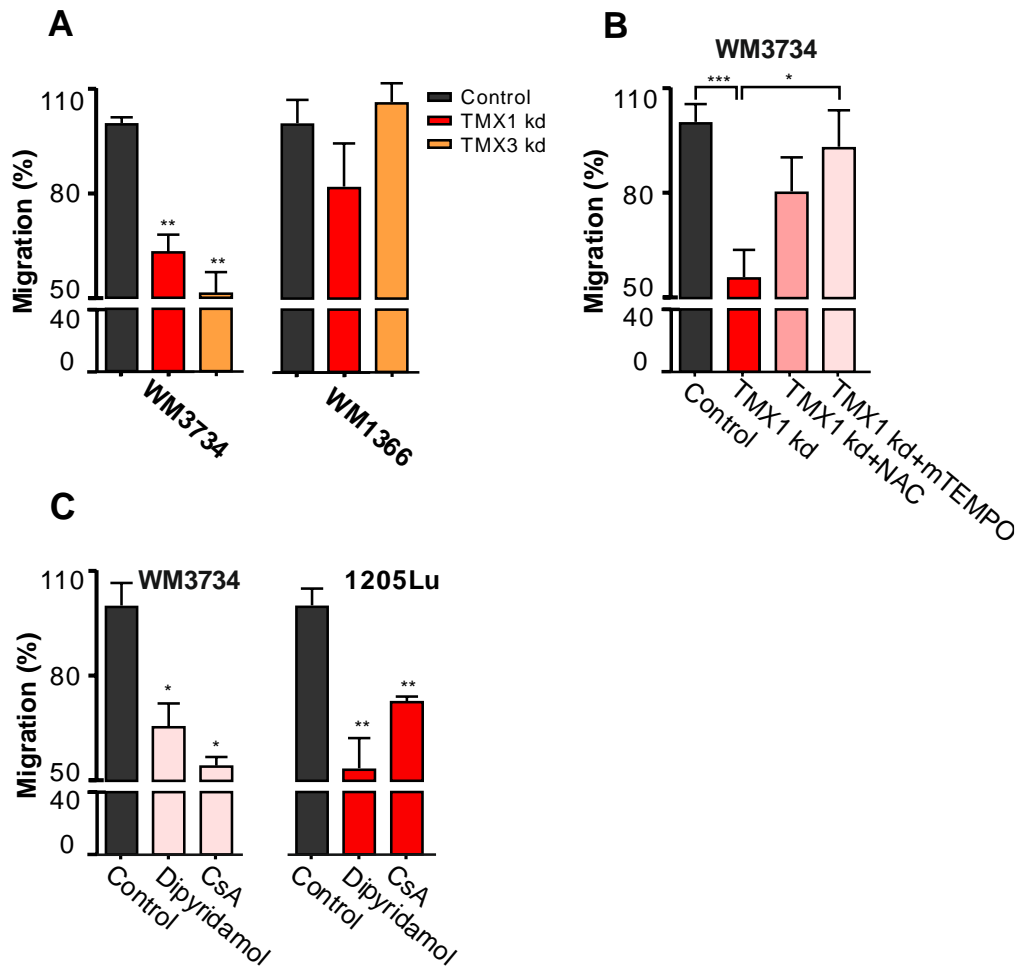


**Figure 23: The migration of melanoma cells is inhibited following TMX silencing or suppression of NFAT, calcineurin.** (A) The migrations of TMX-silenced WM3734 and WM1366 cells were assessed with transwell migration assay 48 hours after the siRNA transfection. Data are normalized to the percentage of control and presented as mean±SEM of 3 independent experiments. (B) The effect of NAC (100µM) and mitochondria targeted antioxidant mTEMPO (100nM) on migration of TMX1-silenced WM3734 was assessed with transwell migration assay 48 hours after the siRNA transfection and antioxidant treatment. Data are normalized to the percentage of control and presented as mean±SEM of 3 independent experiments. (C) The migration of melanoma cells treated with NFAT inhibitor (Dipyridamol, 40µM) and calcineurin inhibitor (CsA, 2µM) for 48 hours was assessed with transwell migration assay. Data are normalized to the percentage of control and presented as mean±SEM of 3 independent experiments.

### 7.8.3 TMX1 silencing does not affect BRAF-inhibitor sensitivity in melanoma

The oncogenic BRAF mutation and downstream hyperactive MAPK signaling pathway are proved to be prevalent in melanoma (257, 258). The combination of BRAF and/or MEK inhibitors is thus often used for treating melanoma. Thus, we tested if the knockdown of TMX proteins had any impact on the BRAF and MAPK signaling and cell drug sensitivity. To this end, we quantified the proliferation of two WM3734 cell clones stably expressing shRNA against TMX1 following treatment with BRAF- (Vemurafenib) and/or MEK inhibitor (Trametinib). As shown in Figure 24A and B, at the clinically relevant concentrations, the drugs elicit the same proliferation inhibition in knockdown cells compared with control cells, in other words, the silencing of TMX1 does not seemingly increase any advantages over these two inhibitors. Hence, we conclude the effects induced by knockdown of TMX proteins are very likely BRAF/MEK independent, and that the TMX-ROS-NFAT axis controls melanoma cells regardless of their BRAF/NRAS mutational status.

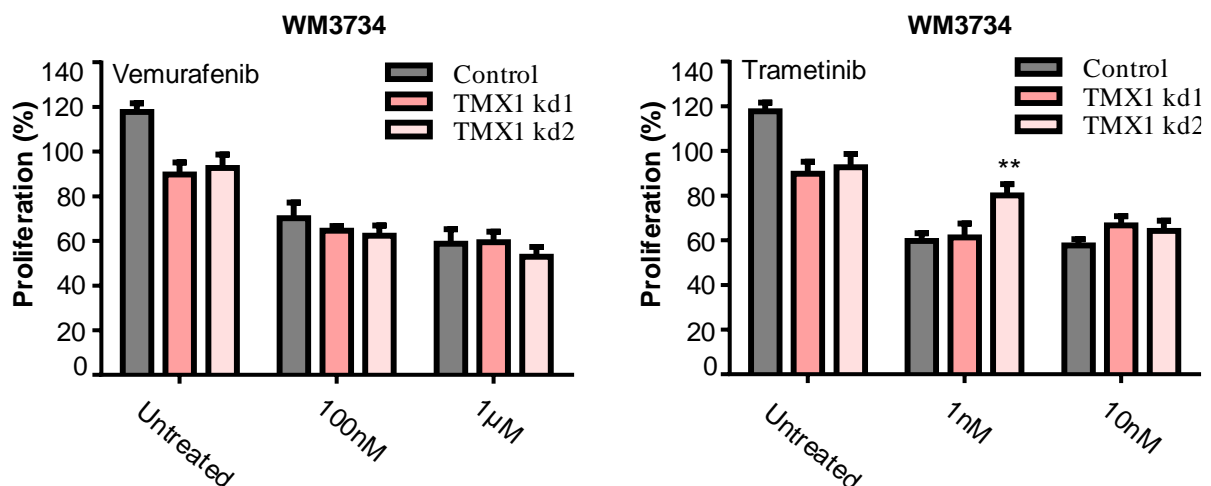


**Figure 24: TMX1 silencing does not affect BRAF and MEK resistance of melanoma cells.**

(A) The proliferation was measured with celltiter blue assay on WM3734 cells with stable knockdown of TMX1 48 hours after the treatment with different concentrations Vemurafenib. Data are normalized to the percentage of control and presented as mean±SEM of 3 independent experiments. (B) The proliferation was measured with celltiter blue assay on WM3734 cells with stable knockdown of TMX1 48 hours after the treatment with different

concentrations of Trametinib. Data are normalized to the percentage of control and presented as mean $\pm$ SEM of 3 independent experiments.

#### **7.8.4 TMX1 silencing affects melanoma tumor growth *in vivo***

Our *in vitro* data strongly support that TMX1, TMX3 and NFAT1 control melanoma proliferation and migration. But regarding the *in vivo* environment such as solid tumor, there are many factors which can lead to a different result. We thus subcutaneously injected WM3734 cells stably expressing shRNA against TMX1 into the immunosuppressed NOD-SCID-IL2-c-null (NSG) mice. As shown in figure 25, in the first 19 days after the inoculation the tumor growth was significantly slower in the mice with TMX1-silenced cells resulting in a significantly smaller tumor volume compared with the control (Figure 25A, B). Surprisingly, by the end of the experiment at 45 days, the tumor volume of TMX1-silenced cells was no longer inhibited (Figure 25C and D), and the rebound of tumor growth from both clones was apparent. These data indicate that silencing of TMX1 suppresses melanoma growth both *in vitro* and *in vivo*, but also implies that melanoma cells could adapt in an *in vivo* setting through re-wiring of signaling pathways or activating other alternative mechanisms. To address the possible adaptive mechanisms, the western blotting was performed with the tumor lysates collected at the end of mouse experiment. The results exclude the possibility that the rebound of tumor growth is caused by the recovery of TMX1 protein expression by showing a still suppressed level of TMX1 in tumors (Panel EV5 D)(249), while one of the clue points to that the re-wiring of AKT signaling pathway is a potential mechanism of adaptation (Panel EV5 E). The tuning of signaling pathways in cancer cells is frequently observed and very complicated, so any concrete conclusion on this topic needs a further and thorough dissection via bioinformatics, large scale proteomics study, which are out of the main aims of this study because of limited time and resources.

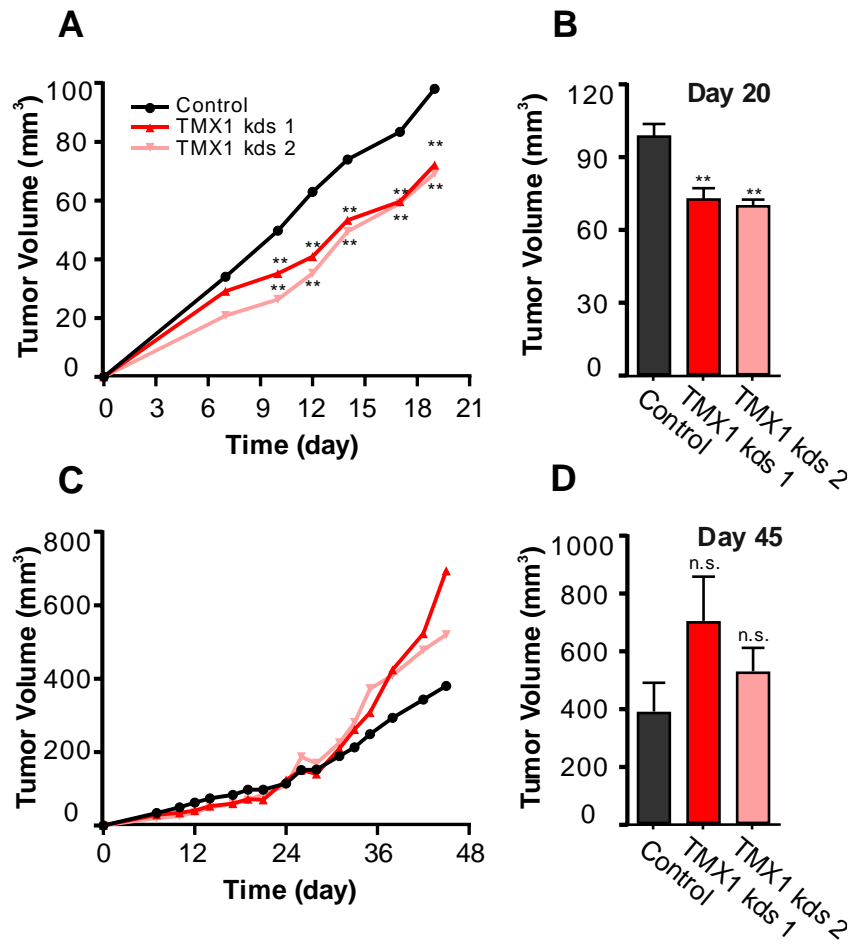


**Figure 25: Melanoma tumor growth is affected following TMX1 silencing.** (A) The tumor volume monitored from 0~20 days after the inoculation with TMX1-silenced WM3734 cell on immune deficient mice. (B) Quantification of tumor volume data at day 20th. Data are presented as mean±SEM of 7 mice for each group. (C) The tumor volume monitored from 0~45 days after the inoculation with TMX1-silenced WM3734 cell on immune deficient mice. (D) Quantification of tumor volume data at day 45th. Data are presented as mean±SEM of 7 mice for each group.

*\*The establishment of TMX1 stable knockdown cell line is done by Xin Zhang. The xenograft experiment, sample collection and stats collection were done by a joint effort of Xin Zhang, Dr. Adina Vultur, Dr. Christina Körbel. Data analysis and presentation were done by Xin Zhang.*

## **8 Discussion**

### **8.1 The TMX proteins and NFAT1 are upregulated in melanoma and correlate with melanoma progression**

As presented in the results section, our analyses on the expression of TMX1, TMX3 and NFAT1 suggest their general upregulation in melanoma cell lines. These results also show that NFAT1 is the predominant NFAT isoform and indicated the existence of NFAT1 positive and NFAT1 negative melanoma cell lines. Accordingly, our data are in line with previous studies, which suggest important role for NFAT in cancer (232, 233).

To further examine the expression of TMX1 and NFAT1 in a clinical perspective, the immunohistochemistry staining (IHC) of healthy skin and melanoma patient biopsies were performed by our collaborators in the dermatology department. As indicated from their result (Panel 1D)(249), in a primary nodular melanoma sample, the healthy melanocytes only express a relatively low level of TMX1 while the melanoma cells express TMX1 proteins on a much higher level. In the healthy tissue including the basal layer and epidermal keratinocytes, the expression of NFAT1 protein is not detectable while the expression in the melanoma cells is significantly higher. The staining from the second case also showed a similar pattern of the expression which confirmed that the TMX1 and NFAT1 are expressed on a higher level in the melanoma patient-derived cells (Panel EV1C).

Along with the progression of cancer, the up-regulation of proteins could be activated temporarily to facilitate the proliferation of the tumor or provide survival advantages such as immune escape, resistance to apoptosis or a pro-aggressive phenotype switch. This up-regulation could also be constant to keep signaling pathways hyper active in the tumor cells and thus circumvent environmental stress factors. Therefore, it is important to examine if the expression of TMX1 and NFAT1 correlate with the progression i.e. aggressiveness of melanoma. For this purpose, the immunohistochemistry staining was performed also on a set

of tumor samples collected from the patients in various stages of melanoma progression. These samples included tumors with thickness less than 2 mm, aggressive tumors (thickness more than 4mm) and metastatic melanoma. To make comparison, the protein abundance in healthy skin, benign naevus and melanoma *in situ* were also examined. As shown from these results (Panel 1E)(249), the abundance of TMX1 is at the lowest level in the healthy epidermis and melanocytic naevus (P1~P2); the *in situ* tumor samples show only a moderate expression (P3~P4). However, the expression increases with the growing thickness of the melanoma tumor (P5~P10). The tumors with a thickness more than 4 mm clearly show the highest expression of TMX1. Over all the metastasis (P11~P13) show the highest expression among all patient samples.

On the other hand, the abundance of NFAT1 is nearly not detectable from either the healthy epidermis, naevus or the *in situ* melanoma (P1~P4). In 2 out of 3 tumors with a thickness more than 2 mm, the NFAT1 expression was not detected (P5~P6), but in the 3rd case only moderate NFAT1 levels were detected (P7). However, in the more advanced cases with thickness more than 4mm and especially in the distant metastases, the abundance of NFAT1 becomes very prominent (P8~P13). Hence, based on the analysis of these 13 patient samples, we conclude, that the TMX1 and NFAT1 expression correlate with the development and invasiveness of the tumor.

Furthermore, an additional IHC set of patient samples based on melanoma staging also confirmed high expression of TMX1 in the aggressive melanomas including superficial melanoma, nodular melanoma, sentinel lymph node metastasis and balloon cell melanoma (Panel EV1D)(249). The results from patient samples show a frequent and significant increase of TMX1, TMX3 and NFAT1 expression in melanomas, which have a strong correlation with disease stage. These results emphasize the clinical importance of TMXs, NFAT proteins and the underlying mechanisms in human melanoma.

## 8.2 The TMXs regulate NFAT1 activation via ROS, not Ca<sup>2+</sup>

Based on the report from Sharma and colleagues (219), we learned that silencing of TMX proteins inhibits NFAT1 nuclear translocation; an indication for a functional link between ER-mitochondria contact sites, gene transcription and disease progression. Since depletion of the ER Ca<sup>2+</sup> store is involved in SOCE, which is necessary in activating calmodulin-calcineurin-NFAT1 signaling cascade, we initially hypothesized that the TMX proteins can affect NFAT1 translocation through their influence on cytosolic calcium transients; a hypothesis that asks for experimental testing.

Our data confirmed that the TMX proteins can regulate NFAT1 activation in melanoma cells. The knockdown of TMX1 and TMX3 inhibits NFAT1 translocation and the expression of downstream effectors such as IL-8 in melanoma cell lines. In the study by Sharma et al., the changes in cytosolic Ca<sup>2+</sup> were identified as a driving factor for the regulation of NFAT1 activation by septins, which prompted us to hypothesize that TMX1 and TMX3 can alter SOCE, probably by influencing STIM activation or ER-PM junctions i.e. STIM-ORAI coupling mechanism. It has been reported that the ER-PM junctions and ER homeostasis can affect STIM activation and STIM/ORAI coupling to control SOCE (260, 261). Nonetheless, the localization of TMX proteins is in the MAMs, which suggests that the TMX proteins might regulate SOCE by altering the mitochondrial calcium uptake (262, 263). However, to our surprise, our results did not show significant changes in SOCE after knockdown of TMX1 and TMX3, a finding that ruled out the possibility of calcium being the major factor at play. This led us to examine other elements than cytosolic Ca<sup>2+</sup> in regulating the NFAT1 translocation.

It has been reported that calcineurin has cysteine residues both in and around its catalytic center, which is a Fe–Zn pair (264). Calcineurin can thus be regulated by the oxidation of either the iron cluster at the active center or the cysteine residues near the pocket, which might

be important for the conformational stability of the catalytic site. Previous studies have shown that  $O_2^-$  and  $H_2O_2$  can deactivate the calcineurin in T-cells and other cells (265-267). In addition, the superoxide dismutase as well as the reducing reagent DTT and the thioredoxin enzyme can reverse/protect the  $H_2O_2$ -induced deactivation of calcineurin (268, 269). Furthermore the calmodulin-binding domain of calcineurin contains methionine residue, which is also sensitive to oxidation and can thus affect the binding and activation of calcineurin (270). Based on these literatures, we suspected that ROS might be responsible for the inhibition of NFAT1 activation in TMX silenced melanoma cells. Thus, we first examined the cellular  $H_2O_2$  levels and found that the knockdown of TMX1 or TMX3 resulted in a higher  $H_2O_2$  concentration. The ROS molecules can play different functional roles depending on their concentration. In the lower range (from nanomolar to a few micromolar),  $H_2O_2$  serves as a signaling molecule (271); however, if the concentration is high enough to cause oxidative damage to biological molecules in the cells, ROS are toxic and can lead to cell death and malignant transformation (272).

Thus, through a series of NFAT1 translocation assays combined with manipulations of extracellular  $H_2O_2$  concentration we found that, in melanoma cells, NFAT1 activation was redox-regulated. Our data suggest that even in the micromolar range,  $H_2O_2$  inhibits NFAT1 activity; additionally, the NFAT1 inhibition caused by knockdown of TMX proteins could be reversed by antioxidants and reducing agents. These data indicate that TMX1 and TMX3 might have a protective role by reducing cellular oxidative stress in melanoma cells. To understand the molecular mechanism of TMX knockdown induced NFAT1 inhibition, we examined the influence of TMX1 and TMX3 knockdown on calcineurin activity in melanoma cells. We found that its activity was suppressed upon knockdown of TMX proteins. In summary, our study suggests the knockdown of TMX proteins leads to a higher ROS levels in

melanoma cells, which are responsible for the inhibition of NFAT1 translocation via inhibition of calcineurin.

### **8.3 The TMXs influence mitochondrial ROS production**

Based on the known functions of TMX proteins, the possible sources of ROS upon their silencing might be as follows: 1) ER lumen, due to disturbances in the redox homeostasis i.e. ER stress; 2) ER-based NADPH oxidases such as NOX4; 3) Mitochondria, through the ER-mitochondria contact sites, the TMX proteins may influence the ROS generation in these organelles (273-275). However, our data indicate that the knockdown of TMX1 does not induce neither the expression of typical ER stress markers, nor higher level of ROS in ER. These findings suggest that the role of TMX proteins in ER stress is probably context-dependent; and other oxidoreductases in the ER might be up-regulated to compensate for the loss of TMX proteins. Nonetheless, based on these negative results from investigation on ER, we started to investigate on the other targets.

The NADPH oxidase 4 is involved in ER stress-related oxidative stress (276). And it has also been reported that TMX3 is an interaction partner of NOX4 (277). Thus, it is intriguing to identify whether NOX4 is relevant to the elevated ROS generation induced by the knockdown of TMX proteins. Our H<sub>2</sub>O<sub>2</sub> measurements in melanoma cells upon TMX1 and NOX4 silencing indicate a certain contribution of NOX4 but also suggest that ROS are generated by additional sources. Concerning the importance of NOX4 in melanoma (278, 279), further investigation in this direction will be interesting.

Based on these findings we tested the mitochondrial parameters and found that the mitochondrial H<sub>2</sub>O<sub>2</sub> levels were dramatically increased after the knockdown of TMX proteins. The mitochondria are the major source of ROS in the cells, considering the special

localization of TMX proteins, these data are not surprising to us. As mentioned previously, mitochondrial ROS production is closely coupled to the respiration and metabolism activities, and the measurements in these two parameters also in turn should confirm that the mitochondria are energized to produce higher level of ROS. These data thus led to questions concerning the mechanism through which TMX proteins regulate mitochondrial ROS production and metabolism.

#### **8.4 The ER-mitochondria contact sites shape mitochondrial dynamics**

Mitochondrial metabolism,  $\text{Ca}^{2+}$  and redox signaling are intrinsically integrated into a complex system for the regulation of cellular functions. Since the TMX proteins are localized in the MAM, their absence might cause consequences for both the structure and the function of ER-mitochondria contact sites, thus has a profound impact on the mitochondrial function.

Our first clue, the elevated mitochondrial ROS, indicates that the mitochondrial metabolism is affected by the knockdown of TMX proteins. Thus, we next investigated mitochondrial calcium uptake in TMX silenced cells. Our data indicates that mitochondrial calcium uptake is increased in both the stable TMX1 knockdown cells and cells with transient silencing of TMX1 following activation of SOCE. The two major sources of calcium i.e. the ER and the cytosol, contributed in different ways: The ER-to-mitochondria calcium transfer was decreased, whereas the PM (cytosol)-to-mitochondria calcium transfer was increased significantly. Further measurements of cellular oxygen consumption and mitochondrial ATP production supported our findings and confirmed that increased calcium uptake led to higher respiratory activity. Thus, we investigated the mitochondrial morphology and the mitochondria positioning to the PM with confocal and electron microscopy in melanoma cells. The data indicates that the total volume and surface area of mitochondria are increased in melanoma cells with stable knockdown of TMX1. Moreover, the mitochondria are re-

positioned to the PM proximity, which may lead to greater exposure of mitochondria to PM-related events.

The mitochondria and the ER are two major endomembrane systems in eukaryotic cells, and they form an extended reticular network. The ER-mitochondria contact sites, as mentioned previously, mediate signaling, lipid exchange and calcium handling to regulate many mitochondrial functions, including metabolic activity, replication and apoptosis (280, 281). Recent studies have revealed that the mitochondria can form contacts with other organelles, such as the PM, lipid droplets, vacuoles, lysosomes and peroxisomes (282). These studies lead to a broader understanding of the roles of mitochondria in cellular functions, and also suggest that the interactions of organelles via the contact sites may have profound influences on mitochondrial behavior (283). In such a context, the exact architecture of the contact sites are very important determining factors (284). Endoplasmic reticulum-mitochondria contact sites have been reported to be 10~30 nm wide (198) and are tethered by specialized membrane proteins in mammalian cells. Moreover, approximately 10 % of the PMs in cells are in contact and are anchored to mitochondria. The disruption of these anchors can redistribute the mitochondria away from the PM (285, 286).

In previous studies, either the ER-mitochondria or PM-mitochondria contact sites were investigated alone. And their impact to the relative distance between organelles, mitochondrial division and distribution were clarified mostly in a yeast model (285, 287, 288). Based on our data, it is plausible to speculate that, together, these two elements determine the apposition of mitochondria relative to the ER and the PM. Under normal conditions, in the presence of TMX proteins, the ER-mitochondria contact sites are intact and the ER-to-mitochondria calcium transfer is sufficient for normal cell function meaning that the mitochondrial ROS generation is under control and thus, the NFAT1 signaling pathway is active. However, if the ER-mitochondria contact sites are disrupted by the loss of TMX

proteins, the mitochondria will become more closely associated with the PM and more distanced from the ER. This will lead to increased mitochondrial calcium levels, which will further promote mitochondrial respiration and contribute to excessive ROS generation. The elevated ROS can then cause NFAT1 inhibition, thus resulting in a negative impact on melanoma cell biology. Our model is in agreement with a previous study that demonstrates that cancer cells are vulnerable to the inhibition of ER-mito calcium transfer (289) and recent findings concerning the protective role played by TMX1 during oxidative stress (290). Based on these evidences, at this point of the study, we conclude that the TMX-ROS-NFAT1 axis plays an important role in melanoma cell pathobiology.

### **8.5 TMXs and NFAT1 promote aggressive melanoma phenotypes**

From the expression analysis, we had already learned that the TMX proteins and NFAT1 were upregulated in human melanomas and that their upregulations were relevant to the progression of the disease. Thus, we examined the proliferation and migration of melanoma cells upon the silencing of TMX proteins and NFAT1. Our data reveal that the knockdown of TMX1/3 or NFAT1 leads to inhibition of both proliferation, migration and invasion of melanoma cells *in vitro*. Notably, the pharmaceutical inhibition of calcineurin and NFAT1 elicits similar effects. Furthermore, the TMX1 knockdown suppresses the growth of tumors in a xenograft mouse model although the tumor cells can adapt by activating AKT and probably also re-wiring other pathways. These data indicate that the attrition of TMX proteins and NFAT1 has a negative impact on melanoma cells; a finding which confirmed our hypothesis regarding the role of mitochondrial contact sites on melanoma pathology.

Yet the results so far indicate that TMX1, TMX3 and NFAT1 play important roles in melanoma cell pathobiology. To explore the connection in human patients and prognosis of melanomas, the integrative bioinformatics analysis was performed by our collaborators,

Thorsten Will and Prof. Dr. Volkhard Helms. By analyzing the Cancer Genome Atlas (TCGA: <https://cancergenome.nih.gov/>) database and focusing on the correlation between the mRNA expression levels of TMX1, TMX3 and NFAT1 and the survival of patients with cutaneous melanoma, their analysis indicates that the high expression of any of the three target genes, TMX1, TMX3 and NFAT1, correlates with a significantly decreased survival expectancy compared with patients with low expression (Panel 7A)(249). The further analysis shows that the high expression of TMX1, TMX3 and NFAT1 also has a negative impact individually on the survival probability of the melanoma patients (Panel EV5J, K, L).

To further identify the impact of TMX proteins and NFAT1 on survival of melanoma patients with different BRAF mutation status, the correlation between the expression of TMX1, TMX3, NFAT1 and BRAF status in a cohort of 97 melanoma patients, which consisted of 49 WT and 48 BRAF V600E melanomas were analyzed. The results (Panel 7B)(249) show that the expression of TMX1/TMX3 is not correlated to the mutational status of BRAF, while the expression of NFAT1 is significantly increased in patients with BRAF V600E mutation. In patients with BRAF V600E mutation, the high expression of NFAT1 does not affect survival probability (Panel 7D). However, the high expression of NFAT1 significantly reduces the survival probability of patients with BRAF WT status (Panel 7C). These data suggest that the TMX-ROS-NFAT1 signaling axis has a more prominent effect in BRAF WT patients, a finding that might be considered in choosing the therapeutic approaches for melanoma patients.

Based on the melanoma patient data and the bioinformatics analysis, it is plausible to conclude that the high expression of TMX and NFAT1 are correlated to an aggressive melanoma phenotype and enhanced melanoma progression; and the experimental data shows their strong impact on intracellular redox regulation and mitochondrial bioenergetics. Given that the influence of this signaling axis is mediated by the regulation of NFAT1, the target

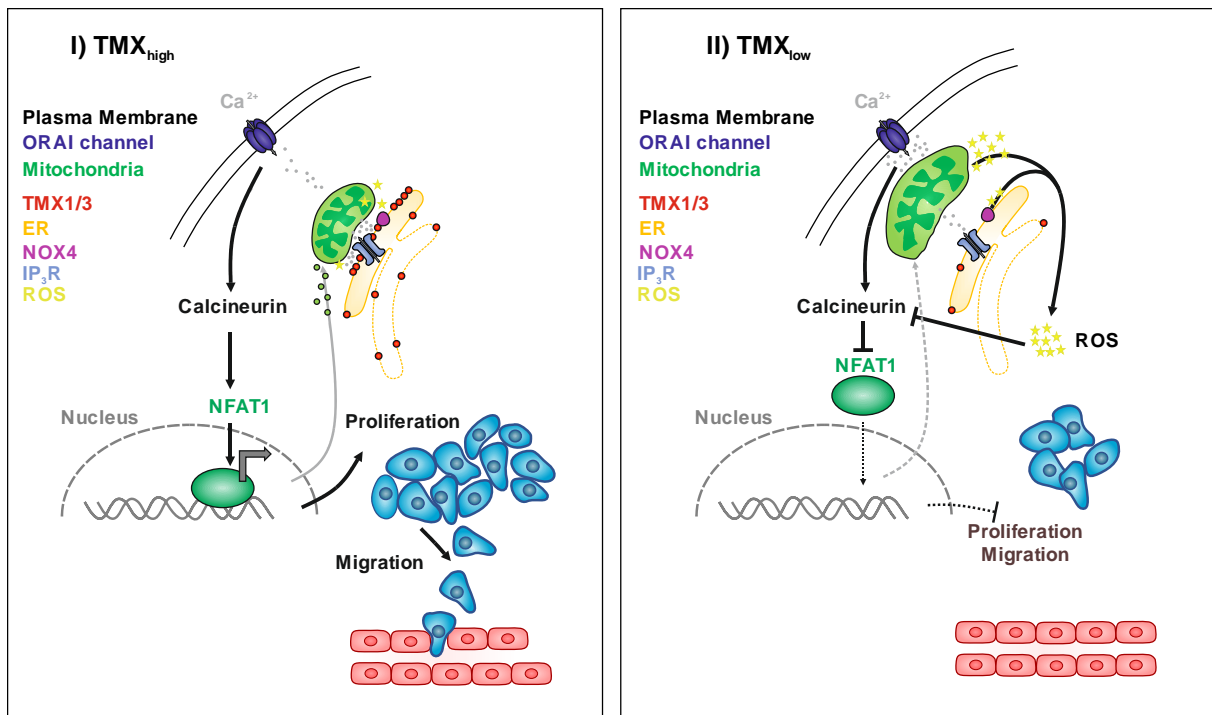
genes of NFAT1 in melanoma cells are of particular interest. To further identify them, two independent published studies, which evaluated the transcriptome of melanoma cells following knockdown of NFAT1 using different approaches (242, 259) were analyzed. It was identified that there were 59 upregulated genes and 56 downregulated genes after NFAT1 knockdown in melanoma cells (List of individual genes published as Table S5)(249).

To address the functional relevance of these genes, the associated annotation data by the Gene Ontology Consortium ([www.geneontology.org](http://www.geneontology.org)) were used for further investigation. The fold-enrichment of genes with different term annotations defined by their background indicates that NFAT1 controls two major groups of genes in melanoma cells, “Mitochondrion-localized” and “Redox-related” (Panel 7F)(249). Furthermore, the fold-enrichment calculations of the transcriptomic data were categorized by the “Hallmarks of cancer”, and the results show that most of the genes under NFAT1 control can be assigned to the hallmark “Deregulating Cellular Energetics”. In addition, the data show that the hallmarks such as cell death resistance, inflammation, evading growth suppressors and immune destruction, proliferation and invasion are also regulated by NFAT1 (Panel 7G).

These analyses confirm our experimental findings and suggest that NFAT1 can influence the cellular redox state by regulating mitochondrial function, thus supporting melanoma cell aggressive phenotype and ultimately lead to lower survival expectancy of melanoma patients. Thus, we conclude that TMX proteins and NFAT1 are pro-tumorigenic and their expression promotes melanoma progression.

## **8.6 The TMX-NFAT1 axis regulates mitochondrial function and redox homeostasis in melanomas**

In our model, the TMX proteins determine the integrity of ER- mitochondria contact sites and thus control NFAT1 activity by modulating the intracellular ROS level. Previous studies have suggested that mitochondrial  $\text{Ca}^{2+}$ , mitochondrial respiration and ROS generation can regulate NFAT activation in different models. In neuron cells, mitochondrial calcium uptake can prolong the activation of PM channels to sustain the calcium influx, which is important for NFAT1 activation (291). The low levels of ROS produced by the mitochondrial respiratory chain during sustained SOCE can also activate NFAT in T-cells and embryo cells (292-294). Based on our findings and the literature, we were able to implement the redox regulation of NFAT1 in our model. Here, we suggest that, in healthy cells, intact ER-mitochondria contact sites can provide normal calcium transfer to the mitochondria so mitochondrial ROS generation is in control, the normal NFAT1 function is unaffected and can be activated readily. As a protective feedback loop, the excessive ROS generated by abnormal metabolism activity can inhibit NFAT1 activity, which will lead to reduced mitochondrial activity and lower ROS production. In melanoma cells, the high expression of TMX proteins enhances the stability of the ER-mitochondria contact sites, while the high expression of NFAT1 increases the mitochondrial capacity to provide more energy to support cancer progression. Simultaneously, the upregulated antioxidant system manages redox balance to prevent negative effects (Graph 5, left). However, the knockdown of TMX1 protein level will disrupt the integrity of ER-mitochondria contact sites, thus causes an over-exposure of mitochondria to PM and calcium influx via channels on it. This will lead to increased mitochondrial  $\text{Ca}^{2+}$  uptake and excessive ROS generation, in turn, the ROS can deactivate NFAT1 signaling by inhibiting Calcineurin and cast negative effect on proliferation and migration of melanoma cells (Graph 5, right).



**Graph 5: Theoretical Model of the TMX-ROS-NFAT1 Signal Axis in Melanomas.**

*\*This conceptual figure is modified from our publication “Redox signals at ER-mitochondria interface control melanoma progression”, Zhang et al, EMBO J. 2019 Aug 1;38(15): e100871.*

## **8.7 ER-mitochondria contact sites and the TMX-ROS-NFAT1 axis in the perspective of melanoma therapeutics**

As noted in the above discussion of our model, our study suggests that the TMX-NFAT1 signaling axis, which contributes to the progression of human melanoma, is tuned by redox signals generated at the ER-mitochondria interface. These findings illustrate the importance of the ER-mitochondria contact sites and TMX-ROS-NFAT1 in melanoma pathology. Thus, it is important to discuss the possible implications of these findings from a clinical perspective.

The research on ER-mitochondria contact sites is still an emerging field regarding cancer biology despite the several recent discoveries. ER-mitochondria communication governs many important cellular functions, including calcium transfer, lipid traffic, mitochondrial

plasticity, apoptosis, autophagy and inflammation (273, 295). Hence, any aberration on its part is associated with pathological conditions including cancer, Alzheimer's (296), obesity and diabetes (297). However, as a functional platform, the structural support provided by the contact sites for the morphology and distribution of mitochondria in cancers, including melanoma, has not been explored thoroughly, perhaps due to the difficulties in targeting it for therapeutic purposes. Nonetheless, our work suggests that, by manipulating the ER-mitochondria contact sites, downstream mitochondrial ROS generation can be elevated and causes inhibition of transcription factors such as NFAT1. This can ultimately lead to the suppression of aggressive melanoma, which might be of clinical interests.

As mentioned previously, the ROS molecules are involved in the formation, metastasis and drug-resistance of melanoma. Abnormal intracellular sources of ROS in melanoma might be aberrant melanosomes, irregular metabolic activity and NADPH oxidases. In cancer cells, it is very commonly that the antioxidant system is upregulated to cope with the increased ROS levels (131). Mitochondria as a major endogenous source of ROS have been linked to cancers including melanoma for a quite long time; previous studies have explored their implications for therapeutics (298, 299). Recently, a series of studies have identified mitochondrial metabolism as an important mechanism for the drug resistance of melanoma (143, 189, 192) and have also highlighted targeting mitochondrial oxidative stress as a potential strategy for addressing drug resistance (158, 300). Our study is in agreement with these findings, and suggests that, in melanoma cells, the mitochondrial ROS can be induced to inhibit critical phosphatases, which could further deactivate downstream pathways such as NFAT1 signaling. Since the expression of the TMX proteins are not correlated to BRAF status in melanoma, their knockdown will trigger general ROS responses which may induce detrimental effects in melanomas regardless of their BRAF status. Additionally, as a responding factor, NFAT1

displays a prominent effect in the patients with BRAF WT phenotype and could thus be targeted for treatment in the sub-population of melanomas.

Studies concerning the role of calcineurin/NFAT1 in melanoma are scarce, although most have noted that NFAT1 expression is related to melanoma growth and metastasis (242, 301). Calcineurin has been frequently discussed in the context of Ca<sup>2+</sup> signaling (302, 303); its inhibition has been reported to have multiple effects on human melanoma (247). It is interesting to note that the expression of calcineurin is also correlated with the malignancy of melanoma and mitochondrial activity in the study conducted by Juhasz and colleagues. Although the inhibition of calcineurin by CsA was found to have different effects on the migration of melanoma cell lines, which can perhaps be attributed to different NFAT levels. Notably, a study on fruit flies stated that calcineurin played a critical role in maintaining metabolic homeostasis, mitochondrial morphology and activity, although, as the downstream effector, NFAT was not in the focus of this research (304). It is likely that calcineurin affects mitochondrial activity through NFAT1 signaling, but a detailed dissection of calcineurin/NFAT1 signaling network will be required to understand the various effects induced by the inhibition of the NFAT1 activation. Overall, our findings emphasize the potential of targeting redox-based processes in melanomas and indicate that calcineurin/NFAT1 may be crucial for the regulation of mitochondrial activity. To this end, additional studies are needed to explore the opportunities for targeted therapeutics against melanoma.

## **8.8 Conclusion**

Melanoma is a cancer caused by various genetic as well as environmental factors. The heterogeneity of melanoma is a reflection of aberrations in signaling pathways caused by mutations, which lead to a reprogrammed metabolic activity, abnormal proliferation and

migration. In this study, we explored the importance of ER-mitochondria contact sites in the pathology of melanoma and dissected a novel redox-driven ER-mitochondria-NFAT1 signaling axis that integrates mitochondrial calcium transfer, bioenergetics and cellular redox homeostasis and contributes to melanoma progression. Our work suggests that ER-mitochondria contact sites can shape calcium and redox signaling in favor of tumor progression, whereas their alterations can in turn limit melanoma proliferation and migration. Accordingly, TMX1, TMX3 and NFAT1 are potential melanoma progression biomarkers as well as candidates for therapeutic targeting.

## 9 References

- (1) Tsatmali, M., Ancans, J., and Thody, A.J. (2002) Melanocyte function and its control by melanocortin peptides. *The journal of histochemistry and cytochemistry : official journal of the Histochemistry Society*. 50, 125-133
- (2) Igyarto, B.Z., and Kaplan, D.H. (2013) Antigen presentation by Langerhans cells. *Current opinion in immunology*. 25, 115-119
- (3) Diepgen, T.L., and Mahler, V. (2002) The epidemiology of skin cancer. *The British journal of dermatology*. 146 Suppl 61, 1-6
- (4) Leiter, U., Eigentler, T., and Garbe, C. (2014) Epidemiology of skin cancer. *Advances in experimental medicine and biology*. 810, 120-140
- (5) Leiter, U., and Garbe, C. (2008) Epidemiology of melanoma and nonmelanoma skin cancer--the role of sunlight. *Advances in experimental medicine and biology*. 624, 89-103
- (6) Eisemann, N., Waldmann, A., Geller, A.C., Weinstock, M.A., Volkmer, B., Greinert, R., Breitbart, E.W., and Katalinic, A. (2014) Non-melanoma skin cancer incidence and impact of skin cancer screening on incidence. *The Journal of investigative dermatology*. 134, 43-50
- (7) Garbe, C., Peris, K., Hauschild, A., Saiag, P., Middleton, M., Bastholt, L., Grob, J.J., Malvehy, J., Newton-Bishop, J., Stratigos, A.J., Pehamberger, H., Eggermont, A.M., European Dermatology, F., European Association of, D.-O., European Organisation for, R., and Treatment of, C. (2016) Diagnosis and treatment of melanoma. European consensus-based interdisciplinary guideline - Update 2016. *European journal of cancer*. 63, 201-217
- (8) Clark, W.H., Jr., From, L., Bernardino, E.A., and Mihm, M.C. (1969) The histogenesis and biologic behavior of primary human malignant melanomas of the skin. *Cancer research*. 29, 705-727
- (9) Armstrong, B.K., and Kricger, A. (2001) The epidemiology of UV induced skin cancer. *Journal of photochemistry and photobiology. B, Biology*. 63, 8-18
- (10) Armstrong, B.K., and Cust, A.E. (2017) Sun exposure and skin cancer, and the puzzle of cutaneous melanoma: A perspective on Fears et al. Mathematical models of age and ultraviolet effects on the incidence of skin cancer among whites in the United States. *American Journal of Epidemiology* 1977; 105: 420-427. *Cancer epidemiology*. 48, 147-156
- (11) Rivers, J.K. (2004) Is there more than one road to melanoma? *Lancet*. 363, 728-730
- (12) (1991) National Institutes of Health summary of the Consensus Development Conference on Sunlight, Ultraviolet Radiation, and the Skin. Bethesda, Maryland, May 8-10, 1989. Consensus Development Panel. *Journal of the American Academy of Dermatology*. 24, 608-612
- (13) Osterlind, A., Tucker, M.A., Stone, B.J., and Jensen, O.M. (1988) The Danish case-control study of cutaneous malignant melanoma. II. Importance of UV-light exposure. *International journal of cancer*. 42, 319-324
- (14) Green, A., Siskind, V., Bain, C., and Alexander, J. (1985) Sunburn and malignant melanoma. *British journal of cancer*. 51, 393-397

- (15) Dubin, N., Pasternack, B.S., and Moseson, M. (1990) Simultaneous assessment of risk factors for malignant melanoma and non-melanoma skin lesions, with emphasis on sun exposure and related variables. *International journal of epidemiology*. 19, 811-819
- (16) Holman, C.D., Armstrong, B.K., and Heenan, P.J. (1986) Relationship of cutaneous malignant melanoma to individual sunlight-exposure habits. *Journal of the National Cancer Institute*. 76, 403-414
- (17) von Thaler, A.K., Kamenisch, Y., and Berneburg, M. (2010) The role of ultraviolet radiation in melanomagenesis. *Experimental dermatology*. 19, 81-88
- (18) Nishigori, C. (2015) Current concept of photocarcinogenesis. *Photochemical & photobiological sciences : Official journal of the European Photochemistry Association and the European Society for Photobiology*. 14, 1713-1721
- (19) Curtin, J.A., Fridlyand, J., Kageshita, T., Patel, H.N., Busam, K.J., Kutzner, H., Cho, K.H., Aiba, S., Brocker, E.B., LeBoit, P.E., Pinkel, D., and Bastian, B.C. (2005) Distinct sets of genetic alterations in melanoma. *The New England journal of medicine*. 353, 2135-2147
- (20) Demierre, M.F., and Sondak, V.K. (2005) Cutaneous melanoma: pathogenesis and rationale for chemoprevention. *Critical reviews in oncology/hematology*. 53, 225-239
- (21) Melnikova, V.O., and Ananthaswamy, H.N. (2005) Cellular and molecular events leading to the development of skin cancer. *Mutation research*. 571, 91-106
- (22) Martens, M.C., Seebode, C., Lehmann, J., and Emmert, S. (2018) Photocarcinogenesis and Skin Cancer Prevention Strategies: An Update. *Anticancer research*. 38, 1153-1158
- (23) Berger, M.F., Hodis, E., Heffernan, T.P., Deribe, Y.L., Lawrence, M.S., Protopopov, A., Ivanova, E., Watson, I.R., Nickerson, E., Ghosh, P., Zhang, H., Zeid, R., Ren, X., Cibulskis, K., Sivachenko, A.Y., Wagle, N., Sucker, A., Sougnez, C., Onofrio, R., Ambrogio, L., Auclair, D., Fennell, T., Carter, S.L., Drier, Y., Stojanov, P., Singer, M.A., Voet, D., Jing, R., Saksena, G., Barretina, J., Ramos, A.H., Pugh, T.J., Stransky, N., Parkin, M., Winckler, W., Mahan, S., Ardlie, K., Baldwin, J., Wargo, J., Schadendorf, D., Meyerson, M., Gabriel, S.B., Golub, T.R., Wagner, S.N., Lander, E.S., Getz, G., Chin, L., and Garraway, L.A. (2012) Melanoma genome sequencing reveals frequent PREX2 mutations. *Nature*. 485, 502-506
- (24) Pleasance, E.D., Cheetham, R.K., Stephens, P.J., McBride, D.J., Humphray, S.J., Greenman, C.D., Varela, I., Lin, M.L., Ordonez, G.R., Bignell, G.R., Ye, K., Alipaz, J., Bauer, M.J., Beare, D., Butler, A., Carter, R.J., Chen, L., Cox, A.J., Edkins, S., Kokko-Gonzales, P.I., Gormley, N.A., Grocock, R.J., Haudenschild, C.D., Hims, M.M., James, T., Jia, M., Kingsbury, Z., Leroy, C., Marshall, J., Menzies, A., Mudie, L.J., Ning, Z., Royce, T., Schulz-Trieglaff, O.B., Spiridou, A., Stebbings, L.A., Szajkowski, L., Teague, J., Williamson, D., Chin, L., Ross, M.T., Campbell, P.J., Bentley, D.R., Futreal, P.A., and Stratton, M.R. (2010) A comprehensive catalogue of somatic mutations from a human cancer genome. *Nature*. 463, 191-196
- (25) Garibyan, L., and Fisher, D.E. (2010) How sunlight causes melanoma. *Current oncology reports*. 12, 319-326
- (26) Goldstein, A.M. (2004) Familial melanoma, pancreatic cancer and germline CDKN2A mutations. *Human mutation*. 23, 630
- (27) Ransohoff, K.J., Jaju, P.D., Tang, J.Y., Carbone, M., Leachman, S., and Sarin, K.Y. (2016) Familial skin cancer syndromes: Increased melanoma risk. *Journal of the American Academy of Dermatology*. 74, 423-434; quiz 435-426

- (28) Bishop, J.N., Harland, M., Randerson-Moor, J., and Bishop, D.T. (2007) Management of familial melanoma. *The Lancet. Oncology*. 8, 46-54
- (29) de Snoo, F.A., Kroon, M.W., Bergman, W., ter Huurne, J.A., Houwing-Duistermaat, J.J., van Mourik, L., Snels, D.G., Breuning, M.H., Willemze, R., Frants, R.R., and Gruis, N.A. (2007) From sporadic atypical nevi to familial melanoma: risk analysis for melanoma in sporadic atypical nevus patients. *Journal of the American Academy of Dermatology*. 56, 748-752
- (30) Aoude, L.G., Pritchard, A.L., Robles-Espinoza, C.D., Wadt, K., Harland, M., Choi, J., Gartside, M., Quesada, V., Johansson, P., Palmer, J.M., Ramsay, A.J., Zhang, X., Jones, K., Symmons, J., Holland, E.A., Schmid, H., Bonazzi, V., Woods, S., Dutton-Regester, K., Stark, M.S., Snowden, H., van Doorn, R., Montgomery, G.W., Martin, N.G., Keane, T.M., Lopez-Otin, C., Gerdes, A.M., Olsson, H., Ingvar, C., Borg, A., Gruis, N.A., Trent, J.M., Jonsson, G., Bishop, D.T., Mann, G.J., Newton-Bishop, J.A., Brown, K.M., Adams, D.J., and Hayward, N.K. (2015) Nonsense mutations in the shelterin complex genes ACD and TERF2IP in familial melanoma. *Journal of the National Cancer Institute*. 107,
- (31) Zuo, L., Weger, J., Yang, Q., Goldstein, A.M., Tucker, M.A., Walker, G.J., Hayward, N., and Dracopoli, N.C. (1996) Germline mutations in the p16INK4a binding domain of CDK4 in familial melanoma. *Nature genetics*. 12, 97-99
- (32) Robles-Espinoza, C.D., Harland, M., Ramsay, A.J., Aoude, L.G., Quesada, V., Ding, Z., Pooley, K.A., Pritchard, A.L., Tiffen, J.C., Petljak, M., Palmer, J.M., Symmons, J., Johansson, P., Stark, M.S., Gartside, M.G., Snowden, H., Montgomery, G.W., Martin, N.G., Liu, J.Z., Choi, J., Makowski, M., Brown, K.M., Dunning, A.M., Keane, T.M., Lopez-Otin, C., Gruis, N.A., Hayward, N.K., Bishop, D.T., Newton-Bishop, J.A., and Adams, D.J. (2014) POT1 loss-of-function variants predispose to familial melanoma. *Nature genetics*. 46, 478-481
- (33) Horn, S., Figl, A., Rachakonda, P.S., Fischer, C., Sucker, A., Gast, A., Kadel, S., Moll, I., Nagore, E., Hemminki, K., Schadendorf, D., and Kumar, R. (2013) TERT promoter mutations in familial and sporadic melanoma. *Science*. 339, 959-961
- (34) Testa, J.R., Cheung, M., Pei, J., Below, J.E., Tan, Y., Sementino, E., Cox, N.J., Dogan, A.U., Pass, H.I., Trusa, S., Hesdorffer, M., Nasu, M., Powers, A., Rivera, Z., Comertpay, S., Tanji, M., Gaudino, G., Yang, H., and Carbone, M. (2011) Germline BAP1 mutations predispose to malignant mesothelioma. *Nature genetics*. 43, 1022-1025
- (35) Yokoyama, S., Woods, S.L., Boyle, G.M., Aoude, L.G., MacGregor, S., Zismann, V., Gartside, M., Cust, A.E., Haq, R., Harland, M., Taylor, J.C., Duffy, D.L., Holohan, K., Dutton-Regester, K., Palmer, J.M., Bonazzi, V., Stark, M.S., Symmons, J., Law, M.H., Schmidt, C., Lanagan, C., O'Connor, L., Holland, E.A., Schmid, H., Maskiell, J.A., Jetann, J., Ferguson, M., Jenkins, M.A., Kefford, R.F., Giles, G.G., Armstrong, B.K., Aitken, J.F., Hopper, J.L., Whiteman, D.C., Pharoah, P.D., Easton, D.F., Dunning, A.M., Newton-Bishop, J.A., Montgomery, G.W., Martin, N.G., Mann, G.J., Bishop, D.T., Tsao, H., Trent, J.M., Fisher, D.E., Hayward, N.K., and Brown, K.M. (2011) A novel recurrent mutation in MITF predisposes to familial and sporadic melanoma. *Nature*. 480, 99-103
- (36) Tang, J., and Chu, G. (2002) Xeroderma pigmentosum complementation group E and UV-damaged DNA-binding protein. *DNA repair*. 1, 601-616
- (37) Gandini, S., Sera, F., Cattaruzza, M.S., Pasquini, P., Zanetti, R., Masini, C., Boyle, P., and Melchi, C.F. (2005) Meta-analysis of risk factors for cutaneous melanoma: III. Family history, actinic damage and phenotypic factors. *European journal of cancer*. 41, 2040-2059

- (38) Ford, D., Bliss, J.M., Swerdlow, A.J., Armstrong, B.K., Franceschi, S., Green, A., Holly, E.A., Mack, T., MacKie, R.M., Osterlind, A., and et al. (1995) Risk of cutaneous melanoma associated with a family history of the disease. The International Melanoma Analysis Group (IMAGE). *International journal of cancer*. 62, 377-381
- (39) Elwood, J.M., Whitehead, S.M., Davison, J., Stewart, M., and Galt, M. (1990) Malignant melanoma in England: risks associated with naevi, freckles, social class, hair colour, and sunburn. *International journal of epidemiology*. 19, 801-810
- (40) Lock-Andersen, J., Drzewiecki, K.T., and Wulf, H.C. (1999) Eye and hair colour, skin type and constitutive skin pigmentation as risk factors for basal cell carcinoma and cutaneous malignant melanoma. A Danish case-control study. *Acta dermato-venereologica*. 79, 74-80
- (41) Dubin, N., Moseson, M., and Pasternack, B.S. (1986) Epidemiology of malignant melanoma: pigmentary traits, ultraviolet radiation, and the identification of high-risk populations. *Recent results in cancer research. Fortschritte der Krebsforschung. Progres dans les recherches sur le cancer*. 102, 56-75
- (42) Landi, M.T., Baccarelli, A., Calista, D., Pesatori, A., Fears, T., Tucker, M.A., and Landi, G. (2001) Combined risk factors for melanoma in a Mediterranean population. *British journal of cancer*. 85, 1304-1310
- (43) Prota, G. (2000) Melanins, melanogenesis and melanocytes: looking at their functional significance from the chemist's viewpoint. *Pigment cell research*. 13, 283-293
- (44) Zanetti, R., Prota, G., Napolitano, A., Martinez, C., Sancho-Garnier, H., Osterlind, A., Sacerdote, C., and Rosso, S. (2001) Development of an integrated method of skin phenotype measurement using the melanins. *Melanoma research*. 11, 551-557
- (45) Rees, J.L. (2003) Genetics of hair and skin color. *Annual review of genetics*. 37, 67-90
- (46) Mitra, D., Luo, X., Morgan, A., Wang, J., Hoang, M.P., Lo, J., Guerrero, C.R., Lennerz, J.K., Mihm, M.C., Wargo, J.A., Robinson, K.C., Devi, S.P., Vanover, J.C., D'Orazio, J.A., McMahon, M., Bosenberg, M.W., Haigis, K.M., Haber, D.A., Wang, Y., and Fisher, D.E. (2012) An ultraviolet-radiation-independent pathway to melanoma carcinogenesis in the red hair/fair skin background. *Nature*. 491, 449-453
- (47) Green, A., MacLennan, R., and Siskind, V. (1985) Common acquired naevi and the risk of malignant melanoma. *International journal of cancer*. 35, 297-300
- (48) Holly, E.A., Kelly, J.W., Shpall, S.N., and Chiu, S.H. (1987) Number of melanocytic nevi as a major risk factor for malignant melanoma. *Journal of the American Academy of Dermatology*. 17, 459-468
- (49) Rokuhara, S., Saida, T., Oguchi, M., Matsumoto, K., Murase, S., and Oguchi, S. (2004) Number of acquired melanocytic nevi in patients with melanoma and control subjects in Japan: Nevus count is a significant risk factor for nonacral melanoma but not for acral melanoma. *Journal of the American Academy of Dermatology*. 50, 695-700
- (50) Bauer, J., and Garbe, C. (2003) Acquired melanocytic nevi as risk factor for melanoma development. A comprehensive review of epidemiological data. *Pigment cell research*. 16, 297-306
- (51) Swerdlow, A.J., English, J., MacKie, R.M., O'Doherty, C.J., Hunter, J.A., and Clark, J. (1984) Benign naevi associated with high risk of melanoma. *Lancet*. 2, 168

- (52) Greene, M.H., Clark, W.H., Jr., Tucker, M.A., Kraemer, K.H., Elder, D.E., and Fraser, M.C. (1985) High risk of malignant melanoma in melanoma-prone families with dysplastic nevi. *Annals of internal medicine*. 102, 458-465
- (53) Swerdlow, A.J., and Green, A. (1987) Melanocytic naevi and melanoma: an epidemiological perspective. *The British journal of dermatology*. 117, 137-146
- (54) Vredenburg, A., Bohringer, S., Boonk, S.E., Gruis, N.A., Out-Luijting, C., Kukutsch, N.A., and Bergman, W. (2014) Acquired melanocytic nevi in childhood and familial melanoma. *JAMA dermatology*. 150, 35-40
- (55) Bray, F., Ferlay, J., Soerjomataram, I., Siegel, R.L., Torre, L.A., and Jemal, A. (2018) Global cancer statistics 2018: GLOBOCAN estimates of incidence and mortality worldwide for 36 cancers in 185 countries. *CA: a cancer journal for clinicians*.
- (56) Schadendorf, D., van Akkooi, A.C.J., Berking, C., Griewank, K.G., Gutzmer, R., Hauschild, A., Stang, A., Roesch, A., and Ugurel, S. (2018) Melanoma. *Lancet*. 392, 971-984
- (57) Chang, A.E., Karnell, L.H., and Menck, H.R. (1998) The National Cancer Data Base report on cutaneous and noncutaneous melanoma: a summary of 84,836 cases from the past decade. The American College of Surgeons Commission on Cancer and the American Cancer Society. *Cancer*. 83, 1664-1678
- (58) Coleman, M.P., Esteve, J., Damiecki, P., Arslan, A., and Renard, H. (1993) Trends in cancer incidence and mortality. *IARC scientific publications*. 1-806
- (59) Garbe, C., and Leiter, U. (2009) Melanoma epidemiology and trends. *Clinics in dermatology*. 27, 3-9
- (60) Karim-Kos, H.E., de Vries, E., Soerjomataram, I., Lemmens, V., Siesling, S., and Coebergh, J.W. (2008) Recent trends of cancer in Europe: a combined approach of incidence, survival and mortality for 17 cancer sites since the 1990s. *European journal of cancer*. 44, 1345-1389
- (61) de Vries, E., Bray, F.I., Coebergh, J.W., and Parkin, D.M. (2003) Changing epidemiology of malignant cutaneous melanoma in Europe 1953-1997: rising trends in incidence and mortality but recent stabilizations in western Europe and decreases in Scandinavia. *International journal of cancer*. 107, 119-126
- (62) Ali, Z., Yousaf, N., and Larkin, J. (2013) Melanoma epidemiology, biology and prognosis. *EJC supplements : EJC : official journal of EORTC, European Organization for Research and Treatment of Cancer ... [et al.]*. 11, 81-91
- (63) Barbaric, J., Sekerija, M., Agius, D., Coza, D., Dimitrova, N., Demetriou, A., Safaei Diba, C., Eser, S., Gavric, Z., Primic-Zakelj, M., Zivkovic, S., Zvolosky, M., Bray, F., Coebergh, J.W., and Znaor, A. (2016) Disparities in melanoma incidence and mortality in South-Eastern Europe: Increasing incidence and divergent mortality patterns. Is progress around the corner? *European journal of cancer*. 55, 47-55
- (64) Forsea, A.M., Del Marmol, V., de Vries, E., Bailey, E.E., and Geller, A.C. (2012) Melanoma incidence and mortality in Europe: new estimates, persistent disparities. *The British journal of dermatology*. 167, 1124-1130
- (65) Dimitriou, F., Krattinger, R., Ramelyte, E., Barysch, M.J., Micaletto, S., Dummer, R., and Goldinger, S.M. (2018) The World of Melanoma: Epidemiologic, Genetic, and Anatomic Differences of Melanoma Across the Globe. *Current oncology reports*. 20, 87

- (66) van der Spek-Keijser, L.M., van der Rhee, H.J., Toth, G., Van Westering, R., Bruijn, J.A., and Coebergh, J.W. (1997) Site, histological type, and thickness of primary cutaneous malignant melanoma in western Netherlands since 1980. *The British journal of dermatology*. 136, 565-571
- (67) Berridge, M.J., and Irvine, R.F. (1984) Inositol trisphosphate, a novel second messenger in cellular signal transduction. *Nature*. 312, 315-321
- (68) Raffaello, A., Mammucari, C., Gherardi, G., and Rizzuto, R. (2016) Calcium at the Center of Cell Signaling: Interplay between Endoplasmic Reticulum, Mitochondria, and Lysosomes. *Trends in biochemical sciences*. 41, 1035-1049
- (69) Stewart, T.A., Yapa, K.T., and Monteith, G.R. (2015) Altered calcium signaling in cancer cells. *Biochimica et biophysica acta*. 1848, 2502-2511
- (70) Hanahan, D., and Weinberg, R.A. (2011) Hallmarks of cancer: the next generation. *Cell*. 144, 646-674
- (71) Monteith, G.R., Prevarskaya, N., and Roberts-Thomson, S.J. (2017) The calcium-cancer signalling nexus. *Nature reviews. Cancer*. 17, 367-380
- (72) Prevarskaya, N., Skryma, R., and Shuba, Y. (2011) Calcium in tumour metastasis: new roles for known actors. *Nature reviews. Cancer*. 11, 609-618
- (73) Aung, C.S., Ye, W., Plowman, G., Peters, A.A., Monteith, G.R., and Roberts-Thomson, S.J. (2009) Plasma membrane calcium ATPase 4 and the remodeling of calcium homeostasis in human colon cancer cells. *Carcinogenesis*. 30, 1962-1969
- (74) VanHouten, J., Sullivan, C., Bazinet, C., Ryoo, T., Camp, R., Rimm, D.L., Chung, G., and Wysolmerski, J. (2010) PMCA2 regulates apoptosis during mammary gland involution and predicts outcome in breast cancer. *Proceedings of the National Academy of Sciences of the United States of America*. 107, 11405-11410
- (75) Deliot, N., and Constantin, B. (2015) Plasma membrane calcium channels in cancer: Alterations and consequences for cell proliferation and migration. *Biochimica et biophysica acta*. 1848, 2512-2522
- (76) Flourakis, M., Lehen'kyi, V., Beck, B., Raphael, M., Vandenberghe, M., Abeele, F.V., Roudbaraki, M., Lepage, G., Mauroy, B., Romanin, C., Shuba, Y., Skryma, R., and Prevarskaya, N. (2010) Orail contributes to the establishment of an apoptosis-resistant phenotype in prostate cancer cells. *Cell death & disease*. 1, e75
- (77) McAndrew, D., Grice, D.M., Peters, A.A., Davis, F.M., Stewart, T., Rice, M., Smart, C.E., Brown, M.A., Kenny, P.A., Roberts-Thomson, S.J., and Monteith, G.R. (2011) ORAI1-mediated calcium influx in lactation and in breast cancer. *Molecular cancer therapeutics*. 10, 448-460
- (78) Monteith, G.R. (2014) Prostate cancer cells alter the nature of their calcium influx to promote growth and acquire apoptotic resistance. *Cancer cell*. 26, 1-2
- (79) Tsavaler, L., Shapero, M.H., Morkowski, S., and Laus, R. (2001) Trp-p8, a novel prostate-specific gene, is up-regulated in prostate cancer and other malignancies and shares high homology with transient receptor potential calcium channel proteins. *Cancer research*. 61, 3760-3769
- (80) Lehen'kyi, V., and Prevarskaya, N. (2011) Oncogenic TRP channels. *Advances in experimental medicine and biology*. 704, 929-945

- (81) Giorgi, C., Ito, K., Lin, H.K., Santangelo, C., Wieckowski, M.R., Lebedzinska, M., Bononi, A., Bonora, M., Duszynski, J., Bernardi, R., Rizzuto, R., Tacchetti, C., Pinton, P., and Pandolfi, P.P. (2010) PML regulates apoptosis at endoplasmic reticulum by modulating calcium release. *Science*. 330, 1247-1251
- (82) Hirobe, T. (2005) Role of keratinocyte-derived factors involved in regulating the proliferation and differentiation of mammalian epidermal melanocytes. *Pigment cell research*. 18, 2-12
- (83) Gordon, P.R., Mansur, C.P., and Gilchrest, B.A. (1989) Regulation of human melanocyte growth, dendricity, and melanization by keratinocyte derived factors. *The Journal of investigative dermatology*. 92, 565-572
- (84) Clark, W.H., Jr., Elder, D.E., Guerry, D.t., Epstein, M.N., Greene, M.H., and Van Horn, M. (1984) A study of tumor progression: the precursor lesions of superficial spreading and nodular melanoma. *Human pathology*. 15, 1147-1165
- (85) Garraway, L.A., Widlund, H.R., Rubin, M.A., Getz, G., Berger, A.J., Ramaswamy, S., Beroukhim, R., Milner, D.A., Granter, S.R., Du, J., Lee, C., Wagner, S.N., Li, C., Golub, T.R., Rimm, D.L., Meyerson, M.L., Fisher, D.E., and Sellers, W.R. (2005) Integrative genomic analyses identify MITF as a lineage survival oncogene amplified in malignant melanoma. *Nature*. 436, 117-122
- (86) Levy, C., Khaled, M., and Fisher, D.E. (2006) MITF: master regulator of melanocyte development and melanoma oncogene. *Trends in molecular medicine*. 12, 406-414
- (87) Miller, A.J., and Mihm, M.C., Jr. (2006) Melanoma. *The New England journal of medicine*. 355, 51-65
- (88) Rosen, L.B., Ginty, D.D., Weber, M.J., and Greenberg, M.E. (1994) Membrane depolarization and calcium influx stimulate MEK and MAP kinase via activation of Ras. *Neuron*. 12, 1207-1221
- (89) James, R.G., Conrad, W.H., and Moon, R.T. (2008) Beta-catenin-independent Wnt pathways: signals, core proteins, and effectors. *Methods in molecular biology*. 468, 131-144
- (90) Chuderland, D., and Seger, R. (2008) Calcium regulates ERK signaling by modulating its protein-protein interactions. *Communicative & integrative biology*. 1, 4-5
- (91) Soboloff, J., Gligorijevic, B., and Zaidi, M.R. (2018) STIM1 (c)AMPs up melanogenesis. *The EMBO journal*. 37,
- (92) Hogan, P.G., Chen, L., Nardone, J., and Rao, A. (2003) Transcriptional regulation by calcium, calcineurin, and NFAT. *Genes & development*. 17, 2205-2232
- (93) Parsons, P.G., Musk, P., Goss, P.D., and Leah, J. (1983) Effects of calcium depletion on human cells in vitro and the anomalous behavior of the human melanoma cell line MM170. *Cancer research*. 43, 2081-2087
- (94) Bogeski, I., Al-Ansary, D., Qu, B., Niemeyer, B.A., Hoth, M., and Peinelt, C. (2010) Pharmacology of ORAI channels as a tool to understand their physiological functions. *Expert review of clinical pharmacology*. 3, 291-303
- (95) Allen, D.H., Lepple-Wienhues, A., and Cahalan, M.D. (1997) Ion channel phenotype of melanoma cell lines. *The Journal of membrane biology*. 155, 27-34

- (96) Oancea, E., Vriens, J., Brauchi, S., Jun, J., Splawski, I., and Clapham, D.E. (2009) TRPM1 forms ion channels associated with melanin content in melanocytes. *Science signaling*. 2, ra21
- (97) Duncan, L.M., Deeds, J., Hunter, J., Shao, J., Holmgren, L.M., Woolf, E.A., Tepper, R.I., and Shyjan, A.W. (1998) Down-regulation of the novel gene melastatin correlates with potential for melanoma metastasis. *Cancer research*. 58, 1515-1520
- (98) Duncan, L.M., Deeds, J., Cronin, F.E., Donovan, M., Sober, A.J., Kauffman, M., and McCarthy, J.J. (2001) Melastatin expression and prognosis in cutaneous malignant melanoma. *Journal of clinical oncology : official journal of the American Society of Clinical Oncology*. 19, 568-576
- (99) Zhiqi, S., Soltani, M.H., Bhat, K.M., Sangha, N., Fang, D., Hunter, J.J., and Setaluri, V. (2004) Human melastatin 1 (TRPM1) is regulated by MITF and produces multiple polypeptide isoforms in melanocytes and melanoma. *Melanoma research*. 14, 509-516
- (100) Biro, T., Toth, B.I., Marincsak, R., Dobrosi, N., Geczy, T., and Paus, R. (2007) TRP channels as novel players in the pathogenesis and therapy of itch. *Biochimica et biophysica acta*. 1772, 1004-1021
- (101) Atoyan, R., Shander, D., and Botchkareva, N.V. (2009) Non-neuronal expression of transient receptor potential type A1 (TRPA1) in human skin. *The Journal of investigative dermatology*. 129, 2312-2315
- (102) Feng, J., Yang, P., Mack, M.R., Dryn, D., Luo, J., Gong, X., Liu, S., Oetjen, L.K., Zholos, A.V., Mei, Z., Yin, S., Kim, B.S., and Hu, H. (2017) Sensory TRP channels contribute differentially to skin inflammation and persistent itch. *Nature communications*. 8, 980
- (103) Yang, P., Feng, J., Luo, J., Madison, M., and Hu, H. (2017) A Critical Role for TRP Channels in the Skin. in *Neurobiology of TRP Channels* (nd, and Emir, T.L.R., ed.)^eds.), pp. 95-111, Boca Raton (FL)
- (104) Ho, J.C., and Lee, C.H. (2015) TRP channels in skin: from physiological implications to clinical significances. *Biophysics*. 11, 17-24
- (105) Guo, H., Carlson, J.A., and Slominski, A. (2012) Role of TRPM in melanocytes and melanoma. *Experimental dermatology*. 21, 650-654
- (106) Hoth, M. (2016) CRAC channels, calcium, and cancer in light of the driver and passenger concept. *Biochimica et biophysica acta*. 1863, 1408-1417
- (107) Parekh, A.B. (2010) Store-operated CRAC channels: function in health and disease. *Nature reviews. Drug discovery*. 9, 399-410
- (108) Hoth, M., and Niemeyer, B.A. (2013) The neglected CRAC proteins: Orai2, Orai3, and STIM2. *Current topics in membranes*. 71, 237-271
- (109) Hoover, P.J., and Lewis, R.S. (2011) Stoichiometric requirements for trapping and gating of Ca<sup>2+</sup> release-activated Ca<sup>2+</sup> (CRAC) channels by stromal interaction molecule 1 (STIM1). *Proceedings of the National Academy of Sciences of the United States of America*. 108, 13299-13304
- (110) Feldman, B., Fedida-Metula, S., Nita, J., Sekler, I., and Fishman, D. (2010) Coupling of mitochondria to store-operated Ca(2+)-signaling sustains constitutive activation of protein kinase B/Akt and augments survival of malignant melanoma cells. *Cell calcium*. 47, 525-537

- (111) Stanisz, H., Stark, A., Kilch, T., Schwarz, E.C., Muller, C.S., Peinelt, C., Hoth, M., Niemeyer, B.A., Vogt, T., and Bogeski, I. (2012) ORAI1 Ca(2+) channels control endothelin-1-induced mitogenesis and melanogenesis in primary human melanocytes. *The Journal of investigative dermatology*. 132, 1443-1451
- (112) Stanisz, H., Saul, S., Muller, C.S., Kappl, R., Niemeyer, B.A., Vogt, T., Hoth, M., Roesch, A., and Bogeski, I. (2014) Inverse regulation of melanoma growth and migration by Orai1/STIM2-dependent calcium entry. *Pigment cell & melanoma research*. 27, 442-453
- (113) Umemura, M., Baljinnayam, E., Feske, S., De Lorenzo, M.S., Xie, L.H., Feng, X., Oda, K., Makino, A., Fujita, T., Yokoyama, U., Iwatsubo, M., Chen, S., Goydos, J.S., Ishikawa, Y., and Iwatsubo, K. (2014) Store-operated Ca<sup>2+</sup> entry (SOCE) regulates melanoma proliferation and cell migration. *PloS one*. 9, e89292
- (114) Sun, J., Lu, F., He, H., Shen, J., Messina, J., Mathew, R., Wang, D., Sarnaik, A.A., Chang, W.C., Kim, M., Cheng, H., and Yang, S. (2014) STIM1- and Orai1-mediated Ca(2+) oscillation orchestrates invadopodium formation and melanoma invasion. *The Journal of cell biology*. 207, 535-548
- (115) Hooper, R., Zhang, X., Webster, M., Go, C., Kedra, J., Marchbank, K., Gill, D.L., Weeraratna, A.T., Trebak, M., and Soboloff, J. (2015) Novel Protein Kinase C-Mediated Control of Orai1 Function in Invasive Melanoma. *Molecular and cellular biology*. 35, 2790-2798
- (116) Cross, C.E., Halliwell, B., Borish, E.T., Pryor, W.A., Ames, B.N., Saul, R.L., McCord, J.M., and Harman, D. (1987) Oxygen radicals and human disease. *Annals of internal medicine*. 107, 526-545
- (117) Finkel, T. (2011) Signal transduction by reactive oxygen species. *The Journal of cell biology*. 194, 7-15
- (118) (1985) Metal chelation therapy, oxygen radicals, and human disease. *Lancet*. 1, 143-145
- (119) Schieber, M., and Chandel, N.S. (2014) ROS function in redox signaling and oxidative stress. *Current biology : CB*. 24, R453-462
- (120) Rhee, S.G. (2006) Cell signaling. H<sub>2</sub>O<sub>2</sub>, a necessary evil for cell signaling. *Science*. 312, 1882-1883
- (121) Forman, H.J., Fukuto, J.M., and Torres, M. (2004) Redox signaling: thiol chemistry defines which reactive oxygen and nitrogen species can act as second messengers. *American journal of physiology. Cell physiology*. 287, C246-256
- (122) Paulsen, C.E., and Carroll, K.S. (2013) Cysteine-mediated redox signaling: chemistry, biology, and tools for discovery. *Chemical reviews*. 113, 4633-4679
- (123) Cairns, R.A., Harris, I.S., and Mak, T.W. (2011) Regulation of cancer cell metabolism. *Nature reviews. Cancer*. 11, 85-95
- (124) Szatrowski, T.P., and Nathan, C.F. (1991) Production of large amounts of hydrogen peroxide by human tumor cells. *Cancer research*. 51, 794-798
- (125) Weinberg, F., Hamanaka, R., Wheaton, W.W., Weinberg, S., Joseph, J., Lopez, M., Kalyanaraman, B., Mutlu, G.M., Budinger, G.R., and Chandel, N.S. (2010) Mitochondrial metabolism and ROS generation are essential for Kras-mediated tumorigenicity. *Proceedings of the National Academy of Sciences of the United States of America*. 107, 8788-8793

- (126) Sullivan, L.B., Martinez-Garcia, E., Nguyen, H., Mullen, A.R., Dufour, E., Sudarshan, S., Licht, J.D., Deberardinis, R.J., and Chandel, N.S. (2013) The proto-oncometabolite fumarate binds glutathione to amplify ROS-dependent signaling. *Molecular cell*. 51, 236-248
- (127) Ishikawa, K., Takenaga, K., Akimoto, M., Koshikawa, N., Yamaguchi, A., Imanishi, H., Nakada, K., Honma, Y., and Hayashi, J. (2008) ROS-generating mitochondrial DNA mutations can regulate tumor cell metastasis. *Science*. 320, 661-664
- (128) Ben-Neriah, Y., and Karin, M. (2011) Inflammation meets cancer, with NF-kappaB as the matchmaker. *Nature immunology*. 12, 715-723
- (129) Sporn, M.B., and Libby, K.T. (2012) NRF2 and cancer: the good, the bad and the importance of context. *Nature reviews. Cancer*. 12, 564-571
- (130) Rojo de la Vega, M., Chapman, E., and Zhang, D.D. (2018) NRF2 and the Hallmarks of Cancer. *Cancer cell*. 34, 21-43
- (131) Gorrini, C., Harris, I.S., and Mak, T.W. (2013) Modulation of oxidative stress as an anticancer strategy. *Nature reviews. Drug discovery*. 12, 931-947
- (132) Trachootham, D., Zhou, Y., Zhang, H., Demizu, Y., Chen, Z., Pelicano, H., Chiao, P.J., Achanta, G., Arlinghaus, R.B., Liu, J., and Huang, P. (2006) Selective killing of oncogenically transformed cells through a ROS-mediated mechanism by beta-phenylethyl isothiocyanate. *Cancer cell*. 10, 241-252
- (133) Bustamante, J., Bredeston, L., Malanga, G., and Mordoh, J. (1993) Role of melanin as a scavenger of active oxygen species. *Pigment cell research*. 6, 348-353
- (134) Sander, C.S., Chang, H., Salzman, S., Muller, C.S., Ekanayake-Mudiyanselage, S., Elsner, P., and Thiele, J.J. (2002) Photoaging is associated with protein oxidation in human skin in vivo. *The Journal of investigative dermatology*. 118, 618-625
- (135) Fuchs, J., Huflejt, M.E., Rothfuss, L.M., Wilson, D.S., Carcamo, G., and Packer, L. (1989) Impairment of enzymic and nonenzymic antioxidants in skin by UVB irradiation. *The Journal of investigative dermatology*. 93, 769-773
- (136) Poswig, A., Wenk, J., Brenneisen, P., Wlaschek, M., Hommel, C., Quel, G., Faisst, K., Dissemmond, J., Briviba, K., Krieg, T., and Scharffetter-Kochanek, K. (1999) Adaptive antioxidant response of manganese-superoxide dismutase following repetitive UVA irradiation. *The Journal of investigative dermatology*. 112, 13-18
- (137) Cheng, G.C., Schulze, P.C., Lee, R.T., Sylvan, J., Zetter, B.R., and Huang, H. (2004) Oxidative stress and thioredoxin-interacting protein promote intravasation of melanoma cells. *Experimental cell research*. 300, 297-307
- (138) Lehtola, K., Laurikainen, L., Leino, L., Ahotupa, M., and Punnonen, K. (1995) Antioxidant enzymes are elevated in dimethylbenz[a]anthracene-induced neoplastic murine keratinocytes containing an active rasHa oncogene. *Journal of cancer research and clinical oncology*. 121, 402-406
- (139) Vural, P., Canbaz, M., and Selcuki, D. (1999) Plasma antioxidant defense in actinic keratosis and basal cell carcinoma. *Journal of the European Academy of Dermatology and Venereology : JEADV*. 13, 96-101
- (140) Wittgen, H.G., and van Kempen, L.C. (2007) Reactive oxygen species in melanoma and its therapeutic implications. *Melanoma research*. 17, 400-409

- (141) Picardo, M., Grammatico, P., Roccella, F., Roccella, M., Grandinetti, M., Del Porto, G., and Passi, S. (1996) Imbalance in the antioxidant pool in melanoma cells and normal melanocytes from patients with melanoma. *The Journal of investigative dermatology*. 107, 322-326
- (142) Schadendorf, D., Zuberbier, T., Diehl, S., Schadendorf, C., and Czarnetzki, B.M. (1995) Serum manganese superoxide dismutase is a new tumour marker for malignant melanoma. *Melanoma research*. 5, 351-353
- (143) Roesch, A., Vultur, A., Bogeski, I., Wang, H., Zimmermann, K.M., Speicher, D., Korbel, C., Laschke, M.W., Gimotty, P.A., Philipp, S.E., Krause, E., Patzold, S., Villanueva, J., Krepler, C., Fukunaga-Kalabis, M., Hoth, M., Bastian, B.C., Vogt, T., and Herlyn, M. (2013) Overcoming intrinsic multidrug resistance in melanoma by blocking the mitochondrial respiratory chain of slow-cycling JARID1B(high) cells. *Cancer cell*. 23, 811-825
- (144) Joosse, A., De Vries, E., van Eijck, C.H., Eggermont, A.M., Nijsten, T., and Coebergh, J.W. (2010) Reactive oxygen species and melanoma: an explanation for gender differences in survival? *Pigment cell & melanoma research*. 23, 352-364
- (145) Verhaegen, M., Bauer, J.A., Martin de la Vega, C., Wang, G., Wolter, K.G., Brenner, J.C., Nikolovska-Coleska, Z., Bengtson, A., Nair, R., Elder, J.T., Van Brocklin, M., Carey, T.E., Bradford, C.R., Wang, S., and Soengas, M.S. (2006) A novel BH3 mimetic reveals a mitogen-activated protein kinase-dependent mechanism of melanoma cell death controlled by p53 and reactive oxygen species. *Cancer research*. 66, 11348-11359
- (146) Stahl, J.M., Sharma, A., Cheung, M., Zimmerman, M., Cheng, J.Q., Bosenberg, M.W., Kester, M., Sandirasegarane, L., and Robertson, G.P. (2004) Deregulated Akt3 activity promotes development of malignant melanoma. *Cancer research*. 64, 7002-7010
- (147) Govindarajan, B., Sligh, J.E., Vincent, B.J., Li, M., Canter, J.A., Nickoloff, B.J., Rodenburg, R.J., Smeitink, J.A., Oberley, L., Zhang, Y., Slingerland, J., Arnold, R.S., Lambeth, J.D., Cohen, C., Hilenski, L., Griendling, K., Martinez-Diez, M., Cuezva, J.M., and Arbiser, J.L. (2007) Overexpression of Akt converts radial growth melanoma to vertical growth melanoma. *The Journal of clinical investigation*. 117, 719-729
- (148) Meyskens, F.L., Jr., McNulty, S.E., Buckmeier, J.A., Tohidian, N.B., Spillane, T.J., Kahlon, R.S., and Gonzalez, R.I. (2001) Aberrant redox regulation in human metastatic melanoma cells compared to normal melanocytes. *Free radical biology & medicine*. 31, 799-808
- (149) Brar, S.S., Kennedy, T.P., Whorton, A.R., Sturrock, A.B., Huecksteadt, T.P., Ghio, A.J., and Hoidal, J.R. (2001) Reactive oxygen species from NAD(P)H:quinone oxidoreductase constitutively activate NF-kappaB in malignant melanoma cells. *American journal of physiology. Cell physiology*. 280, C659-676
- (150) Bergman, M.R., Cheng, S., Honbo, N., Piacentini, L., Karliner, J.S., and Lovett, D.H. (2003) A functional activating protein 1 (AP-1) site regulates matrix metalloproteinase 2 (MMP-2) transcription by cardiac cells through interactions with JunB-Fra1 and JunB-FosB heterodimers. *The Biochemical journal*. 369, 485-496
- (151) Kim, M.H., Cho, H.S., Jung, M., Hong, M.H., Lee, S.K., Shin, B.A., Ahn, B.W., and Jung, Y.D. (2005) Extracellular signal-regulated kinase and AP-1 pathways are involved in reactive oxygen species-induced urokinase plasminogen activator receptor expression in human gastric cancer cells. *International journal of oncology*. 26, 1669-1674

- (152) Cen, D., Gonzalez, R.I., Buckmeier, J.A., Kahlon, R.S., Tohidian, N.B., and Meyskens, F.L., Jr. (2002) Disulfiram induces apoptosis in human melanoma cells: a redox-related process. *Molecular cancer therapeutics*. 1, 197-204
- (153) Cen, D., Brayton, D., Shahandeh, B., Meyskens, F.L., Jr., and Farmer, P.J. (2004) Disulfiram facilitates intracellular Cu uptake and induces apoptosis in human melanoma cells. *Journal of medicinal chemistry*. 47, 6914-6920
- (154) Massaro, R.R., Faiao-Flores, F., Rebecca, V.W., Sandri, S., Alves-Fernandes, D.K., Pennacchi, P.C., Smalley, K.S.M., and Maria-Engler, S.S. (2017) Inhibition of proliferation and invasion in 2D and 3D models by 2-methoxyestradiol in human melanoma cells. *Pharmacological research*. 119, 242-250
- (155) Revesz, L., Edgren, M.R., and Wainson, A.A. (1994) Selective toxicity of buthionine sulfoximine (BSO) to melanoma cells in vitro and in vivo. *International journal of radiation oncology, biology, physics*. 29, 403-406
- (156) Huang, P., Feng, L., Oldham, E.A., Keating, M.J., and Plunkett, W. (2000) Superoxide dismutase as a target for the selective killing of cancer cells. *Nature*. 407, 390-395
- (157) Dobos, J., Timar, J., Bocsi, J., Burian, Z., Nagy, K., Barna, G., Petak, I., and Ladanyi, A. (2004) In vitro and in vivo antitumor effect of 2-methoxyestradiol on human melanoma. *International journal of cancer*. 112, 771-776
- (158) Cierlitz, M., Chauvistre, H., Bogeski, I., Zhang, X., Hauschild, A., Herlyn, M., Schadendorf, D., Vogt, T., and Roesch, A. (2015) Mitochondrial oxidative stress as a novel therapeutic target to overcome intrinsic drug resistance in melanoma cell subpopulations. *Experimental dermatology*. 24, 155-157
- (159) Fruehauf, J.P., and Meyskens, F.L., Jr. (2007) Reactive oxygen species: a breath of life or death? *Clinical cancer research : an official journal of the American Association for Cancer Research*. 13, 789-794
- (160) Fruehauf, J.P., and Trapp, V. (2008) Reactive oxygen species: an Achilles' heel of melanoma? *Expert review of anticancer therapy*. 8, 1751-1757
- (161) Feissner, R.F., Skalska, J., Gaum, W.E., and Sheu, S.S. (2009) Crosstalk signaling between mitochondrial Ca<sup>2+</sup> and ROS. *Frontiers in bioscience*. 14, 1197-1218
- (162) Brookes, P.S., Yoon, Y., Robotham, J.L., Anders, M.W., and Sheu, S.S. (2004) Calcium, ATP, and ROS: a mitochondrial love-hate triangle. *American journal of physiology. Cell physiology*. 287, C817-833
- (163) Brookes, P.S., Levonen, A.L., Shiva, S., Sarti, P., and Darley-Usmar, V.M. (2002) Mitochondria: regulators of signal transduction by reactive oxygen and nitrogen species. *Free radical biology & medicine*. 33, 755-764
- (164) Denton, R.M. (2009) Regulation of mitochondrial dehydrogenases by calcium ions. *Biochimica et biophysica acta*. 1787, 1309-1316
- (165) Griffiths, E.J., and Rutter, G.A. (2009) Mitochondrial calcium as a key regulator of mitochondrial ATP production in mammalian cells. *Biochimica et biophysica acta*. 1787, 1324-1333
- (166) Baughman, J.M., Perocchi, F., Girgis, H.S., Plovanich, M., Belcher-Timme, C.A., Sancak, Y., Bao, X.R., Strittmatter, L., Goldberger, O., Bogorad, R.L., Kotliansky, V., and

- Mootha, V.K. (2011) Integrative genomics identifies MCU as an essential component of the mitochondrial calcium uniporter. *Nature*. 476, 341-345
- (167) J, O.U., Ryu, S.Y., Jhun, B.S., Hurst, S., and Sheu, S.S. (2014) Mitochondrial ion channels/transporters as sensors and regulators of cellular redox signaling. *Antioxidants & redox signaling*. 21, 987-1006
- (168) Viola, H.M., Arthur, P.G., and Hool, L.C. (2007) Transient exposure to hydrogen peroxide causes an increase in mitochondria-derived superoxide as a result of sustained alteration in L-type Ca<sup>2+</sup> channel function in the absence of apoptosis in ventricular myocytes. *Circulation research*. 100, 1036-1044
- (169) Liu, S.S. (1999) Cooperation of a "reactive oxygen cycle" with the Q cycle and the proton cycle in the respiratory chain--superoxide generating and cycling mechanisms in mitochondria. *Journal of bioenergetics and biomembranes*. 31, 367-376
- (170) Han, D., Antunes, F., Canali, R., Rettori, D., and Cadenas, E. (2003) Voltage-dependent anion channels control the release of the superoxide anion from mitochondria to cytosol. *The Journal of biological chemistry*. 278, 5557-5563
- (171) Heinen, A., Camara, A.K., Aldakkak, M., Rhodes, S.S., Riess, M.L., and Stowe, D.F. (2007) Mitochondrial Ca<sup>2+</sup>-induced K<sup>+</sup> influx increases respiration and enhances ROS production while maintaining membrane potential. *American journal of physiology. Cell physiology*. 292, C148-156
- (172) Nulton-Persson, A.C., and Szwedda, L.I. (2001) Modulation of mitochondrial function by hydrogen peroxide. *The Journal of biological chemistry*. 276, 23357-23361
- (173) Cleeter, M.W., Cooper, J.M., Darley-Usmar, V.M., Moncada, S., and Schapira, A.H. (1994) Reversible inhibition of cytochrome c oxidase, the terminal enzyme of the mitochondrial respiratory chain, by nitric oxide. Implications for neurodegenerative diseases. *FEBS letters*. 345, 50-54
- (174) Jekabsone, A., Ivanoviene, L., Brown, G.C., and Borutaite, V. (2003) Nitric oxide and calcium together inactivate mitochondrial complex I and induce cytochrome c release. *Journal of molecular and cellular cardiology*. 35, 803-809
- (175) Herrington, J., Park, Y.B., Babcock, D.F., and Hille, B. (1996) Dominant role of mitochondria in clearance of large Ca<sup>2+</sup> loads from rat adrenal chromaffin cells. *Neuron*. 16, 219-228
- (176) Boitier, E., Rea, R., and Duchen, M.R. (1999) Mitochondria exert a negative feedback on the propagation of intracellular Ca<sup>2+</sup> waves in rat cortical astrocytes. *The Journal of cell biology*. 145, 795-808
- (177) Bereiter-Hahn, J., and Voth, M. (1994) Dynamics of mitochondria in living cells: shape changes, dislocations, fusion, and fission of mitochondria. *Microscopy research and technique*. 27, 198-219
- (178) Brookes, P.S., and Darley-Usmar, V.M. (2004) Role of calcium and superoxide dismutase in sensitizing mitochondria to peroxynitrite-induced permeability transition. *American journal of physiology. Heart and circulatory physiology*. 286, H39-46
- (179) Rooney, T.A., Renard, D.C., Sass, E.J., and Thomas, A.P. (1991) Oscillatory cytosolic calcium waves independent of stimulated inositol 1,4,5-trisphosphate formation in hepatocytes. *The Journal of biological chemistry*. 266, 12272-12282

- (180) Suzuki, Y.J., and Ford, G.D. (1992) Superoxide stimulates IP<sub>3</sub>-induced Ca<sup>2+</sup> release from vascular smooth muscle sarcoplasmic reticulum. *The American journal of physiology.* 262, H114-116
- (181) Kaplan, P., Babusikova, E., Lehotsky, J., and Dobrota, D. (2003) Free radical-induced protein modification and inhibition of Ca<sup>2+</sup>-ATPase of cardiac sarcoplasmic reticulum. *Molecular and cellular biochemistry.* 248, 41-47
- (182) Goldhaber, J.I. (1996) Free radicals enhance Na<sup>+</sup>/Ca<sup>2+</sup> exchange in ventricular myocytes. *The American journal of physiology.* 271, H823-833
- (183) Kowaltowski, A.J., Castilho, R.F., and Vercesi, A.E. (2001) Mitochondrial permeability transition and oxidative stress. *FEBS letters.* 495, 12-15
- (184) Daiber, A. (2010) Redox signaling (cross-talk) from and to mitochondria involves mitochondrial pores and reactive oxygen species. *Biochimica et biophysica acta.* 1797, 897-906
- (185) Vander Heiden, M.G., Cantley, L.C., and Thompson, C.B. (2009) Understanding the Warburg effect: the metabolic requirements of cell proliferation. *Science.* 324, 1029-1033
- (186) Hall, A., Meyle, K.D., Lange, M.K., Klima, M., Sanderhoff, M., Dahl, C., Abildgaard, C., Thorup, K., Moghimi, S.M., Jensen, P.B., Bartek, J., Guldborg, P., and Christensen, C. (2013) Dysfunctional oxidative phosphorylation makes malignant melanoma cells addicted to glycolysis driven by the (V600E)BRAF oncogene. *Oncotarget.* 4, 584-599
- (187) Abildgaard, C., Dahl, C., Basse, A.L., Ma, T., and Guldborg, P. (2014) Bioenergetic modulation with dichloroacetate reduces the growth of melanoma cells and potentiates their response to BRAFV600E inhibition. *Journal of translational medicine.* 12, 247
- (188) Scott, D.A., Richardson, A.D., Filipp, F.V., Knutzen, C.A., Chiang, G.G., Ronai, Z.A., Osterman, A.L., and Smith, J.W. (2011) Comparative metabolic flux profiling of melanoma cell lines: beyond the Warburg effect. *The Journal of biological chemistry.* 286, 42626-42634
- (189) Vazquez, F., Lim, J.H., Chim, H., Bhalla, K., Girnun, G., Pierce, K., Clish, C.B., Granter, S.R., Widlund, H.R., Spiegelman, B.M., and Puigserver, P. (2013) PGC1alpha expression defines a subset of human melanoma tumors with increased mitochondrial capacity and resistance to oxidative stress. *Cancer cell.* 23, 287-301
- (190) Abildgaard, C., and Guldborg, P. (2015) Molecular drivers of cellular metabolic reprogramming in melanoma. *Trends in molecular medicine.* 21, 164-171
- (191) Parmenter, T.J., Kleinschmidt, M., Kinross, K.M., Bond, S.T., Li, J., Kaadige, M.R., Rao, A., Sheppard, K.E., Hugo, W., Pupo, G.M., Pearson, R.B., McGee, S.L., Long, G.V., Scolyer, R.A., Rizos, H., Lo, R.S., Cullinane, C., Ayer, D.E., Ribas, A., Johnstone, R.W., Hicks, R.J., and McArthur, G.A. (2014) Response of BRAF-mutant melanoma to BRAF inhibition is mediated by a network of transcriptional regulators of glycolysis. *Cancer discovery.* 4, 423-433
- (192) Haq, R., Shoag, J., Andreu-Perez, P., Yokoyama, S., Edelman, H., Rowe, G.C., Frederick, D.T., Hurley, A.D., Nellore, A., Kung, A.L., Wargo, J.A., Song, J.S., Fisher, D.E., Arany, Z., and Widlund, H.R. (2013) Oncogenic BRAF regulates oxidative metabolism via PGC1alpha and MITF. *Cancer cell.* 23, 302-315

- (193) Haq, R., Fisher, D.E., and Widlund, H.R. (2014) Molecular pathways: BRAF induces bioenergetic adaptation by attenuating oxidative phosphorylation. *Clinical cancer research : an official journal of the American Association for Cancer Research*. 20, 2257-2263
- (194) Barbi de Moura, M., Vincent, G., Fayewicz, S.L., Bateman, N.W., Hood, B.L., Sun, M., Suhan, J., Duensing, S., Yin, Y., Sander, C., Kirkwood, J.M., Becker, D., Conrads, T.P., Van Houten, B., and Moschos, S.J. (2012) Mitochondrial respiration--an important therapeutic target in melanoma. *PloS one*. 7, e40690
- (195) Ho, J., de Moura, M.B., Lin, Y., Vincent, G., Thorne, S., Duncan, L.M., Hui-Min, L., Kirkwood, J.M., Becker, D., Van Houten, B., and Moschos, S.J. (2012) Importance of glycolysis and oxidative phosphorylation in advanced melanoma. *Molecular cancer*. 11, 76
- (196) Elbaz, Y., and Schuldiner, M. (2011) Staying in touch: the molecular era of organelle contact sites. *Trends in biochemical sciences*. 36, 616-623
- (197) Friedman, J.R., and Voeltz, G.K. (2011) The ER in 3D: a multifunctional dynamic membrane network. *Trends in cell biology*. 21, 709-717
- (198) Csordas, G., Renken, C., Varnai, P., Walter, L., Weaver, D., Buttle, K.F., Balla, T., Mannella, C.A., and Hajnoczky, G. (2006) Structural and functional features and significance of the physical linkage between ER and mitochondria. *The Journal of cell biology*. 174, 915-921
- (199) Ruby, J.R., Dyer, R.F., and Skalko, R.G. (1969) Continuities between mitochondria and endoplasmic reticulum in the mammalian ovary. *Zeitschrift fur Zellforschung und mikroskopische Anatomie*. 97, 30-37
- (200) Vance, J.E. (1990) Phospholipid synthesis in a membrane fraction associated with mitochondria. *The Journal of biological chemistry*. 265, 7248-7256
- (201) Friedman, J.R., Webster, B.M., Mastronarde, D.N., Verhey, K.J., and Voeltz, G.K. (2010) ER sliding dynamics and ER-mitochondrial contacts occur on acetylated microtubules. *The Journal of cell biology*. 190, 363-375
- (202) Knott, A.B., Perkins, G., Schwarzenbacher, R., and Bossy-Wetzel, E. (2008) Mitochondrial fragmentation in neurodegeneration. *Nature reviews. Neuroscience*. 9, 505-518
- (203) Rowland, A.A., and Voeltz, G.K. (2012) Endoplasmic reticulum-mitochondria contacts: function of the junction. *Nature reviews. Molecular cell biology*. 13, 607-625
- (204) van Vliet, A.R., Verfaillie, T., and Agostinis, P. (2014) New functions of mitochondria associated membranes in cellular signaling. *Biochimica et biophysica acta*. 1843, 2253-2262
- (205) Pinton, P., Giorgi, C., and Pandolfi, P.P. (2011) The role of PML in the control of apoptotic cell fate: a new key player at ER-mitochondria sites. *Cell death and differentiation*. 18, 1450-1456
- (206) Giorgi, C., Wieckowski, M.R., Pandolfi, P.P., and Pinton, P. (2011) Mitochondria associated membranes (MAMs) as critical hubs for apoptosis. *Communicative & integrative biology*. 4, 334-335
- (207) Betz, C., Stracka, D., Prescianotto-Baschong, C., Frieden, M., Demaurex, N., and Hall, M.N. (2013) Feature Article: mTOR complex 2-Akt signaling at mitochondria-associated endoplasmic reticulum membranes (MAM) regulates mitochondrial physiology. *Proceedings of the National Academy of Sciences of the United States of America*. 110, 12526-12534

- (208) Colombi, M., Molle, K.D., Benjamin, D., Rattenbacher-Kiser, K., Schaefer, C., Betz, C., Thiemeyer, A., Regenass, U., Hall, M.N., and Moroni, C. (2011) Genome-wide shRNA screen reveals increased mitochondrial dependence upon mTORC2 addiction. *Oncogene*. 30, 1551-1565
- (209) Bravo, R., Vicencio, J.M., Parra, V., Troncoso, R., Munoz, J.P., Bui, M., Quiroga, C., Rodriguez, A.E., Verdejo, H.E., Ferreira, J., Iglewski, M., Chiong, M., Simmen, T., Zorzano, A., Hill, J.A., Rothermel, B.A., Szabadkai, G., and Lavandero, S. (2011) Increased ER-mitochondrial coupling promotes mitochondrial respiration and bioenergetics during early phases of ER stress. *Journal of cell science*. 124, 2143-2152
- (210) Sano, R., Annunziata, I., Patterson, A., Moshiach, S., Gomero, E., Opferman, J., Forte, M., and d'Azzo, A. (2009) GM1-ganglioside accumulation at the mitochondria-associated ER membranes links ER stress to Ca(2+)-dependent mitochondrial apoptosis. *Molecular cell*. 36, 500-511
- (211) Chami, M., Oules, B., Szabadkai, G., Tacine, R., Rizzuto, R., and Paterlini-Brechot, P. (2008) Role of SERCA1 truncated isoform in the proapoptotic calcium transfer from ER to mitochondria during ER stress. *Molecular cell*. 32, 641-651
- (212) Staunton, M.J., and Gaffney, E.F. (1995) Tumor type is a determinant of susceptibility to apoptosis. *American journal of clinical pathology*. 103, 300-307
- (213) Glinsky, G.V., Glinsky, V.V., Ivanova, A.B., and Hueser, C.J. (1997) Apoptosis and metastasis: increased apoptosis resistance of metastatic cancer cells is associated with the profound deficiency of apoptosis execution mechanisms. *Cancer letters*. 115, 185-193
- (214) Soengas, M.S., and Lowe, S.W. (2003) Apoptosis and melanoma chemoresistance. *Oncogene*. 22, 3138-3151
- (215) Beck, D., Niessner, H., Smalley, K.S., Flaherty, K., Paraiso, K.H., Busch, C., Sinnberg, T., Vasseur, S., Iovanna, J.L., Driessen, S., Stork, B., Wesselborg, S., Schaller, M., Biedermann, T., Bauer, J., Lasithiotakis, K., Weide, B., Eberle, J., Schitteck, B., Schadendorf, D., Garbe, C., Kulms, D., and Meier, F. (2013) Vemurafenib potently induces endoplasmic reticulum stress-mediated apoptosis in BRAFV600E melanoma cells. *Science signaling*. 6, ra7
- (216) Ma, X.H., Piao, S.F., Dey, S., McAfee, Q., Karakousis, G., Villanueva, J., Hart, L.S., Levi, S., Hu, J., Zhang, G., Lazova, R., Klump, V., Pawelek, J.M., Xu, X., Xu, W., Schuchter, L.M., Davies, M.A., Herlyn, M., Winkler, J., Koumenis, C., and Amaravadi, R.K. (2014) Targeting ER stress-induced autophagy overcomes BRAF inhibitor resistance in melanoma. *The Journal of clinical investigation*. 124, 1406-1417
- (217) Cerezo, M., Lehraiki, A., Millet, A., Rouaud, F., Plaisant, M., Jaune, E., Botton, T., Ronco, C., Abbe, P., Amdouni, H., Passeron, T., Hofman, V., Mograbi, B., Dabert-Gay, A.S., Debayle, D., Alcor, D., Rabhi, N., Annicotte, J.S., Heliot, L., Gonzalez-Pisfil, M., Robert, C., Morera, S., Vigouroux, A., Gual, P., Ali, M.M.U., Bertolotto, C., Hofman, P., Ballotti, R., Benhida, R., and Rocchi, S. (2016) Compounds Triggering ER Stress Exert Anti-Melanoma Effects and Overcome BRAF Inhibitor Resistance. *Cancer cell*. 30, 183
- (218) Hill, D.S., Martin, S., Armstrong, J.L., Flockhart, R., Tonison, J.J., Simpson, D.G., Birch-Machin, M.A., Redfern, C.P., and Lovat, P.E. (2009) Combining the endoplasmic reticulum stress-inducing agents bortezomib and fenretinide as a novel therapeutic strategy for metastatic melanoma. *Clinical cancer research : an official journal of the American Association for Cancer Research*. 15, 1192-1198

- (219) Sharma, S., Quintana, A., Findlay, G.M., Mettlen, M., Baust, B., Jain, M., Nilsson, R., Rao, A., and Hogan, P.G. (2013) An siRNA screen for NFAT activation identifies septins as coordinators of store-operated Ca<sup>2+</sup> entry. *Nature*. 499, 238-242
- (220) Matsuo, Y., Akiyama, N., Nakamura, H., Yodoi, J., Noda, M., and Kizaka-Kondoh, S. (2001) Identification of a novel thioredoxin-related transmembrane protein. *The Journal of biological chemistry*. 276, 10032-10038
- (221) Meng, X., Zhang, C., Chen, J., Peng, S., Cao, Y., Ying, K., Xie, Y., and Mao, Y. (2003) Cloning and identification of a novel cDNA coding thioredoxin-related transmembrane protein 2. *Biochemical genetics*. 41, 99-106
- (222) Haugstetter, J., Blicher, T., and Ellgaard, L. (2005) Identification and characterization of a novel thioredoxin-related transmembrane protein of the endoplasmic reticulum. *The Journal of biological chemistry*. 280, 8371-8380
- (223) Roth, D., Lynes, E., Riemer, J., Hansen, H.G., Althaus, N., Simmen, T., and Ellgaard, L. (2009) A di-arginine motif contributes to the ER localization of the type I transmembrane ER oxidoreductase TMX4. *The Biochemical journal*. 425, 195-205
- (224) Harding, H.P., Zhang, Y., Zeng, H., Novoa, I., Lu, P.D., Calton, M., Sadri, N., Yun, C., Popko, B., Paules, R., Stojdl, D.F., Bell, J.C., Hettmann, T., Leiden, J.M., and Ron, D. (2003) An integrated stress response regulates amino acid metabolism and resistance to oxidative stress. *Molecular cell*. 11, 619-633
- (225) Haynes, C.M., Titus, E.A., and Cooper, A.A. (2004) Degradation of misfolded proteins prevents ER-derived oxidative stress and cell death. *Molecular cell*. 15, 767-776
- (226) Matsuo, Y., and Hirota, K. (2017) Transmembrane thioredoxin-related protein TMX1 is reversibly oxidized in response to protein accumulation in the endoplasmic reticulum. *FEBS open bio*. 7, 1768-1777
- (227) Lynes, E.M., Bui, M., Yap, M.C., Benson, M.D., Schneider, B., Ellgaard, L., Berthiaume, L.G., and Simmen, T. (2012) Palmitoylated TMX and calnexin target to the mitochondria-associated membrane. *The EMBO journal*. 31, 457-470
- (228) Raturi, A., Gutierrez, T., Ortiz-Sandoval, C., Ruangkittisakul, A., Herrera-Cruz, M.S., Rockley, J.P., Gesson, K., Ourdev, D., Lou, P.H., Lucchinetti, E., Tahbaz, N., Zaugg, M., Baksh, S., Ballanyi, K., and Simmen, T. (2016) TMX1 determines cancer cell metabolism as a thiol-based modulator of ER-mitochondria Ca<sup>2+</sup> flux. *The Journal of cell biology*. 214, 433-444
- (229) Shaw, J.P., Utz, P.J., Durand, D.B., Toole, J.J., Emmel, E.A., and Crabtree, G.R. (2010) Identification of a putative regulator of early T cell activation genes. *Science*. 1988. 241: 202-205. *Journal of immunology*. 185, 4972-4975
- (230) Rao, A., Luo, C., and Hogan, P.G. (1997) Transcription factors of the NFAT family: regulation and function. *Annual review of immunology*. 15, 707-747
- (231) Horsley, V., Aliprantis, A.O., Polak, L., Glimcher, L.H., and Fuchs, E. (2008) NFATc1 balances quiescence and proliferation of skin stem cells. *Cell*. 132, 299-310
- (232) Mancini, M., and Toker, A. (2009) NFAT proteins: emerging roles in cancer progression. *Nature reviews. Cancer*. 9, 810-820
- (233) Muller, M.R., and Rao, A. (2010) NFAT, immunity and cancer: a transcription factor comes of age. *Nature reviews. Immunology*. 10, 645-656

- (234) Pena, J.A., Losi-Sasaki, J.L., and Gooch, J.L. (2010) Loss of calcineurin Aalpha alters keratinocyte survival and differentiation. *The Journal of investigative dermatology*. 130, 135-140
- (235) Mammucari, C., Tommasi di Vignano, A., Sharov, A.A., Neilson, J., Havrda, M.C., Roop, D.R., Botchkarev, V.A., Crabtree, G.R., and Dotto, G.P. (2005) Integration of Notch 1 and calcineurin/NFAT signaling pathways in keratinocyte growth and differentiation control. *Developmental cell*. 8, 665-676
- (236) Flockhart, R.J., Diffey, B.L., Farr, P.M., Lloyd, J., and Reynolds, N.J. (2008) NFAT regulates induction of COX-2 and apoptosis of keratinocytes in response to ultraviolet radiation exposure. *FASEB journal : official publication of the Federation of American Societies for Experimental Biology*. 22, 4218-4227
- (237) Nicolas, M., Wolfer, A., Raj, K., Kummer, J.A., Mill, P., van Noort, M., Hui, C.C., Clevers, H., Dotto, G.P., and Radtke, F. (2003) Notch1 functions as a tumor suppressor in mouse skin. *Nature genetics*. 33, 416-421
- (238) Sommerer, C., Hartschuh, W., Enk, A., Meuer, S., Zeier, M., and Giese, T. (2008) Pharmacodynamic immune monitoring of NFAT-regulated genes predicts skin cancer in elderly long-term renal transplant recipients. *Clinical transplantation*. 22, 549-554
- (239) Flockhart, R.J., Armstrong, J.L., Reynolds, N.J., and Lovat, P.E. (2009) NFAT signalling is a novel target of oncogenic BRAF in metastatic melanoma. *British journal of cancer*. 101, 1448-1455
- (240) Levin-Gromiko, U., Koshelev, V., Kushnir, P., Fedida-Metula, S., Voronov, E., and Fishman, D. (2014) Amplified lipid rafts of malignant cells constitute a target for inhibition of aberrantly active NFAT and melanoma tumor growth by the aminobisphosphonate zoledronic acid. *Carcinogenesis*. 35, 2555-2566
- (241) Perotti, V., Baldassari, P., Molla, A., Vegetti, C., Bersani, I., Maurichi, A., Santinami, M., Anichini, A., and Mortarini, R. (2016) NFATc2 is an intrinsic regulator of melanoma dedifferentiation. *Oncogene*. 35, 2862-2872
- (242) Shoshan, E., Braeuer, R.R., Kamiya, T., Mobley, A.K., Huang, L., Vasquez, M.E., Velazquez-Torres, G., Chakravarti, N., Ivan, C., Prieto, V., Villares, G.J., and Bar-Eli, M. (2016) NFAT1 Directly Regulates IL8 and MMP3 to Promote Melanoma Tumor Growth and Metastasis. *Cancer research*. 76, 3145-3155
- (243) Skarmoutsou, E., Bevelacqua, V., F, D.A., Russo, A., Spandidos, D.A., Scalisi, A., Malaponte, G., and Guarneri, C. (2018) FOXP3 expression is modulated by TGFbeta1/NOTCH1 pathway in human melanoma. *International journal of molecular medicine*. 42, 392-404
- (244) Tan, B., Anaka, M., Deb, S., Freyer, C., Ebert, L.M., Chueh, A.C., Al-Obaidi, S., Behren, A., Jayachandran, A., Cebon, J., Chen, W., and Mariadason, J.M. (2014) FOXP3 over-expression inhibits melanoma tumorigenesis via effects on proliferation and apoptosis. *Oncotarget*. 5, 264-276
- (245) Franco-Molina, M.A., Miranda-Hernandez, D.F., Mendoza-Gamboa, E., Zapata-Benavides, P., Coronado-Cerda, E.E., Sierra-Rivera, C.A., Saavedra-Alonso, S., Tamez-Guerra, R.S., and Rodriguez-Padilla, C. (2016) Silencing of Foxp3 delays the growth of murine melanomas and modifies the tumor immunosuppressive environment. *OncoTargets and therapy*. 9, 243-253

- (246) Ciechomska, I., Legat, M., Golab, J., Wesolowska, A., Kurzaj, Z., Mackiewicz, A., and Kaminska, B. (2005) Cyclosporine A and its non-immunosuppressive derivative NIM811 induce apoptosis of malignant melanoma cells in in vitro and in vivo studies. *International journal of cancer*. 117, 59-67
- (247) Juhasz, T., Matta, C., Veress, G., Nagy, G., Szijgyarto, Z., Molnar, Z., Fodor, J., Zakany, R., and Gergely, P. (2009) Inhibition of calcineurin by cyclosporine A exerts multiple effects on human melanoma cell lines HT168 and WM35. *International journal of oncology*. 34, 995-1003
- (248) Fang, D., Nguyen, T.K., Leishear, K., Finko, R., Kulp, A.N., Hotz, S., Van Belle, P.A., Xu, X., Elder, D.E., and Herlyn, M. (2005) A tumorigenic subpopulation with stem cell properties in melanomas. *Cancer research*. 65, 9328-9337
- (249) Zhang, X., Gibhardt, C.S., Will, T., Stanisz, H., Korbelt, C., Mitkovski, M., Stejerean, I., Cappello, S., Pacheu-Grau, D., Dudek, J., Tahbaz, N., Mina, L., Simmen, T., Laschke, M.W., Menger, M.D., Schon, M.P., Helms, V., Niemeyer, B.A., Rehling, P., Vultur, A., and Bogeski, I. (2019) Redox signals at the ER-mitochondria interface control melanoma progression. *The EMBO journal*. 38, e100871
- (250) Boveris, A., and Chance, B. (1973) The mitochondrial generation of hydrogen peroxide. General properties and effect of hyperbaric oxygen. *The Biochemical journal*. 134, 707-716
- (251) Quintana, A., Schwindling, C., Wenning, A.S., Becherer, U., Rettig, J., Schwarz, E.C., and Hoth, M. (2007) T cell activation requires mitochondrial translocation to the immunological synapse. *Proceedings of the National Academy of Sciences of the United States of America*. 104, 14418-14423
- (252) Block, K., Gorin, Y., and Abboud, H.E. (2009) Subcellular localization of Nox4 and regulation in diabetes. *Proceedings of the National Academy of Sciences of the United States of America*. 106, 14385-14390
- (253) Van Buul, J.D., Fernandez-Borja, M., Anthony, E.C., and Hordijk, P.L. (2005) Expression and localization of NOX2 and NOX4 in primary human endothelial cells. *Antioxidants & redox signaling*. 7, 308-317
- (254) Bedard, K., and Krause, K.H. (2007) The NOX family of ROS-generating NADPH oxidases: physiology and pathophysiology. *Physiological reviews*. 87, 245-313
- (255) von Lohneysen, K., Noack, D., Wood, M.R., Friedman, J.S., and Knaus, U.G. (2010) Structural insights into Nox4 and Nox2: motifs involved in function and cellular localization. *Molecular and cellular biology*. 30, 961-975
- (256) Friedl, P., Locker, J., Sahai, E., and Segall, J.E. (2012) Classifying collective cancer cell invasion. *Nature cell biology*. 14, 777-783
- (257) Sumimoto, H., Imabayashi, F., Iwata, T., and Kawakami, Y. (2006) The BRAF-MAPK signaling pathway is essential for cancer-immune evasion in human melanoma cells. *The Journal of experimental medicine*. 203, 1651-1656
- (258) Poulidakos, P.I., and Rosen, N. (2011) Mutant BRAF melanomas--dependence and resistance. *Cancer cell*. 19, 11-15
- (259) Aibar, S., Gonzalez-Blas, C.B., Moerman, T., Huynh-Thu, V.A., Imrichova, H., Hulselmans, G., Rambow, F., Marine, J.C., Geurts, P., Aerts, J., van den Oord, J., Atak, Z.K.,

- Wouters, J., and Aerts, S. (2017) SCENIC: single-cell regulatory network inference and clustering. *Nature methods*. 14, 1083-1086
- (260) Soboloff, J., Rothberg, B.S., Madesh, M., and Gill, D.L. (2012) STIM proteins: dynamic calcium signal transducers. *Nature reviews. Molecular cell biology*. 13, 549-565
- (261) Carrasco, S., and Meyer, T. (2011) STIM proteins and the endoplasmic reticulum-plasma membrane junctions. *Annual review of biochemistry*. 80, 973-1000
- (262) Demaurex, N., Poburko, D., and Frieden, M. (2009) Regulation of plasma membrane calcium fluxes by mitochondria. *Biochimica et biophysica acta*. 1787, 1383-1394
- (263) Deak, A.T., Blass, S., Khan, M.J., Groschner, L.N., Waldeck-Weiermair, M., Hallstrom, S., Graier, W.F., and Malli, R. (2014) IP3-mediated STIM1 oligomerization requires intact mitochondrial Ca<sup>2+</sup> uptake. *Journal of cell science*. 127, 2944-2955
- (264) Yu, L., Golbeck, J., Yao, J., and Rusnak, F. (1997) Spectroscopic and enzymatic characterization of the active site dinuclear metal center of calcineurin: implications for a mechanistic role. *Biochemistry*. 36, 10727-10734
- (265) Rhee, S.G., Bae, Y.S., Lee, S.R., and Kwon, J. (2000) Hydrogen peroxide: a key messenger that modulates protein phosphorylation through cysteine oxidation. *Science's STKE : signal transduction knowledge environment*. 2000, pe1
- (266) Reiter, T.A., Abraham, R.T., Choi, M., and Rusnak, F. (1999) Redox regulation of calcineurin in T-lymphocytes. *Journal of biological inorganic chemistry : JBIC : a publication of the Society of Biological Inorganic Chemistry*. 4, 632-644
- (267) Ghosh, M.C., Wang, X., Li, S., and Klee, C. (2003) Regulation of calcineurin by oxidative stress. *Methods in enzymology*. 366, 289-304
- (268) Wang, X., Culotta, V.C., and Klee, C.B. (1996) Superoxide dismutase protects calcineurin from inactivation. *Nature*. 383, 434-437
- (269) Bogumil, R., Namgaladze, D., Schaarschmidt, D., Schmachtel, T., Hellstern, S., Mutzel, R., and Ullrich, V. (2000) Inactivation of calcineurin by hydrogen peroxide and phenylarsine oxide. Evidence for a dithiol-disulfide equilibrium and implications for redox regulation. *European journal of biochemistry*. 267, 1407-1415
- (270) Carruthers, N.J., and Stemmer, P.M. (2008) Methionine oxidation in the calmodulin-binding domain of calcineurin disrupts calmodulin binding and calcineurin activation. *Biochemistry*. 47, 3085-3095
- (271) Thannickal, V.J., and Fanburg, B.L. (2000) Reactive oxygen species in cell signaling. *American journal of physiology. Lung cellular and molecular physiology*. 279, L1005-1028
- (272) Ralph, S.J., Rodriguez-Enriquez, S., Neuzil, J., Saavedra, E., and Moreno-Sanchez, R. (2010) The causes of cancer revisited: "mitochondrial malignancy" and ROS-induced oncogenic transformation - why mitochondria are targets for cancer therapy. *Molecular aspects of medicine*. 31, 145-170
- (273) Senft, D., and Ronai, Z.A. (2015) UPR, autophagy, and mitochondria crosstalk underlies the ER stress response. *Trends in biochemical sciences*. 40, 141-148
- (274) Malhotra, J.D., and Kaufman, R.J. (2007) Endoplasmic reticulum stress and oxidative stress: a vicious cycle or a double-edged sword? *Antioxidants & redox signaling*. 9, 2277-2293

- (275) Appenzeller-Herzog, C., Banhegyi, G., Bogeski, I., Davies, K.J., Delaunay-Moisan, A., Forman, H.J., Gorlach, A., Kietzmann, T., Laurindo, F., Margittai, E., Meyer, A.J., Riemer, J., Rutzler, M., Simmen, T., Sitia, R., Toledano, M.B., and Touw, I.P. (2016) Transit of H<sub>2</sub>O<sub>2</sub> across the endoplasmic reticulum membrane is not sluggish. *Free radical biology & medicine*. 94, 157-160
- (276) Li, G., Scull, C., Ozcan, L., and Tabas, I. (2010) NADPH oxidase links endoplasmic reticulum stress, oxidative stress, and PKR activation to induce apoptosis. *The Journal of cell biology*. 191, 1113-1125
- (277) Prior, K.K., Wittig, I., Leisegang, M.S., Groenendyk, J., Weissmann, N., Michalak, M., Jansen-Durr, P., Shah, A.M., and Brandes, R.P. (2016) The Endoplasmic Reticulum Chaperone Calnexin Is a NADPH Oxidase NOX4 Interacting Protein. *The Journal of biological chemistry*. 291, 7045-7059
- (278) Yamaura, M., Mitsushita, J., Furuta, S., Kiniwa, Y., Ashida, A., Goto, Y., Shang, W.H., Kubodera, M., Kato, M., Takata, M., Saida, T., and Kamata, T. (2009) NADPH oxidase 4 contributes to transformation phenotype of melanoma cells by regulating G2-M cell cycle progression. *Cancer research*. 69, 2647-2654
- (279) Meitzler, J.L., Makhlof, H.R., Antony, S., Wu, Y., Butcher, D., Jiang, G., Juhasz, A., Lu, J., Dahan, I., Jansen-Durr, P., Pircher, H., Shah, A.M., Roy, K., and Doroshov, J.H. (2017) Decoding NADPH oxidase 4 expression in human tumors. *Redox biology*. 13, 182-195
- (280) Kornmann, B., Currie, E., Collins, S.R., Schuldiner, M., Nunnari, J., Weissman, J.S., and Walter, P. (2009) An ER-mitochondria tethering complex revealed by a synthetic biology screen. *Science*. 325, 477-481
- (281) Friedman, J.R., Lackner, L.L., West, M., DiBenedetto, J.R., Nunnari, J., and Voeltz, G.K. (2011) ER tubules mark sites of mitochondrial division. *Science*. 334, 358-362
- (282) Eisenberg-Bord, M., Shai, N., Schuldiner, M., and Bohnert, M. (2016) A Tether Is a Tether: Tethering at Membrane Contact Sites. *Developmental cell*. 39, 395-409
- (283) Klecker, T., Bockler, S., and Westermann, B. (2014) Making connections: interorganelle contacts orchestrate mitochondrial behavior. *Trends in cell biology*. 24, 537-545
- (284) Giacomello, M., and Pellegrini, L. (2016) The coming of age of the mitochondria-ER contact: a matter of thickness. *Cell death and differentiation*. 23, 1417-1427
- (285) Frieden, M., Arnaudeau, S., Castelbou, C., and Demaurex, N. (2005) Subplasmalemmal mitochondria modulate the activity of plasma membrane Ca<sup>2+</sup>-ATPases. *The Journal of biological chemistry*. 280, 43198-43208
- (286) Fowler, S.L., Akins, M., Zhou, H., Figeys, D., and Bennett, S.A. (2013) The liver connexin32 interactome is a novel plasma membrane-mitochondrial signaling nexus. *Journal of proteome research*. 12, 2597-2610
- (287) Filadi, R., Greotti, E., Turacchio, G., Luini, A., Pozzan, T., and Pizzo, P. (2015) Mitofusin 2 ablation increases endoplasmic reticulum-mitochondria coupling. *Proceedings of the National Academy of Sciences of the United States of America*. 112, E2174-2181
- (288) Lackner, L.L., Ping, H., Graef, M., Murley, A., and Nunnari, J. (2013) Endoplasmic reticulum-associated mitochondria-cortex tether functions in the distribution and inheritance

of mitochondria. *Proceedings of the National Academy of Sciences of the United States of America*. 110, E458-467

(289) Cardenas, C., Muller, M., McNeal, A., Lovy, A., Jana, F., Bustos, G., Urra, F., Smith, N., Molgo, J., Diehl, J.A., Ridky, T.W., and Foskett, J.K. (2016) Selective Vulnerability of Cancer Cells by Inhibition of Ca<sup>2+</sup> Transfer from Endoplasmic Reticulum to Mitochondria. *Cell reports*. 15, 219-220

(290) Phan, V., Schmidt, J., Matyash, V., Malchow, S., Thanisch, M., Lorenz, C., Diepolder, I., Schulz, J.B., Stenzel, W., Roos, A., and Gess, B. (2018) Characterization of Naive and Vitamin C-Treated Mouse Schwann Cell Line MSC80: Induction of the Antioxidative Thioredoxin Related Transmembrane Protein 1. *Journal of proteome research*. 17, 2925-2936

(291) Kim, M.S., and Usachev, Y.M. (2009) Mitochondrial Ca<sup>2+</sup> cycling facilitates activation of the transcription factor NFAT in sensory neurons. *The Journal of neuroscience : the official journal of the Society for Neuroscience*. 29, 12101-12114

(292) Chen, Y., Yuen, W.H., Fu, J., Huang, G., Melendez, A.J., Ibrahim, F.B., Lu, H., and Cao, X. (2007) The mitochondrial respiratory chain controls intracellular calcium signaling and NFAT activity essential for heart formation in *Xenopus laevis*. *Molecular and cellular biology*. 27, 6420-6432

(293) Murphy, M.P., and Siegel, R.M. (2013) Mitochondrial ROS fire up T cell activation. *Immunity*. 38, 201-202

(294) Sena, L.A., Li, S., Jairaman, A., Prakriya, M., Ezponda, T., Hildeman, D.A., Wang, C.R., Schumacker, P.T., Licht, J.D., Perlman, H., Bryce, P.J., and Chandel, N.S. (2013) Mitochondria are required for antigen-specific T cell activation through reactive oxygen species signaling. *Immunity*. 38, 225-236

(295) Pinton, P., Giorgi, C., Siviero, R., Zecchini, E., and Rizzuto, R. (2008) Calcium and apoptosis: ER-mitochondria Ca<sup>2+</sup> transfer in the control of apoptosis. *Oncogene*. 27, 6407-6418

(296) Area-Gomez, E., and Schon, E.A. (2016) Mitochondria-associated ER membranes and Alzheimer disease. *Current opinion in genetics & development*. 38, 90-96

(297) Tubbs, E., and Rieusset, J. (2017) Metabolic signaling functions of ER-mitochondria contact sites: role in metabolic diseases. *Journal of molecular endocrinology*. 58, R87-R106

(298) Trachootham, D., Alexandre, J., and Huang, P. (2009) Targeting cancer cells by ROS-mediated mechanisms: a radical therapeutic approach? *Nature reviews. Drug discovery*. 8, 579-591

(299) Fulda, S., Galluzzi, L., and Kroemer, G. (2010) Targeting mitochondria for cancer therapy. *Nature reviews. Drug discovery*. 9, 447-464

(300) Corazao-Rozas, P., Guerreschi, P., Jendoubi, M., Andre, F., Jonneaux, A., Scalbert, C., Garcon, G., Malet-Martino, M., Balayssac, S., Rocchi, S., Savina, A., Formstecher, P., Mortier, L., Kluza, J., and Marchetti, P. (2013) Mitochondrial oxidative stress is the Achilles' heel of melanoma cells resistant to Braf-mutant inhibitor. *Oncotarget*. 4, 1986-1998

(301) Braeuer, R.R., Zigler, M., Kamiya, T., Dobroff, A.S., Huang, L., Choi, W., McConkey, D.J., Shoshan, E., Mobley, A.K., Song, R., Raz, A., and Bar-Eli, M. (2012) Galectin-3 contributes to melanoma growth and metastasis via regulation of NFAT1 and autotaxin. *Cancer research*. 72, 5757-5766

- (302) Yang, Y., and Qian, Q. (2014) Wnt5a/Ca (2+) /calcineurin/nuclear factor of activated T signaling pathway as a potential marker of pediatric melanoma. *Journal of cancer research and therapeutics*. 10 Suppl, C83-88
- (303) Yang, Y., Guo, W., Ma, J., Xu, P., Zhang, W., Guo, S., Liu, L., Ma, J., Shi, Q., Jian, Z., Liu, L., Wang, G., Gao, T., Han, Z., and Li, C. (2018) Downregulated TRPV1 Expression Contributes to Melanoma Growth via the Calcineurin-ATF3-p53 Pathway. *The Journal of investigative dermatology*. 138, 2205-2215
- (304) Pfluger, P.T., Kabra, D.G., Aichler, M., Schriever, S.C., Pfuhlmann, K., Garcia, V.C., Lehti, M., Weber, J., Kutschke, M., Rozman, J., Elrod, J.W., Hevener, A.L., Feuchtinger, A., Hrabe de Angelis, M., Walch, A., Rollmann, S.M., Aronow, B.J., Muller, T.D., Perez-Tilve, D., Jastroch, M., De Luca, M., Molkentin, J.D., and Tschop, M.H. (2015) Calcineurin Links Mitochondrial Elongation with Energy Metabolism. *Cell metabolism*. 22, 838-850

## **10 Register of Graphs, Tables and Figures**

### **Graphs**

Graph 1: Anatomy of the Human Skin (Adapted from official website: university of California San Francisco/Melanoma Surgery/Department of Surgery)

Graph 2: Biologic Events and Molecular Changes in the Progression of Melanoma. (Adapted from Arlo J. Miller and Martin C. Mihm, N Engl J Med 2006; 355:51-65.)

Graph 3: The Ca<sup>2+</sup>-NFAT Signaling pathway. (Adapted from Martin R. Müller and Anjana Rao, Nat Rev Immunol 2010; 10:645-656.)

Graph 4: Zeiss Cell Observer Z1 imaging setup.

Graph 5: Theoretical model of TMX-ROS-NFAT1 signal axis in melanoma.

### **Tables**

Table 1: Chemicals

Table 2: Solutions and Medium

Table 3: Recipes for home-made solutions

Table 4: Primer for PCR

Table 5: siRNA and shRNA

Table 6: Primary antibodies

Table 7: Commercially available kits

Table 8: Peripheral materials

Table 9: Devices

Table 10: LED sets on the Zeiss Colibri 2 system

Table 11: Emission filters and dichroic mirror sets

Table 12: Objectives on the Zeiss Cell observer

Table 13: Cameras for live cell imaging

Table 14: Olympus IX70 components

Table 15: Panel of Cell Lines Used for the Current Study

Table 16: Genetically Encoded Protein Sensors

Table 17: Programs used for the transfection by electroporation

## **Figures**

Figure 1: mRNA expression of TMX1 and TMX3 in melanoma cell lines.

Figure 2: mRNA expression of NFAT in melanoma cell lines.

Figure 3: Nuclear import of NFAT1 in melanoma cell.

Figure 4: NFAT1 translocation is inhibited following TMX silencing in melanoma cell lines.

Figure 5: IL-8 secretion from melanoma cells is decreased following TMX silencing.

Figure 6: Cytosolic calcium measurement on WM3734 cells following TMX silencing.

Figure 7: Cytosolic H<sub>2</sub>O<sub>2</sub> concentration was elevated by TMX silencing.

Figure 8: The NFAT1 translocation is inhibited by extracellular H<sub>2</sub>O<sub>2</sub> in a dose-dependent manner.

Figure 9: The inhibition of NFAT1 activation induced by TMX1 silencing can be rescued by antioxidants.

Figure 10: The phosphatase activity of calcineurin is inhibited by TMX silencing.

Figure 11: The calcineurin activity could be inhibited by H<sub>2</sub>O<sub>2</sub> in melanoma.

Figure 12: The silencing of TMX does not trigger ER stress in melanoma cells.

Figure 13: The ER lumen is not a major source of H<sub>2</sub>O<sub>2</sub> in melanoma cells following TMX1 silencing.

Figure 14: TMX silencing induces significant increase of mitochondrial ROS.

Figure 15: Mitochondrial calcium uptake is increased following TMX1 silencing.

Figure 16: The PM to mitochondria calcium transfer is increased following TMX1 silencing.

Figure 17: The basal mitochondrial ATP level is increased following TMX1 silencing.

Figure 18: Mitochondrial repositioning towards the plasma membrane in melanoma cells following TMX1 silencing.

Figure 19: Mitochondrial repositioning disturbed redox homeostasis in MAM.

Figure 20: The NOX4 is an alternative source of excessive cellular ROS.

Figure 21: The proliferation of melanoma cells is inhibited following TMX silencing.

Figure 22: The proliferation of melanoma cells is inhibited by suppression of NFAT.

Figure 23: The migration of melanoma cells is inhibited following TMX silencing or suppression of NFAT, calcineurin.

Figure 24: TMX1 silencing does not affect BRAF and MEK resistance of melanoma cells.

Figure 25: The melanoma tumor growth is affected following TMX silencing.

## **11 Declaration**

According to § 7 Abs. 1 Nr. 4, I hereby declare to the best of my knowledge as follows. The experimental data in the present study is a collective effort with the stated collaborators and co-workers with permission, no other parties are unspecified for their aids and resources in this project. The concepts and data directly or indirectly adopted from other sources are all specified in the manuscript.

### **Writings and Figures**

This work cited and contained altered paragraphs and figures from the published first author publication “Redox signals at the ER-mitochondria interface control melanoma progression”, Zhang *et al*, EMBO J. 2019 Aug 1;38(15): e100871. The contributions for the generation of experimental data from other group members, collaborators are specified in the figure legends.

### **Collaboration and access to laboratory resources**

The Wistar Institute (Philadelphia, U.S.A) transferred the WM3734 melanoma cell line for this study. This study was performed in collaboration with the following institutions: Center for Bioinformatics, Saarland University, Saarbruecken, Germany; Department of Dermatology Venereology and Allergology, University Medical Center, Georg-August-University, Goettingen, Germany; Institute for Clinical and Experimental Surgery, Saarland University, Homburg, Germany; Department of Cellular Biochemistry, University Medical Center, Georg-August-University, Goettingen, Germany; Department of Cell Biology, University of Alberta, Edmonton, Alberta, Canada; Light Microscopy Facility, Max Planck Institute for Experimental Medicine, Goettingen; Molecular Biophysics, Center for Integrative Physiology and Molecular Medicine, Saarland University, Homburg, Germany; Max Plank Institute for Biophysical Chemistry, Goettingen, Germany.

Date and Place:

Signature:

## 12 Publications

1. Zhang, X., Gibhardt, C. S., Will, T., Stanisz, H., Korbel, C., Mitkovski, M., Stejerean, I., Cappello, S., Pacheu-Grau, D., Dudek, J., Tahbaz, N., Mina, L., Simmen, T., Laschke, M. W., Menger, M. D., Schon, M. P., Helms, V., Niemeyer, B. A., Rehling, P., Vultur, A., and Bogeski, I. (2019) Redox signals at the ER-mitochondria interface control melanoma progression. *The EMBO journal* 38, e100871
2. Akula, A. K., Zhang, X., Viotti, J. S., Nestvogel, D., Rhee, J. S., Ebrecht, R., Reim, K., Wouters, F., Liepold, T., Jahn, O., Bogeski, I., and Dresbach, T. (2019) The Calmodulin Binding Region of the Synaptic Vesicle Protein Mover Is Required for Homomeric Interaction and Presynaptic Targeting. *Frontiers in molecular neuroscience* 12, 249
3. Zhang, X., Gibhardt, C. S., Cappello, S., Zimmermann, K. M., Vultur, A., Bogeski, I. (2018) Measuring mitochondrial ROS in mammalian cells with a genetically encoded protein sensor. *Bio-protocol*, 8(2).
4. Gibhardt, C. S., Zimmermann, K. M., Zhang, X., Belousov, V. V., and Bogeski, I. (2016) Imaging calcium and redox signals using genetically encoded fluorescent indicators. *Cell calcium* 60, 55-64
5. Cierlitz, M., Chauvistre, H., Bogeski, I., Zhang, X., Hauschild, A., Herlyn, M., Schadendorf, D., Vogt, T., and Roesch, A. (2015) Mitochondrial oxidative stress as a novel therapeutic target to overcome intrinsic drug resistance in melanoma cell subpopulations. *Experimental dermatology* 24, 155-157
6. Wang, Y., Sun, C., Mao, A., Zhang, X., Zhou, X., Wang, Z., and Zhang, H. (2015) Radiosensitization to X-ray radiation by telomerase inhibitor MST-312 in human hepatoma HepG2 cells. *Life sciences* 123, 43-50
7. Di, C. X., Yang, L. N., Zhang, H., An, L. Z., Zhang, X., Ma, X. F., Sun, C., Wang, X. H., Yang, R., Wu, Z. H., and Si, J. (2013) Effects of carbon-ion beam or X-ray irradiation on anti-apoptosis Dnnp73 expression in HeLa cells. *Gene* 515, 208-213
8. Di, C., Yang, L., Zhang, H., Ma, X., Zhang, X., Sun, C., Li, H., Xu, S., An, L., Li, X., and Bai, Z. (2013) Mechanisms, function and clinical applications of Dnnp73. *Cell cycle* 12, 1861-1867
9. Zhou, X., Zhang, X., Xie, Y., Tanaka, K., Wang, B., and Zhang, H. (2013) DNA-PKcs inhibition sensitizes cancer cells to carbon-ion irradiation via telomere capping disruption. *Plos One* 8, e72641
10. Li, H. Y., Zhang, H., Miao, G. Y., Xie, Y., Sun, C., Di, C. X., Liu, Y., Liu, Y. Y., Zhang, X., Ma, X. F., Xu, S., Gan, L., and Zhou, X. (2013) Simulated microgravity conditions and carbon ion irradiation induce spermatogenic cell apoptosis and sperm DNA damage. *Biomedical and environmental sciences : BES* 26, 726-734

11. Zhou, X., Liu, X., Zhang, X., Zhou, R., He, Y., Li, Q., Wang, Z., and Zhang, H. (2012) Non-randomized mtDNA damage after ionizing radiation via charge transport. *Scientific reports* 2, 780
12. Zhang, X., Zhou, X., Chen, R., and Zhang, H. (2012) Radiosensitization by inhibiting complex I activity in human hepatoma HepG2 cells to X-ray radiation. *Journal of radiation research* 53, 257-263
13. Zhou, X., Li, N., Wang, Y., Wang, Y., Zhang, X., and Zhang, H. (2011) Effects of X-irradiation on mitochondrial DNA damage and its supercoiling formation change. *Mitochondrion* 11, 886-892

## **13 Curriculum Vitae**

\*The curriculum vitae was removed from the electronic version of the doctoral thesis for reasons of data protection.

(Aus datenschutzrechtlichen Gründen wird der Lebenslauf in der elektronischen Fassung der Dissertation nicht veröffentlicht.)

